INVESTIGATION OF PHYSIOLOGICAL AND MOLECULAR MECHANISMS CONFERRING DIURNAL VARIATION IN AUXINIC HERBICIDE EFFICACY

by

CHRISTOPHER R. JOHNSTON

(Under the Direction of William Vencill)

ABSTRACT

The efficacy of auxinic herbicides has been shown to vary with the time of day in which applications are made, however little is known about the mechanisms causing this phenomenon. Investigating the differential *in planta* behavior of these herbicides across different times of application may grant an ability to advise which properties of auxinic herbicide activity are desirable when applications must be made around the clock. Furthermore, determining under which environmental conditions this phenomenon is most prone to occurring may grant growers valuable information to inform future application strategies. Radiolabeled herbicide experiments demonstrated a likely increase in ATP-binding cassette subfamily B (ABCB)-mediated 2,4-D and dicamba transport in Palmer amaranth (*Amaranthus palmeri* S. Watson) at simulated dawn compared to mid-day, as dose response models indicated that many orders of magnitude higher concentrations of N-1-naphthylphthalamic acid (NPA) and verapamil are required to inhibit translocation by 50% at simulated sunrise compared to mid-day. Gas chromatographic analysis displayed that the log of ethylene evolution in *A. palmeri* was 0.32 µL kg FW^{-1} h^{-1} higher when dicamba was applied during mid-day compared to sunrise. Furthermore, it was found that inhibition of translocation via 2,3,5-triiodobenzoic acid resulted in an increased amount of 2,4-

D-induced ethylene evolution at sunrise, and the inhibition of dicamba translocation via NPA reversed the difference in ethylene evolution across time of application. Molecular experiments showed that expression of 9-cis-epoxycarotenoid dioxygenase biosynthesis gene *NCED1* was increased with dawn applications, while there was a notable lack of trends observed across times of day and across herbicides with *ACS1*, encoding 1-aminocyclopropane-1-carboxylic acid synthase. Growth chamber studies indicated that temperature and day/night temperature differential affect percent control of *A. palmeri* with 2,4-D and dicamba applications more than humidity. Time of application effects were observed with 2,4-D across different temperature regimens, but not dicamba. Across different temperature differentials, a time of application effect observed with dicamba was eliminated upon increasing the rate. The formation of H_2O_2 was closely associated with phytotoxicity resulting from 2,4-D and dicamba applications.

INDEX WORDS: Palmer amaranth (*Amaranthus palmeri* S. Watson), Auxinic herbicide, N-1-naphthylphthalamic acid, Verapamil, 2,3,5-triiodobenzoic acid, 2,4-D, Dicamba, Herbicide translocation, Ethylene evolution, 1-aminocyclopropane-1-carboxylic acid synthase, 9-cis-epoxycarotenoid dioxygenase, Temperature, Temperature differential, Humidity, Hydrogen peroxide

INVESTIGATION OF PHYSIOLOGICAL AND MOLECULAR MECHANISMS CONFERRING DIURNAL VARIATION IN AUXINIC HERBICIDE EFFICACY

by

CHRISTOPHER R. JOHNSTON

B.S., Virginia Polytechnic Institute and State University, 2011

M.S., The University of Georgia, 2014

A Dissertation Submitted to the Graduate Faculty of The University of Georgia in Partial Fulfillment of the Requirements for the Degree

DOCTOR OF PHILOSOPHY

ATHENS, GEORGIA

2019

INVESTIGATION OF PHYSIOLOGICAL AND MOLECULAR MECHANISMS CONFERRING DIURNAL VARIATION IN AUXINIC HERBICIDE EFFICACY

by

CHRISTOPHER R. JOHNSTON

Major Professor: William Vencill

Committee: Timothy Grey
Stanley Culpepper
Mark Czarnota
Gerald Henry

Electronic Version Approved:

Suzanne Barbour
Dean of the Graduate School
The University of Georgia
May 2019

DEDICATION

This dissertation is dedicated to my mother, Susan Ward, and my late father, Robert Johnston, for their unconditional love and encouragement, and to all the wonderful people that have been put in my life during my journey in Georgia.

ACKNOWLEDGEMENTS

First and foremost, I would like to thank Dr. William Vencill for providing me with the guidance to allow me to carry out this research, and for the dedication of time to mentor me in all aspects during my studies. Through his support I have been able to gain an indispensable and formidable further understanding of how to conduct quality research with real-world implications.

I would like to express a great degree of gratitude for my committee members, Dr. Timothy Grey, Dr. Stanley Culpepper, Dr. Mark Czarnota and Dr. Gerald Henry for providing me with all the additional perspectives and training necessary to effectively execute this research. Their input into not only my own research but my professional development as a whole is more than I could ask for. I also give the warmest of thanks to Dr. Anish Malladi, who selflessly gave a great deal of his time to show me the fundamentals of gas chromatography and qRT-PCR. Without his laboratory space and equipment this research would not have been possible.

I would like to express special appreciation to Dr. William Miller, Dr. Rhett Jackson, Dr. Todd Rasmussen, and Dr. Matthew Levi for their guidance and professorship during my teaching assistantship. The example they set was instrumental in furthering my knowledge of what is necessary to run a teaching appointment at a major university. I cannot express enough love and gratitude for my students in CRSS 3060 and CRSS 4340/6340L. The ability to guide them and give my time to furthering their understanding of science was truly a special privilege. They helped me more than I would have imagined by giving this chapter of my life even greater purpose.

I have to give a sincere appreciation for my fellow graduate students and colleagues for their friendship and support, namely Chase Straw, Zack Sanders, Josh Andrews, Aaron Joslin, Rachel Ryland, Kishan Mahmud, Nadia Noor, Andy Bisceglia, Dr. Kate Cassity-Duffey, John Rema, Pietro Sica, Kurk Lance, Jacob Kalina, Nehru Mantripragada, Shan Jing, John Doyle, Andres Mayorga, and Dr. Nick Basinger. I have to give a special thanks to Taylor Randell and Joseph Gaines for their technical assistance, taking over for me so I could go to sleep after spending all-nighters in the lab.

Finally, I have to give thanks to God for the strength and courage to carry this work out, to all my great friends for their support, and the town of Athens as a whole for the beautiful experiences and memories.

Christopher R. Johnston

The University of Georgia

November 22, 2018.

TABLE OF CONTENTS

Page

LIST OF TABLES

Page

LIST OF FIGURES

Page

CHAPTER 1

INTRODUCTION AND LITERATURE REVIEW

Time of Day Effects

The time of day in which herbicides are applied can vary across different agronomic systems. Growers may apply herbicides around dawn or dusk to reduce drift potential and increase the duration of spray droplet retention on leaves before evaporation, or simply because farm size may require applications be made at these times to cover all acreage (Sellers et al. 2003; Prasad et al. 1967; Dalazen and Merotto 2016). Despite these commonplace practices, the efficacy of many herbicides have been shown to vary depending on what time of day they are applied (Sellers et al. 2004; Lee and Oliver 1982; Kudsk and Kristensen 1992; Stopps et al. 2013). This variation in herbicide efficacy offers a challenge to growers that must make applications at various times of day, as the resulting reduced efficacy from applications made at times with lower herbicide performance may require additional herbicide applications. In situations where additional applications cannot be made or are ineffective, consequential weed control failures may reduce crop productivity or harvestability.

Numerous processes may contribute to differential herbicide efficacy resulting from the time of day in which an herbicide is applied. Specifically, a time of day of application effect has been reported with PROTOX-inhibiting herbicides, glyphosate, glufosinate, and auxinic herbicides (Culpepper 2014; Sharkhuu et al. 2014; Dalazen and Merotto 2016; McCue and Conn 1990; Sellers et al. 2003; Sellers et al. 2004; Weaver and Nylund 1963; Stewart et al. 2009; Skuterud et al. 1998; Bovey et al. 1972). There is however a pronounced lack of understanding

in the mechanisms conferring this effect with auxinic herbicides. Factors responsible for auxin translocation have been shown to have varying degrees of activity depending on time of day (Nozue and Maloof 2006; Covington and Harmer 2007; Nozue et al. 2011; Blakeslee et al. 2004). This has implications concerning auxinic herbicide translocation and may be a critical factor involved in differential efficacy (Nozue and Maloof 2006; Covington and Harmer 2007; Johnston et al. 2018). This is further supported by the fact that previous literature has correlated the degree of herbicide translocation with phytotoxicity (Beriault et al. 1999). However, translocation is likely not the only factor responsible for differential efficacy of auxinic herbicides. Circadian regulation has been linked to the perception and signaling of auxin, at least on the transcriptional level, with the majority of auxin-induced genes showing peak expression around mid-day (Covington and Harmer 2007). Furthermore, the synthesis and signaling of ethylene, a major hormone product resulting from auxinic herbicide applications, has also been shown to display circadian rhythms (Covington and Harmer 2007; Thain et al. 2004; Macháčková et al. 1997; Finlayson et al. 1999; Chincinska et al. 2013).

Auxinic Herbicides

There are four major chemical classes of auxinic herbicides: the phenoxyalkanoic acids (e.g. 2,4-D, MCPA), the benzoic acids (including dicamba), the pyridine-carboxylic acids (e.g. clopyralid, picloram, triclopyr), and the newer quinoline-carboxylic acids (including quinclorac) (Grossmann 2009; Cobb and Reade 2010). Auxinic herbicides (WSSA Group 4) work by mimicking the activity of natural auxin hormones, namely indole-3-acetic acid (IAA) (Cobb and Reade 2010; Sterling and Hall 1997). Herbicides of this class have been widely used since the late 1940s for dicot weed control in grass crops due to a favorable selectivity profile conferring a

lack of phytotoxicity towards grasses (Cobb and Reade 2010; Grossmann 2000). This selectivity favoring phytotoxic action only in dicot weeds is presumed to be due to differential metabolism and target-site sensitivity (Grossmann 2003; Sterling and Hall 1997; Kelley and Riechers 2007). As weak acids, ionized auxinic herbicides display a charge separation conferred via a negative charge on the carboxyl group and a positive charge on the benzene ring (Farrimond 1978). This is believed to be essential for proper auxin functioning.

Overall Mechanism of Action. The mechanism of action of auxinic herbicides is a complicated picture involving multiple points of transport, perception, and regulation. Nonetheless, much ground has been covered in recent years to elucidate these processes. Despite being mimics of natural auxins, auxinic herbicides, especially at higher doses, escape the natural regulatory system that plants have developed for these hormones and cause runaway auxin-inducible responses (Kelley and Riechers 2007). These auxinic herbicide-induced responses are typically reported to occur in three stages. In the first stage, membrane permeability is altered via proton efflux by H^+-ATPases, causing stomatal opening and cell elongation (Cobb and Reade 2010). This in combination with increases in the sugar and amino acid pools results in an initial stimulation of photosynthesis. Coinciding with these processes is an upregulation of gene expression, namely the 1-aminocyclopropane-1-carboxylic acid synthase (*ACS*) and 9-*cis*-epoxycarotenoid dioxygenase (*NCED*) genes within hours after treatment (Grossmann 2009; Grossmann 2003; Hansen and Grossmann 2000). Both *ACS* and *NCED* encode the major enzymes involved in upregulation of the biosynthesis of the hormones ethylene and abscisic acid (ABA), respectively (Yang and Hoffmann 1984; Song 2014). Epinastic symptoms such as stem twisting and leaf curling are sometimes first noted during this phase. The presence of reactive

oxygen species (ROS) is heavily associated with epinasty and overall phytotoxic response. Production of ROS is partly caused by the eventual accumulation of ABA resulting from *NCED* upregulation, ultimately inducing stomatal closure and inhibiting photosynthesis (following the initial transient stimulation) (Grossmann et al. 2001). Abscisic acid has also been noted to upregulate the activity of NADPH-oxidases in addition to stimulating superoxide dismutase activity, which are both suggested to be involved in hydrogen peroxide production which eventually results in lipid peroxidation (Romero-Puertas et al. 2004; Grossmann 2009; Dat et al. 2000). Activation of enzymes involved in ureide and fatty acid metabolism as well as jasmonic acid production are also involved in ROS accumulation (Pazmino et al. 2011; reviewed in Song 2014).

In the second phase of herbicidal activity, the initial increases in plant photosynthetic and metabolic processes become fueled by plant reserves, beginning the descent into unsustainable growth and eventual inhibition (Cobb and Reade 2010). Adventitious shoot and root growth is often observed at this point (Sanders and Pallett 1987). The aforementioned stomatal closure and reduction in photosynthetic processes eventually leads to the third phase in which cell anatomical breakdown, tissue destruction, and senescence occur before ultimate plant death (Grossmann 2009; Song 2014).

Perception. Auxin perception is primarily carried out via the auxin-binding protein 1 (ABP1) and transport inhibitor response 1 (TIR1), which are associated with the initiation of cell elongation and auxin-inducible gene expression, respectively (Braun et al. 2008; Napier et al. 2002; Macdonald 1997; Dharmasiri et al. 2005a; Dharmasiri et al. 2005b). More recently, TIR1-like proteins known as auxin-signaling F-box proteins (AFBs) have been identified, with AFB4

and AFB5 specifically displaying selective preferences for different auxinic herbicides (Walsh et al. 2006; Gleason 2011; Prigge et al. 2016). Other AFB proteins have no known affinity profile for auxinic herbicides.

ABP1 is found most abundantly in the endoplasmic reticulum, but the functional component responsible for perception occurs with plasma membrane-bound ABP1 located in a low-pH apoplast, allowing for auxin binding (Kelley and Riechers 2007). It is believed that auxin binding to ABP1 results in upregulated protein kinase activity, phosphorylating H^+-ATPases that subsequently create an electrochemical gradient via pumping protons and acidifying the apoplast (Macdonald 1997; DeLong et al. 2002; Hager 2003). Associated with proton pumping is a destabilizing effect resulting from mobilization of Ca^{2+} ions (Arif and Newman 1993). Both the creation of an electrochemical gradient and Ca^{2+} flux are believed to decrease the integrity of cell walls, allowing for auxin-induced cell elongation.

Upregulation of auxin-inducible genes is carried out via the binding of dimerized auxin response factors (ARFs) to auxin response elements (AuxREs) present on such genes (Hagen and Guilfoyle 2002). Under low auxin conditions, binding of ARFs to AuxREs is inhibited via the association of ARFs with a repressor protein, Aux/IAA (Mockaitis and Estelle 2008). Both the TIR1 and AFB proteins, now known to be auxin receptors, are associated with a Skp1-cullin-F-box protein ubiquitin ligase (SCF), resulting in a $SCF^{TIR1/AFB}$ complex (Dharmasiri et al. 2005a). In the presence of high auxin concentrations or auxinic herbicides, the TIR1/AFB proteins on this complex are bridged and bound to Aux/IAAs via the auxin/auxinic herbicide molecule itself, signaling the ubiquitination and subsequent degradation of Aux/IAAs via the 26S proteasome (Dharmasiri et al. 2005a; Kepinski and Leyser 2005; Hagen and Guilfoyle 2002; reviewed in

Grossmann 2009). Upon the binding of Aux/IAAs to ARFs, the ARFs are then free to dimerize and bind to AuxRE sequences on auxin-inducible genes (Hagen and Guilfoyle 2002).

Transport. Due to their similar chemical properties, auxinic herbicides are transported in plants via many of the same mechanisms as natural auxins. While mass flow of auxins through the phloem is one mechanism of auxin transport, the activity of plasma membrane-localized efflux proteins are responsible for cell-to-cell movement which can take place over long and short distances (Zažímalová et al. 2010). Specifically, the polar localization of such proteins across the plasma membrane determine the direction of cell-to-cell movement.

Plasma membrane-localized proteins of the ATP-binding cassette subfamily B (ABCB) have been known to play a large part in general transport of auxins and auxinic herbicides, namely ABCB1, ABCB4, and ABCB19 proteins (Kubeš et al. 2012; Yang and Murphy 2009; Schulz and Segobye 2016). In the case of ABCB proteins, ATP hydrolysis is used to propel the substrate (i.e. auxin or auxinic herbicide molecule) across plasma membranes (Hollenstein et al. 2007). Auxin efflux is also known to be facilitated by PIN-formed transporter proteins (PINs) (Gälweiler et al. 1998; Zažímalová et al. 2007). PIN proteins are trafficked from cell endosomes to the plasma membrane where they are able to facilitate polar auxin export (Geldner et al. 2001; Wiśniewska et al. 2006). While 2,4-D translocation is not dependent on PIN proteins, the inhibition of PIN proteins by 2,3,5-triiodobenzoic acid (TIBA) has been shown to reduce 2,4-D translocation (Covington and Harmer 2007; Goggin et al. 2016). Therefore, PIN proteins are likely to be partially responsible for auxinic herbicide translocation in general. In addition to the aforementioned auxin efflux proteins, members of the AUX/LAX protein family have been shown to function in auxin influx (reviewed in Swarup and Péret 2012). Specifically, AUX1 has

been shown to display permease-like behavior resulting in increased auxin uptake in a pH-regulated manner (Yang et al. 2006; Carrier et al. 2008).

2,4-D

The herbicide 2,4-dichlorophenoxyacetic acid (2,4-D), a phenoxyalkanoic acid, is generally regarded to be the first selective weed control agent, originally widely used in cereal crops (Sterling and Hall 1997; Grossmann 2003; Grossmann 2009). The mechanism of herbicidal activity of 2,4-D is consistent with other auxin analogues, generally causing a massive upregulation of auxin-inducible processes. Changes in membrane permeability to cations and mobilization of carbohydrate reserves occurs, followed by plant growth disturbances and production of ethylene, abscisic acid, and radical oxygen species (ROS) ultimately leads to senescence and tissue breakdown (Cobb and Reade 2010; Abeles 1973; Kraft et al. 2007; Dat et al. 2000; reviewed in Grossmann 2009).

Foliar applications are the most prevalent method of applying 2,4-D for weed control, as it is rapidly absorbed into the leaf (Cobb and Reade 2010). Upon entry into the cell apoplast, 2,4-D exists primarily in the lipophilic acid form which allows for ready movement into the phloem (Sterling 1994). The herbicide is quickly ionized due to the high pH in the phloem and is subsequently trapped and allowed to move in a classical source-to-sink manner (Ashton and Crafts 1981; Sterling and Hall 1997). Since it is a weak acid herbicide, it is phloem mobile and has the ability to disperse throughout the plant in multiple directions (Sterling and Hall 1997; Ashton and Crafts 1981).

The selectivity of 2,4-D towards dicot plants grant it a diverse array of utility in agronomic settings, with uses in turf, cereal crops, pastures, and aquatic situations as well as

directed applications in fruit crops (Senseman 2007; Grossmann 2003). Furthermore, the advent of 2,4-D-resistant crops has allowed for non-directed broadcast applications to be made throughout the season on increased amounts of acreage (Egan et al. 2011). Resistance in crops is achieved via insertion of transgenic aryloxyalkanoate dioxygenase that allows for rapid metabolism of 2,4-D to the non-active metabolite dichlorophenol (Skelton 2015). In 2014, the United States Department of Agriculture approved the use of 2,4-D-resistant soybean and corn, followed by approval for use in cotton in 2016 (Keim 2014; Barr and Zeller 2016).

Resistance to auxinic herbicides is not as widespread as other chemistries, nonetheless it has been reported to be a significant concern, especially with the advent of 2,4-D-resistant crops (Egan et al. 2011). Multiple mechanisms of resistance to 2,4-D have been reported in various weeds, suggesting a definite ability to select for resistance-conferring traits in multiple physiological processes. Resistance via a potential target-site alteration has been reported in wild mustard (*Sinapis arvensis* L.) (Webb and Hall 1995). Wild radish (*Raphanus raphanistrum* L.) resistance has been attributed to reduced translocation, potentially due to altered auxin transporter activity (Goggin et al. 2016). Rapid metabolism has been identified as the mechanism of 2,4-D resistance in waterhemp [*Amaranthus tuberculatus* (Moq.) J.D. Sauer] (Figueiredo et al. 2017).

Dicamba

The benzoic acid derivative 3,6-dichloro-2-methoxybenzoic acid (dicamba) is a widely used herbicide with a selectivity profile similar to 2,4-D, generally only having phytotoxic properties on dicot weeds (Senseman 2007; Chang and Vanden Born 1971; Grossmann 2003). Dicamba possesses similar auxinic activity to 2,4-D and other synthetic auxin analogues, which

is associated with increases in auxin signaling resulting in production of ethylene and abscisic acid as well as ROS accumulation (Cobb and Reade 2010; Abeles 1973; Kraft et al. 2007; Dat et al. 2000; reviewed in Grossmann 2009).

Foliar applications of dicamba are generally the most prevalent method of administration on target weeds (Senseman 2007). As with other synthetic auxins, dicamba is a weak acid which contributes to phloem mobility (Sterling and Hall 1997; Ashton and Crafts 1981). Entry into the phloem results in ionization and subsequent "trapping" allowing for source-to-sink movement in multiple directions (Ashton and Crafts 1981; Sterling and Hall 1997; see above). Consistently, rapid translocation has been positively correlated with phytotoxicity in susceptible species, with herbicide generally accumulating in meristematic tissues as well as roots (Chang and Vanden Born 1968; Gorrell et al. 1988).

Dicamba is utilized in many agronomic systems, with selective PRE and POST use in corn, as well as POST applications in sorghum, small grains, pastures and asparagus (Senseman 2007). Additionally, POST dicamba use has greatly increased with the commercialization of cotton and soybeans tolerant to dicamba, approved by the Environmental Protection Agency in 2016, which allows for over-the-top applications over large acreage in two crops traditionally susceptible to auxinic herbicides (Hartzler 2017; EPA 2017). The mechanism of dicamba detoxification in resistant crops is conferred by the presence of transgenic dicamba monooxygenase which metabolizes dicamba into an herbicidally inactive metabolite 3,6-dichlorosalicylic acid (Behrens et al. 2007). The release of dicamba-resistant crops was coupled with the introduction of low volatility formulations of the herbicide, including Xtendimax™ with VaporGrip™ Technology, as well as the new N,N-Bis-(3-aminopropyl)methylamine salt formulation contained in the Engenia™ herbicide product (Anonymous 2015, Anonymous 2016,

Johnston et al. 2018). However, during the 2017 growing season, more than a dozen states reported large amounts of dicamba-induced injury in non-resistant soybeans, resulting in the introduction of new requirements by the Environmental Protection Agency for the 2018 growing season and again in the 2019 growing season (Hightower 2017; Begemann 2017; Anonymous 2018).

Resistance to dicamba is more uncommon than many other herbicide chemistries. Dicamba resistance in Kochia [*Bassia scoparia* (L.) A.J. Scott] has been reported in the northern United States and Canada; however, the mechanism of resistance is currently unknown due to the lack of differential absorption, translocation, or metabolism between susceptible and resistant biotypes (Cranston et al. 2001). However, resistance in wild mustard [*Brassica kaber* (DC.) L.C. Wheeler] has been reported to be conferred by a single dominant nuclear-encoded allele (Jasieniuk et al. 1995). Despite a relatively low incidence of dicamba resistant weeds, alleles may now conceivably be selected for at a higher rate as a result of increased use in resistant crops.

Biosynthesis and Action of Auxin-Induced Hormones

Ethylene Biosynthesis. Ethylene biosynthesis begins with methionine. The enzyme S-adenosylmethionine synthase (SAMS) converts methionine into S-adenosylmethionine (SAM) (Pech et al. 2004). Following this reaction is the generation of 1-aminocyclopropane-1-carboxylic acid (ACC) from SAM via the ACC synthase (ACS) enzyme, which is encoded by numerous genes in *Arabidopsis* as well as in other plants (Kende 1993; Tsuchisaka and Theologis 2004; Taiz and Zeiger 2010). This is generally regarded as the rate-limiting step of ethylene biosynthesis in the majority of plant species, and ACC is the immediate precursor of

ethylene (Yang and Hoffman 1984). Finally, ACC is converted to ethylene via the ACC oxidase enzyme (ACO) in a reaction involving oxygen (McKeon et al. 1995; Kende 1993). Like ACS, ACO is encoded by a multigene family in plants (Barry et al. 1996). Ethylene itself has been shown to regulate ACO and ACS activity through feedback loops (Petruzzelli et al. 2000).

Abscisic Acid Biosynthesis. The synthesis of abscisic acid in higher plants involves reactions in both the terpenoid and carotenoid biosynthesis pathways. The major initial precursor is a C_5 isopentenyl diphosphate, which is condensed three times via geranylgeranyl diphosphate synthase in order to produce the C_{20} intermediate geranylgeranyl diphosphate (Buchanan et al. 2000; Nambara and Marion-Poll 2005). Geranylgeranyl diphosphate is then dimerized into a diphosphate intermediate prior to the C_{40} compound phytoene via phytoene synthase (Dogbo et al. 1988). This step serves as the major rate-limiting step in carotenoid biosynthesis, and is followed by intensive desaturase activity that finally produces β-carotene via lycopene cyclase (Lindgren et al. 2003; Buchanan et al. 2000). The carotenoid alcohol zeaxanthin is then produced from β-carotene via a hydroxylation reaction (Depka et al. 1998). The major epoxidation steps of the plastid-localized xanthophyll cycle are responsible for the ultimate conversion of zeaxanthin to violaxanthins via the enzyme zeaxanthin epoxidase (Marin et al. 1996; Nambara and Marion-Poll 2005; reviewed in Xiong and Zhu 2003). Following this step, *trans*-violaxanthin is converted to *trans*-neoxanthin via an enzyme product formed from an *ABA4* locus identified in *Arabidopsis* (Taiz and Zeiger 2010). An unknown enzyme isomerizes *trans*-neoxanthin to 9-*cis*-neoxanthin, which along with 9-*cis*-violaxanthin is a substrate for NCED that carries out the major committed and rate-limiting step for ABA biosynthesis (Schwartz et al. 2003). The product of this reaction is the C_{15} compound xanthoxal. Xanthoxal

is exported to the cytoplasm, where it is converted into ABA-aldehyde by a short-chain alcohol dehydrogenase/reductase (Cheng et al. 2002; González-Guzmán et al. 2002). ABA-aldehyde is finally oxidized into the carboxylic acid ABA via abscisic aldehyde oxidase (González-Guzmán et al. 2004).

Auxin-Induction of Hormones and Associated Responses. The induction of ethylene and ABA accumulation in auxin/auxinic herbicide-treated plants involves several key mechanisms and phenomena that occur prior to the eventual perception of both hormones via the regular signaling pathway. In addition to the aforementioned auxin-induced upregulation of *ACS* genes, regulation at the post-transcriptional level is also noted to play a role in stimulating the biosynthesis of ethylene in response to auxins (Hansen and Grossmann 2000; Woeste et al. 1999; Tsuchisaka and Theologis 2004). The upregulated biosynthesis of ethylene itself has been shown to be the key cause of the eventual inhibition of growth observed with a full phytotoxic response to auxins and auxinic herbicides (Sterling and Hall 1997; Grossmann 1998). Interestingly, the oxidation of ACC during the biosynthesis of ethylene results in cyanide production, causing an additional phytotoxic response (Grossmann 1998).

Auxinic herbicide-induced ABA formation is closely correlated with the classical effects of the hormone, including stomatal closure and inhibition of photosynthesis-related processes (Grossmann et al. 1996; Scheltrup and Grossmann 1995; Buchanan et al. 2000). Hansen and Grossmann (2000) provided support for a hypothesis in which ethylene stimulates the conversion of epoxy-carotenoids into the ABA precursor xanthoxal, a step occurring directly before in the abscisic aldehyde oxidase-mediated reaction that finally leads to ABA (Taiz and Zeiger 2010). Indeed, the production of ACC and resulting ethylene have been confirmed to result in increases

in xanthoxal, further supporting this hypothesis (Grossmann et al. 2001). In summary, it appears that stimulation of ethylene biosynthesis via gene upregulation and/or post-transcriptional mechanisms precede auxin-induced increases in ABA production via stimulation of downstream ABA precursor formation.

Ethylene Perception. Ethylene signaling takes place through a network of receptors and transcription factors that ultimately lead to the induction of ethylene response genes. Multiple ethylene receptors have been identified, which are redundant in function (Hua and Meyerowitz 1998). Interestingly, ethylene receptors, of which Ethylene-Response 1 and 2 (ETR1 and ETR2), ETHYLENE-RESPONSE SENSOR 1 and 2 (ERS1 and ERS2) and EIN4 have been identified, are actually negative regulators of the ethylene response; that is, receptors that actively repress the ethylene response in the absence of ethylene (Hua et al. 1998; Taiz and Zeiger 2010; Thain et al. 2004). In the absence of ethylene, the protein kinase CONSTITUTIVE TRIPLE RESPONSE1 (CTR1) is activated by ethylene receptors and CTR1 phosphorylates and inactivates the ETHYLENE-INSENSITIVE2 (EIN2) protein, repressing the ethylene response pathway (Ju et al. 2012). An active EIN2 protein is necessary for activating ethylene responses (Alonso et al. 1999). When ethylene is present and binds to receptors, the negative regulatory action of receptors is inhibited, which in turn inhibits the activity of CTR1 allowing EIN2 to localize in the nucleus and reach EIN3 (Ju et al. 2012). Once EIN2 is localized in the nucleus it stabilizes EIN3 along with EIN3-LIKE1 (EIL1) transcription factors (An et al. 2010). Finally, stabilized EIN3 (or related proteins such as EIL1) homodimers bind to the promoter region of ETHYLENE RESPONSE FACTOR 1 (ERF1), which results in activation and transcription of ethylene-inducible genes (An et al. 2010; Solano et al. 1998).

Abscisic Acid Perception. Signaling of ABA involves a complex network of receptors and secondary messengers that regulate many ABA-inducible processes. To date, several receptors to ABA have been identified, including the PYR/PYL/RCAR family, GTG, and CHLH, located in the cytosol/nucleus, plasma membrane, and plastid, respectively (Taiz and Zeiger 2010). Members of the PYR/PYL/RCAR family are able to directly bind ABA, resulting in a conformational change allowing for this receptor to interact with repressor Protein Phosphatase 2C (PP2C) (Miyazono et al. 2009; Nishimura et al. 2009; Kim et al. 2012). This interaction results in deactivation of the inhibitory action of PP2C, resulting in phosphorylation of Sucrose Non-fermenting Related Kinase2 (SnRK2) (Umezawa et al. 2009). SnRK2s activate both ABA-responsive element binding factors (ABFs) which are able to bind to ABA-responsive elements on ABA-inducible genes, promoting expression of these genes (Kagaya et al. 2002; Taiz and Zeiger 2010; reviewed in Kim et al. 2012). The status of GTG as an actual ABA receptor is controversial in accordance with conflicting evidence based on *gtg* mutant responses to ABA (Pandey et al. 2009; Jaffé et al. 2012; Taiz and Zieger 2010). Similarly, the exact mechanism of the activity of the plastid-localized CHLH is yet to be fully elucidated, although partial loss-of-function mutations have been shown to confer hyposensitive responses to ABA, providing evidence that perception of the hormone occurs within the plastid (Shen et al. 2006; Taiz and Zeiger 2010). The same sources indicated that an unknown interaction between ABA-bound CHLH may occur with PP2C in addition to potentially upregulating ABA-inducible genes.

A variety of secondary messengers are instrumental in ABA-induced responses. Heavily involved in these responses, especially with respect to stomatal closure, is the regulation of Ca^{2+} fluxes from the plasma membrane as well as vacuoles and other intracellular organelles

(McAinsh and Pittman 2009). Activation of these Ca^{2+}-influx channels is known to be at least partially carried out via ROS formed by NADPH oxidase (Romero-Puertas et al. 2004; Grossmann 2009; Dat et al. 2000; Kwak et al. 2003). Calcineurin B-like proteins are able to bind Ca^{2+}, resulting in conformational changes allowing for interaction with many different regulatory proteins (Luan et al. 2002). Regulatory activity of Ca^{2+} on kinases and phosphatases that affect protein function is also noted (Taiz and Zeiger 2010). Effects of ABA on lipid metabolism results in increased abundance/activity of many secondary messengers, including phospholipase C, an enzyme that increases concentrations of the ABA sensitivity-conferring inositol triphosphate, as well as phosphatase and kinase-binding phosphatidic acid that results from ABA-induced phospholipase D activation (Sanchez and Chua 2001; Xiong et al. 2001; Wilson et al. 2009; Zhang et al. 2005; Taiz and Zeiger 2010).

Phytochromes and Phytochrome Regulation

Phytochromes. Phytochromes are photoreceptors that are responsible primarily for perception of red to far-red light quality. Phytochromes are known to exhibit a novel photoreversibility between two separate conformations. The Pr form, which absorbs the red light abundant in sunlight (~660 nm), is converted to Pfr, which is considered the physiologically active conformation of the protein that induces gene expression and signaling (Buchanan et al. 2000; Taiz and Zeiger 2010). In the dark, the Pfr conformation absorbs far-red light (~730 nm) which is present at higher proportions in the absence of sunlight, causing the protein to assume the inactive Pr conformation. The fully-elucidated mechanism of conformational changes has not been conclusively published, although it is known that the Pr conformation is localized mainly in the cytoplasm, whereas the Pfr form is transported to the nucleus (Yamaguchi et al. 1999;

Kircher et al. 2002; Nagy and Schäfer 2002; Schäfer and Bowler 2002). This translocation is initiated via the conformational change, which allows sequences necessary for localization in the nucleus to be exposed (Montgomery and Lagarias 2002; Taiz and Zeiger 2010). Translocation of Pfr to the nucleus is consistent with the fact that Pfr is the form that induces gene expression (Yamaguchi et al. 1999; Schäfer and Bowler 2002). Active phytochrome is a protein kinase that autophosphorylates and then phosphorylates other proteins (Yeh and Lagarias 1998).

Phytochromes are typically 120 kDa in size as a monomer, although the 240 kDa homodimeric form is necessary for binding the light-sensing component, a tetrapyrrole chromophore, which is bound to the N-terminal domain of two monomers (Sakamoto and Nagatani 1996; Montgomery and Lagarias 2002). The most well-cited phytochrome that is generally regarded as most developmentally important, phytochrome B (phyB), is present at the greatest proportion in sunlight, which rapidly degrades phytochrome A (phyA) (Smith 2000; Møller et al. 2002; Nagy and Schäfer 2002). However, phyA is stable in the dark and makes up the majority of the phytochrome transcript pool in the absence of sunlight (Quail et al. 1995).

Phytochrome-Interacting Factors. Plants are able to finely modulate responses to phytochrome activity via basic helix-loop-helix transcriptional regulator proteins known as phytochrome-interacting factors (PIFs). In sunlight, PIFs are bound to the nuclear-localized Pfr conformation of phytochrome via a phytochrome binding domain (Lorrain et al. 2008). When PIFs are bound to Pfr, they are targeted to the 26S proteasome where they are degraded (Shen et al. 2005). In the absence of sunlight, PIFs accumulate in the nucleus and upregulate expression of genes involved in the shade avoidance response (Lorrain et al. 2008; reviewed in Leivar and Monte 2014). In addition to Pfr binding, DELLA proteins which are repressors of gibberellic

acid responses can also bind PIFs in the light, preventing interaction with response elements on shade-inducible genes (Sun 2008; de Lucas et al. 2008; Feng et al. 2008; Taiz and Zeiger 2010). In the dark and in the presence of gibberellic acid, the complex of a gibberellic acid receptor GID1 and an F-box protein SCF^{SLY1} ubiquitinate DELLAs and target them for degradation in the 26S proteasome, thus preventing repression of PIFs (McGinnis et al. 2003; Dill et al. 2004; reviewed in Li et al. 2016).

Phytochrome and PIF regulation of auxin-related processes. As auxinic herbicides are analogues of natural auxins such as IAA, their activity is likely subject to many of the same regulatory mechanisms conferred by phytochrome signaling. As far as regulation of auxin transport, some PIN proteins have been shown to exhibit differential regulation depending on time of day, potentially due in part to factors that interact with phytochrome (Nozue and Maloof 2006; Covington and Harmer 2007; Nozue et al. 2011; Blakeslee et al. 2004). This provides potential evidence that the activity/expression of certain auxin transporters are critical factors involved in the differences in auxinic herbicide efficacy depending on time of application. It has been demonstrated in previous research that PIF4 and/or PIF5 can function to upregulate the activity of PIN3, which may explain the increased translocation of auxinic herbicides observed with dawn applications (Nozue et al. 2011; Johnston et al. 2018).

Auxin biosynthesis is known to be regulated by phytochrome. Hersch et al. (2014) noted a potential for PIFs to mediate the ability of phytochrome to induce auxin production. This same research noted that PIF4 and PIF5 control light intensity-mediated regulation of auxin sensitivity. Phytochrome B is noted to increase the transcriptional stability of the sucrose transporter SUT4 in potato, which has been proposed to be a link between photoreceptor perception and

phytohormone biosynthesis (Chincinska et al. 2013). Additionally, there are also reported effects of phytochrome on auxin sensitivity/perception. Reed (2001) mentioned the ability of light to potentially stabilize Aux/IAA proteins, possibly through differential phosphorylation by phytochrome A, which has direct implications on auxinic herbicide perception.

Ethylene production resulting from auxinic herbicide activity is potentially mediated by phytochrome as well. Finlayson et al. (1999) illustrated that phyB function was a major mechanism necessary for the generation of diurnal ethylene rhythms in *Sorghum*. The same research illustrated that the part of the ethylene biosynthetic pathway that most closely correlated with ethylene levels in plants depended on the R:FR light ratio. Bours et al. (2013) noted that ethylene signaling by EIN2 and ACS2 act downstream of phytochrome B. The same research indicated a link between PIF3 and EIN3 activity in light. Furthermore, the production of the ACC conjugate 1-(malonylamino)-cyclopropane-1-carboxylic acid was reported to be promoted by light (Jiao et al. 1987; Vangronsveld et al. 1988).

Palmer Amaranth

Palmer amaranth (*Amaranthus palmeri* S. Watson) is an extremely troublesome warm-season annual broadleaf weed found primarily throughout the southern United States. The presence of this weed is particularly problematic in soybeans and cotton, where yield reductions have been reported to range from ~50-80% at high weed densities (Klingaman and Oliver 1994; Morgan et al. 2001; Bensch et al. 2003). Peanut (*Arachis hypogea* L.) is also among the crops most vulnerable to *A. palmeri* infestation (Ward et al. 2013). Due to its tall stature, *A. palmeri* has also been noted to interfere heavily with corn yield, with the highest yield reductions noted when weeds emerged at the same time as corn (Massinga et al. 2001; Culpepper et al 2006).

Amaranthus palmeri has several growth and reproductive characteristics that lend to its highly competitive nature with crops. In a growth comparison of several *Amaranthus* species, *A. palmeri* was noted to have the highest rate of height increase, tissue volume, dry weight, and leaf area compared to common waterhemp (*Amaranthus rudis* Sauer), redroot pigweed (*Amaranthus retroflexus* L.), and tumble pigweed (*Amaranthus albus* L.) (Horak and Loughin 2000). As with other members of the *Amaranthus* genus, *A. palmeri* is a C_4 species, which is a novel evolutionary trait for dicots (Wang et al. 1993; Ehleringer et al. 1997). Furthermore, *A. palmeri* has been noted to be able to produce well over 500,000 seeds on a single female plant, which in addition to its obligate outcrossing results in a high degree of genetic variation in small geographic areas, increasing the risk of adaptation to certain management practices thus aiding further spread (Keeley et al. 1987; Radosevich et al. 2007).

Amaranthus palmeri has been placed in the order Caryophyllales, family Amaranthaceae, and subfamily Amaranthoideae (Müller and Borsch 2005; Sage et al. 2007; Sauer 1967; Assad et al. 2017). The current distribution of heavy *A. palmeri* infestation roughly runs longitudinally from the southernmost majority of California to southern New York and Massachusetts, from where it extends to the southern edge of the entire United States except for the peninsular region of Florida (Anonymous 2009). This distribution overlaps with its native region of the southern Great Plains of North America, where it is present in a variety of cultivated areas as well as rights-of-way and natural landscapes (Anonymous 2009). *Amaranthus palmeri* has been noted to have a chromosome count of 2n = 34, similar to spiny amaranth (*Amaranthus spinosus* L.) to which it has been designated a sister taxa (Gaines et al. 2012; Grant 1959; Wassom and Tranel 2005). From this information it is suggested that the species is a distantly diverged tetraploid (Ward et al. 2013).

Amaranthus palmeri produces unbranched inflorescences that can reach up to 0.5 m in length (Assad et al. 2017; Anonymous 2009). The species has a prominent taproot which gives rise to fibrous roots, anchoring its erect stature (Anonymous 2009). The absence of hairs on all tissues, wide ovate to rhomboid leaves, petioles that are longer than the leaves, a lack of branching on seedheads, and occasional variegation in the form of a single chevron-like mark on the middle of leaves are some of the additional identifying characteristics that separate *A. palmeri* from other members of the genus (Legleiter and Johnson 2013).

An obligate outcrossing summer annual, *A. palmeri* is one of the dioecious species of the *Amaranthus* genus (Franssen et al. 2001; Assad et al. 2017). Fertilization of female flowers is most commonly carried out via wind pollination (Ward et al. 2013). The far-traveling heavy pollen load produced by males contributes to the great genetic variability observed with the species (Walkington 1960; Sosnoskie et al. 2007). Low levels of hybridization between *A. palmeri* and other common weedy *Amaranthus* spp. have been reported to fall in the range of 0.01 to 0.4% (Gaines et al. 2012).

Amaranthus palmeri produces small seeds not exceeding 2 mm that are subject to water and animal-facilitated dispersal in addition to spread via contaminated agricultural products and equipment (Legleiter and Johnston 2013; Norsworthy et al. 2009; Ward et al. 2013). The highest rate of germination occurs when seeds are no more than 1.3 cm deep in the soil and in the presence of light (Keeley et al. 1984; Jha et al. 2010). The emergence of seeds has been reported to increase with increasing temperature up until 35°C at which germination begins to decline, reaching a lack of germination at 50°C (Steckel et al. 2004; Guo and Al-Khatib 2003; Ward et al. 2013). While the viability of seeds has been reported to fall below 15% after 3 years of burial, it has been speculated that seeds deep within the seedbank may remain viable for longer periods of

time and emerge if brought closer to the soil surface where germination conditions are more favorable (Sosnoskie et al. 2011; Ward et al. 2013).

Similar to several other members of the *Amaranthus* genus, *A. palmeri* residues contain volatile allelochemicals reported to inhibit emergence of several vegetable crops (Connick et al. 1987). These chemicals include 3-pentanone as well as the other aliphatic compounds 1-hexanol, 2-heptanol, 2-heptanone, 3-methyl-1-butanol, hexanal, ethanol, acetaldehyde, 2-methyl-1-propanol, and 1-pentanol (Bradow and Connick 1988). The presence of *A. palmeri* residue in fields has been reported to result in decreased fresh weight of carrot [*Daucus carota* subsp. *sativus* (Hoffm.) Schübl. & G. Martens] and onion (*Allium cepa* L.) (Bradow and Connick 1987). The same research established that allelochemicals volatilized from soil containing *A. palmeri* residues inhibited germination of carrot and tomato (*Solanum lycopersicum* L.). The roots of grain sorghum have also been reported to be highly sensitive to residues of this weed (Menges 1988).

Palmer Amaranth Control

With the advent of resistant crops, weed control systems utilizing glyphosate were the main source of *A. palmeri* control for some time (Culpepper and York 1998; Ward et al. 2013). Since the discovery of glyphosate-resistant *A. palmeri* in Georgia in 2005, over half of the states in the United States have reported glyphosate resistance in the species, particularly in the southern region of the country (Culpepper et al. 2006; Heap 2017; Culpepper et al. 2010). The mechanism of resistance to glyphosate is conferred by a novel gene amplification mechanism, resulting in a greatly-increased number of copies of the EPSP synthase gene targeted by glyphosate in susceptible plants (Gaines et al. 2010). This results in an inability for glyphosate

to disrupt the function of this enzyme due to its overabundance, allowing its normal function to be carried out even in the presence of the herbicide at normal rates. In response to the widespread development of glyphosate resistance, applications of residual herbicides increased in addition to use of the postemergence herbicide glufosinate (Sosnoskie and Culpepper 2014). Use of glufosinate in combination with residual herbicides has been noted to provide ~80 to 90% control of glyphosate-resistant *A. palmeri* in cotton (MacRae et al. 2007). Similarly, the use of the residual herbicide fluometuron followed by three applications of glufosinate was noted to result in effective mid-season *A. palmeri* control, with the use of fluometuron granting greater flexibility in glufosinate application timing (Bond and Eubank 2011). It was also around this time that reports of increased use of tillage, hand-weeding, and cover cropping surfaced (Sosnoskie and Culpepper 2014; Montgomery et al. 2017). Sosnoskie et al. (2012) reported the use of hand-weeding reduced but did not eliminate the *A. palmeri* seedbank.

The introduction of the dicamba-resistant crop with stacked traits for glyphosate and glufosinate resistance have dawned a new era of postemergence *A. palmeri* control options (Anonymous 2015; Anonymous 2016; Johnston et al. 2018). In North Carolina, Vann et al. (2017) reported 99% *A. palmeri* control in dicamba + glufosinate + glyphosate resistant cotton when postemergence glufosinate + dicamba applications (not currently labeled) were made twice, or once in addition to glufosinate or dicamba alone, followed by layby glyphosate + diuron + *S*-metolachlor application. Similarly, ≥ 99% control of *A. palmeri* has been reported using preemergence acetochlor followed by two glufosinate + dicamba applications, or preemergence acetochlor + dicamba followed by postemergence applications of glufosinate and glufosinate + dicamba in dicamba-resistant cotton in Georgia (Cahoon et al. 2015). Additionally, 2,4-D + glyphosate-resistant crops have introduced an alternative postemergence control option

also utilizing an auxinic herbicide (Keim 2014; Barr and Zeller 2016; Chahal et al. 2017). The use of glyphosate + 2,4-D in Nebraska, a new postemergence corn and soybean control option, was noted to provide an 88 to 92% reduction in glyphosate-resistant *A. palmeri* biomass (Chahal et al. 2017). These new postemergence options can be effective when combined with cultural practices to provide ample control of *A. palmeri*. The use of a wheat and hairy vetch cover-cropping system in dicamba-resistant soybeans in Tennessee was noted to provide ≥ 98% control when used in conjunction with dicamba + glyphosate (Montgomery et al. 2017).

In addition to glyphosate resistance, *A. palmeri* has developed resistance in various parts of the United States to other herbicide mechanisms of action. *Amaranthus palmeri* resistance to acetolactate synthase (ALS) herbicides, likely conferred by base substitutions in the highly-variable sequence of *ALS*, is widespread and results in cross-resistance to other members of the same herbicide mechanism of action (Tranel et al. 2004; Ward et al. 2013; Wise et al. 2009). The spread of this trait is highly dominant (Tranel and Wright 2002). Resistance to the dinitroaniline herbicides benefin, ethalfluralin, isopropalin, pendimethalin, and trifluralin has been demonstrated, but to date no exact mechanism of resistance has been reported (Gossett et al. 1992; Heap 2017). Similar to the dinitroanilines, the resistance to atrazine reported in the southern and Great Plains of the United States, and the resistance to 4-hydroxyphenylpyruvate dioxygenase in Kansas, has no defined mechanism (Heap 2017; Ward et al. 2013; Thompson et al. 2012). Resistance to PROTOX-inhibiting herbicides in Tennessee and Arkansas have been tied to a glycine deletion at the 210 position in PPO2, however this is not believed to be the full causal mechanism behind resistance in this case (Giacomini et al. 2017).

Amaranthus palmeri is noted to be sensitive to the fungal pathogens *Phomopsis amaranthicola* (Rosskopf, Charudattan, Shabana and Benny) and *Microsphaeropsis amaranthi*

(Ell. & Barth.), with proposed use of conidial suspensions of the two pathogens for biological control (Ortiz-Ribbing and Williams 2006). Similarly, *Myrothecium verrucaria* (Alb. & Schwein.) Ditmar (1813) is reported to be an effective fungal bioherbicide with activity on both glyphosate-resistant and -susceptible biotypes (Hoagland et al. 2013). To date, no effective biological control programs have been implemented on a wide scale.

Objective

The reduced efficacy of auxinic herbicides observed with near-dawn and -dusk applications is economically problematic and has implications on resistance management. The investigation of the mechanisms conferring this phenomenon would grant important insight into which *in planta* behaviors of auxinic herbicide chemistries are undesirable when applications must be made very early or late in the day. Such information may help advise the development of new herbicides, as well as inform growers under which conditions that reductions in control are most likely to occur due to the aforementioned diurnal variation. The objectives of this research were to evaluate: (1) how transport protein activity varies with time of 2,4-D and dicamba application, (2) how 2,4-D and dicamba application time and the inhibition of translocation affect ethylene evolution, (3) whether or not expression of genes inducible by 2,4-D and dicamba are differentially affected by applications at different times of day, and (4) how different simulated environmental conditions affect the diurnal variation in 2,4-D and dicamba activity, and resulting H_2O_2 formation.

References

Abeles FB (1973) Ethylene in plant biology. New York, NY: Academic Press

Alonso JM, Hirayama T, Roman G, Nourizadeh S, Ecker JR (1999) EIN2, a bifunctional transducer of ethylene and stress responses in Arabidopsis. Science 284:2148-2152

An F, Zhao Q, Ji Y, Li W, Jiang Z, Yu X, Zhang C, Han Y, He W, Liu Y (2010) Ethylene-induced stabilization of ETHYLENE INSENSITIVE3 and EIN3-LIKE1 is mediated by proteasomal degradation of EIN3 binding F-box 1 and 2 that requires EIN2 in Arabidopsis. Plant Cell 22:2384

Anonymous (2009) Weeds of the South. Athens, GA: University of Georgia Press

Anonymous (2015) Xtendimax™ with VaporGrip™ Technology herbicide product label and brochure. Monsanto Canada Inc. Publication. Winnipeg, MB: Monsanto Canada. 35 p

Anonymous (2016) Engenia™ herbicide product label. BASF Corporation Publication. Research Triangle Park, NC: BASF. 22 p

Anonymous (2018) Xtendimax™ with VaporGrip™ Technology herbicide product label. Monsanto Company Publication. St. Louis, MO: Monsanto Company. 8 p

Arif I, Newman IA (1993) Proton efflux from oat coleoptile cells and exchange with wall calcium after IAA or fusicoccin treatment. Planta 189:377-383

Ashton F, Crafts AS (1981) Mode of action of herbicides. Toronto, Canada: John Wiley & Sons, Inc.

Assad R, Reshi ZA, Jan S, Rashid I (2017) Biology of amaranths. Bot. Rev. 83:382-436

Barr V, Zeller J (2016) Dow AgroSciences launches Enlist Cotton for the 2016 season. Dow AgroSciences. <http://www.dowagro.com/en-us/usag/news-and-

resources/newsroom/2016/january/06/dow-agrosciences-launches-enlist-cotton-for-the-2016-season>

Barry CS, Blume B, Bouzayen M, Cooper W, Hamilton AJ, Grierson D (1996) Differential expression of the 1-aminocyclopropane-1-carboxylate oxidase gene family of tomato. Plant J. 9:525-535

Begemann S (2017) EPA imposes new requirements for dicamba. Farm J., Inc. <https://www.agweb.com/article/epa-imposes-new-requirements-for-dicamba-naa-sonja-begemann/>

Behrens MR, Mutlu N, Chakraborty S, Dumitru R, Jiang WZ, LaVallee BJ, Herman PL, Clemente TE, Weeks DP (2007) Dicamba resistance: enlarging and preserving biotechnology-based weed management strategies. Science 316:1185-1188

Bensch CN, Horak MJ, Peterson D (2003) Interference of redroot pigweed (*Amaranthus retroflexus*), Palmer amaranth (*A. palmeri*), and common waterhemp (*A. rudis*) in soybean. Weed Sci. 51:37-43

Beriault JN, Horsman GP, Devine MD (1999) Phloem transport of D,L-glufosinate and acetyl-L-glufosinate in glufosinate-resistant and -susceptible *Brassica napus*. Plant Physiol. 121:619-627

Blakeslee JJ, Bandyopadhyay A, Peer WA, Makam SN, Murphy AS (2004) Relocalization of the PIN1 auxin efflux facilitator plays a role in phototropic responses. Plant Physiol. 134:28-31

Bond JA, Eubank TW (2011) Comparison of Ignite application programs in LibertyLink cotton. Proc. Southern Weed Sci. Soc. Las Cruces, NM: Southern Weed Science Society. p. 14

Bours R, van Zanten M, Pierik R, Bouwmeester H, van der Krol A (2013) Antiphase light and temperature cycles affect PHYTOCHROME B-controlled ethylene sensitivity and biosynthesis, limiting leaf movement and growth of Arabidopsis. Plant Physiol. 163:882-895

Bovey RW, Haas RH, Meyer RE (1972) Daily and seasonal response of huisache and Macartney rose to herbicides. Weed Sci. 20:577-580

Bradow JM, Connick WJ (1987) Allelochemicals from Palmer amaranth, *Amaranthus palmeri* S. Wats. J. Chem. Ecol. 13:185-202

Bradow JM, Connick WJ (1988) Seed germination inhibition by volatile alcohols and other compounds associated with *Amaranthus palmeri* residues. J. Chem. Ecol. 14:1633-1648

Braun N, Wyrzykowska J, Muller P, David K, Couch D, Perrot-Rechenmann C, Fleming AJ (2008) Conditional repression of AUXIN BINDING PROTEIN1 reveals that it coordinates cell division and cell expansion during postembryonic shoot development in Arabidopsis and tobacco. Plant Cell 20:2746-2762

Buchanan BB, Gruissem W, Jones RL (2000) Biochemistry & Molecular Biology of Plants. Rockville, MD: The American Society of Plant Biologists.

Cahoon CW, York AC, Jordan DL, Everman WJ, Seagroves RW, Culpepper AS, Eure PM (2015) Palmer amaranth (*Amaranthus palmeri*) management in dicamba-resistant cotton. Weed Technol. 29:758-770

Carrier DJ, Bakar NTA, Swarup R, Callaghan R, Napier RM, Bennett MJ, Kerr ID (2008) The binding of auxin to the Arabidopsis auxin influx transporter AUX1. Plant Physiol. 148:529-535

Chahal PS, Varanasi VK, Jugulam M, Jhala AJ (2017) Glyphosate-resistant Palmer amaranth (*Amaranthus palmeri*) in Nebraska: Confirmation, EPSPS gene amplification, and response to POST corn and soybean herbicides. Weed Technol. 31:80-93

Chang F, Born WV (1971) Dicamba uptake, translocation, metabolism, and selectivity. Weed Sci. 19:113-117

Chang F, Vanden Born W (1968) Translocation of dicamba in Canada thistle. Weed Sci. 16:176-181

Cheng WH, Endo A, Zhou L, Penney J, Chen HC, Arroyo A, Leon P, Nambara E, Asami T, Seo M, Koshiba T, Sheen J (2002) A unique short-chain dehydrogenase/reductase in Arabidopsis glucose signaling and abscisic acid biosynthesis and functions. Plant Cell 14:2723-2743

Chincinska I, Gier K, Krugel U, Liesche J, He HX, Grimm B, Harren FJM, Cristescu SM, Kuhn C (2013) Photoperiodic regulation of the sucrose transporter StSUT4 affects the expression of circadian-regulated genes and ethylene production. Front. Plant Sci. 4:26

Cobb AH, Reade JPH (2010) Herbicides and plant physiology. 2nd edn. West Sussex, United Kingdom: Wiley-Blackwell

Connick WJ, Bradow JM, Legendre MG, Vail SL, Menges RM (1987) Identification of volatile allelochemicals from *Amaranthus palmeri* S. Wats. J. Chem. Ecol. 13:463-472

Covington MF, Harmer SL (2007) The circadian clock regulates auxin signaling and responses in Arabidopsis. PLoS Biol. 5:e222

Cranston HJ, Kern AJ, Hackett JL, Miller EK, Maxwell BD, Dyer WE (2001) Dicamba resistance in kochia. Weed Sci. 49:164-170

Culpepper AS, Grey TL, Vencill WK, Kichler JM, Webster TM, Brown SM, York AC, Davis JW, Hanna WW (2006) Glyphosate-resistant Palmer amaranth (*Amaranthus palmeri*) confirmed in Georgia. Weed Sci. 54:620-626

Culpepper AS, Webster TM, Sosnoskie LM, York AC (2010) Glyphosate-resistant Palmer amaranth in the United States. *In* V. K. Nandula ed. Glyphosate Resistance in Crops and Weeds: History, Development, and Management. Hoboken, NJ: Wiley. Pp. 195-212

Culpepper AS, York AC (1998) Weed management in glyphosate-tolerant cotton. J. Cotton Sci. 2:174-185

Culpepper S (2014) Application time of day influence on Roundup, Reflex, and Clarity. Unpublished raw data

Dalazen G, Merotto A (2016) Physiological and genetic bases of the circadian clock in plants and their relationship with herbicides efficacy. Planta Daninha 34:191-198

Dat J, Vandenabeele S, Vranová E, Van Montagu M, Inzé D, Van Breusegem F (2000) Dual action of the active oxygen species during plant stress responses. Cell. Mol. Life Sci. 57:779-795

de Lucas M, Daviere JM, Rodriguez-Falcon M, Pontin M, Iglesias-Pedraz JM, Lorrain S, Fankhauser C, Blazquez MA, Titarenko E, Prat S (2008) A molecular framework for light and gibberellin control of cell elongation. Nature 451:480-U411

DeLong A, Mockaitis K, Christensen S (2002) Protein phosphorylation in the delivery of and response to auxin signals. *In* Perrot-Rechenmann C, Hagen G eds. Auxin Molecular Biology. Dordrecht, Netherlands: Springer Dordrecht Pp. 285-303

Depka B, Jahns P, Trebst A (1998) beta-carotene to zeaxanthin conversion in the rapid turnover of the D1 protein of photosystem II. FEBS Lett. 424:267-270

Dharmasiri N, Dharmasiri S, Estelle M (2005a) The F-box protein TIR1 is an auxin receptor. Nature 435:441

Dharmasiri N, Dharmasiri S, Weijers D, Lechner E, Yamada M, Hobbie L, Ehrismann JS, Jürgens G, Estelle M (2005b) Plant development is regulated by a family of auxin receptor F box proteins. Dev. Cell 9:109-119

Dill A, Thomas SG, Hu JH, Steber CM, Sun TP (2004) The Arabidopsis F-box protein SLEEPY1 targets gibberellin signaling repressors for gibberellin-induced degradation. Plant Cell 16:1392-1405

Dogbo O, Laferriere A, Dharlingue A, Camara B (1988) Carotenoid biosynthesis - isolation and characterization of a bifunctional enzyme catalyzing the synthesis of phytoene. Proc. Natl. Acad. Sci. 85:7054-7058

Egan JF, Maxwell BD, Mortensen DA, Ryan MR, Smith RG (2011) 2,4-dichlorophenoxyacetic acid (2,4-D)–resistant crops and the potential for evolution of 2,4-D–resistant weeds. Proc. Natl. Acad. Sci. 108:E37

Ehleringer JR, Cerling TE, Helliker BR (1997) C_4 photosynthesis, atmospheric CO_2, and climate. Oecologia 112:285-299

EPA (2017) Registration of dicamba for use on genetically engineered crops. United States Environmental Protection Agency. <https://www.epa.gov/ingredients-used-pesticide-products/registration-dicamba-use-genetically-engineered-crops>

Farrimond JA, Elliott MC, Clack DW (1978) Charge separation as a component of the structural requirements for hormone activity. Nature 274:401-402

Feng SH, Martinez C, Gusmaroli G, Wang Y, Zhou JL, Wang F, Chen LY, Yu L, Iglesias-Pedraz JM, Kircher S, Schafer E, Fu XD, Fan LM, Deng XW (2008) Coordinated

regulation of Arabidopsis thaliana development by light and gibberellins. Nature 451:475-U479

Figueiredo MR, Leibhart LJ, Reicher ZJ, Tranel PJ, Nissen SJ, Westra P, Bernards ML, Kruger GR, Gaines TA, Jugulam M (2017) Metabolism of 2, 4-dichlorophenoxyacetic acid contributes to resistance in a common waterhemp (*Amaranthus tuberculatus*) population. Pest Manag. Sci.:doi:10.1002/ps/4811

Finlayson SA, Lee IJ, Mullet JE, Morgan PW (1999) The mechanism of rhythmic ethylene production in sorghum. The role of phytochrome B and simulated shading. Plant Physiol. 119:1083-1089

Franssen AS, Skinner DZ, Al-Khatib K, Horak MJ, Kulakow PA (2001) Interspecific hybridization and gene flow of ALS resistance in *Amaranthus* species. Weed Sci. 49:598-606

Gaines TA, Ward SM, Bukun B, Preston C, Leach JE, Westra P (2012) Interspecific hybridization transfers a previously unknown glyphosate resistance mechanism in *Amaranthus* species. Evol. Appl. 5:29-38

Gaines TA, Zhang WL, Wang DF, Bukun B, Chisholm ST, Shaner DL, Nissen SJ, Patzoldt WL, Tranel PJ, Culpepper AS, Grey TL, Webster TM, Vencill WK, Sammons RD, Jiang JM, Preston C, Leach JE, Westra P (2010) Gene amplification confers glyphosate resistance in *Amaranthus palmeri*. Proc. Natl. Acad. Sci. 107:1029-1034

Gälweiler L, Guan C, Müller A, Wisman E, Mendgen K, Yephremov A, Palme K (1998) Regulation of polar auxin transport by AtPIN1 in Arabidopsis vascular tissue. Science 282:2226-2230

Geldner N, Friml J, Stierhof Y-D, Jürgens G, Palme K (2001) Auxin transport inhibitors block PIN1 cycling and vesicle trafficking. Nature 413:425

Giacomini DA, Umphres AM, Nie H, Mueller TC, Steckel LE, Young BG, Scott RC, Tranel PJ (2017) Two new *PPX2* mutations associated with resistance to PPO-inhibiting herbicides in *Amaranthus palmeri*. Pest Manag. Sci. 2017:10.1002/ps.4581

Gleason C, Foley RC, Singh KB (2011) Mutant analysis in Arabidopsis provides insight into the molecular mode of action of the auxinic herbicide dicamba. PLoS One 6:e17245

Goggin DE, Cawthray GR, Powles SB (2016) 2,4-D resistance in wild radish: reduced herbicide translocation via inhibition of cellular transport. J. Exp. Bot. 67:3223-3235

González-Guzmán M, Abia D, Salinas J, Serrano R, Rodríguez PL (2004) Two new alleles of the abscisic aldehyde oxidase 3 gene reveal its role in abscisic acid biosynthesis in seeds. Plant Physiol. 135:325-333

Gonzalez-Guzman M, Apostolova N, Belles JM, Barrero JM, Piqueras P, Ponce MR, Micol JL, Serrano R, Rodriguez PL (2002) The short-chain alcohol dehydrogenase ABA2 catalyzes the conversion of xanthoxin to abscisic aldehyde. Plant Cell 14:1833-1846

Gorrell RM, Bingham SW, Foy CL (1988) Translocation and fate of dicamba, picloram, and triclopyr in horsenettle, *Solanum carolinense*. Weed Sci. 36:447-452

Gossett BJ, Murdock EC, Toler JE (1992) Resistance of Palmer amaranth (*Amaranthus palmeri*) to the dinitroaniline herbicides. Weed Technol. 6:587-591

Grant WF (1959) Cytogenetic studies in *Amaranthus*. II. Natural interspecific hybridization between *A. dubius* and *A. spinosus*. Can. J. Bot. 37:1063-1070

Grossmann K (1998) Quinclorac belongs to a new class of highly selective auxin herbicides. Weed Sci. 46:707-716

Grossmann K (2000) Mode of action of auxin herbicides: a new ending to a long, drawn out story. Trends Plant Sci. 5:506-508

Grossmann K (2003) Mediation of herbicide effects by hormone interactions. J. Plant Growth Regul. 22:109-122

Grossmann K (2009) Auxin herbicides: current status of mechanism and mode of action. Pest Manag. Sci. 66:113-120

Grossmann K, Kwiatkowski J, Tresch S (2001) Auxin herbicides induce H_2O_2 overproduction and tissue damage in cleavers (*Galium aparine* L.). J. Exp. Bot. 52:1811-1816

Grossmann K, Scheltrup F, Kwiatkowski J, Caspar G (1996) Induction of abscisic acid is a common effect of auxin herbicides in susceptible plants. J. Plant Physiol. 149:475-478

Guo PG, Al-Khatib K (2003) Temperature effects on germination and growth of redroot pigweed (*Amaranthus retroflexus*), Palmer amaranth (*A. palmeri*), and common waterhemp (*A. rudis*). Weed Sci. 51:869-875

Hagen G, Guilfoyle T (2002) Auxin-responsive gene expression: genes, promoters and regulatory factors. Plant Mol. Biol. 49:373-385

Hager A (2003) Role of the plasma membrane H^+-ATPase in auxin-induced elongation growth: historical and new aspects. J. Plant Res. 116:483-505

Hansen H, Grossmann K (2000) Auxin-induced ethylene triggers abscisic acid biosynthesis and growth inhibition. Plant Physiol. 124:1437-1448

Hartzler B (2017) Dicamba: Past, present, and future. Proc. Integ. Crop Manag. Conf. 12

Heap I (2017) The international survey of herbicide resistant weeds. <http://www.weedscience.org/>

Hersch M, Lorrain S, de Wit M, Trevisan M, Ljung K, Bergmann S, Fankhauser C (2014) Light intensity modulates the regulatory network of the shade avoidance response in Arabidopsis. Proc. Natl. Acad. Sci. 111:6515-6520

Hightower M (2017) Dicamba drift: Arkansas researchers find all formulations volatile; 876 injury reports. AgFax <https://agfax.com/2017/08/10/dicamba-drift-arkansas-has-876-injury-complaints-researchers-find-all-formulations-are-volatile/>

Hoagland RE, Teaster ND, Boyette CD (2013) Bioherbicidal effects of *Myrothecium verrucaria* on glyphosate-resistant and-susceptible Palmer amaranth biotypes. Allelopathy J. 31:367-376

Hollenstein K, Dawson RJ, Locher KP (2007) Structure and mechanism of ABC transporter proteins. Curr. Opin. Str. Biol. 17:412-418

Horak MJ, Loughin TM (2000) Growth analysis of four *Amaranthus* species. Weed Sci. 48:347-355

Hua J, Meyerowitz EM (1998) Ethylene responses are negatively regulated by a receptor gene family in *Arabidopsis thaliana*. Cell 94:261-271

Hua J, Sakai H, Nourizadeh S, Chen QHG, Bleecker AB, Ecker JR, Meyerowitz EM (1998) EIN4 and ERS2 are members of the putative ethylene receptor gene family in Arabidopsis. Plant Cell 10:1321-1332

Jaffé FW, Freschet GEC, Valdes BM, Runions J, Terry MJ, Williams LE (2012) G protein-coupled receptor-type G proteins are required for light-dependent seedling growth and fertility in Arabidopsis. Plant Cell 24:3649-3668

Jasieniuk M, Morrison IN, Brûlé-Babel AL (1995) Inheritance of dicamba resistance in wild mustard (*Brassica kaber*). Weed Sci. 43:192-195

Jha P, Norsworthy JK, Riley MB, Bridges W (2010) Annual changes in temperature and light requirements for germination of Palmer amaranth (*Amaranthus palmeri*) seeds retrieved from soil. Weed Sci. 58:426-432

Jiao XZ, Yip WK, Yang SF (1987) The effect of light and phytochrome on 1-aminocyclopropane-1-carboxylic acid metabolism in etiolated wheat seedling leaves. Plant Physiol. 85:643-647

Johnston CR, Eure PM, Grey TL, Culpepper AS, Vencill WK (2018) Time of application influences translocation of auxinic herbicides in Palmer amaranth (*Amaranthus palmeri*). Weed Sci. 66:4-14

Ju CL, Yoon GM, Shemansky JM, Lin DY, Ying ZI, Chang JH, Garrett WM, Kessenbrock M, Groth G, Tucker ML, Cooper B, Kieber JJ, Chang C (2012) CTR1 phosphorylates the central regulator EIN2 to control ethylene hormone signaling from the ER membrane to the nucleus in Arabidopsis. Proc. Natl. Acad. Sci. 109:19486-19491

Kagaya Y, Hobo T, Murata M, Ban A, Hattori T (2002) Abscisic acid-induced transcription is mediated by phosphorylation of an abscisic acid response element binding factor, TRAB1. Plant Cell 14:3177-3189

Keeley PE, Carter CH, Thullen RJ (1987) Influence of planting date on growth of Palmer amaranth (*Amaranthus palmeri*). Weed Sci. 35:199-204

Keim B (2014) New generation of GM crops puts agriculture in a ‘crisis situation’. Wired: Science. <https://www.wired.com/?p=1573313>

Kelley KB, Riechers DE (2007) Recent developments in auxin biology and new opportunities for auxinic herbicide research. Pestic. Biochem. Physiol. 89:1-11

Kende H (1993) Ethylene biosynthesis. Annu. Rev. Plant Physiol. Plant Mol. Biol. 44:283-307

Kepinski S, Leyser O (2005) The Arabidopsis F-box protein TIR1 is an auxin receptor. Nature 435:446

Kim H, Hwang H, Hong JW, Lee YN, Ahn IP, Yoon IS, Yoo SD, Lee S, Lee SC, Kim BG (2012) A rice orthologue of the ABA receptor, OsPYL/RCAR5, is a positive regulator of the ABA signal transduction pathway in seed germination and early seedling growth. J. Exp. Bot. 63:1013-1024

Kircher S, Gil P, Kozma-Bognar L, Fejes E, Speth V, Husselstein-Muller T, Bauer D, Adam E, Schafer E, Nagy F (2002) Nucleocytoplasmic partitioning of the plant photoreceptors phytochrome A, B, C, D, and E is regulated differentially by light and exhibits a diurnal rhythm. Plant Cell 14:1541-1555

Klingaman TE, Oliver LR (1994) Palmer amaranth (*Amaranthus palmeri*) interference in soybeans (*Glycine max*). Weed Sci. 42:523-527

Kraft M, Kuglitsch R, Kwiatkowski J, Frank M, Grossmann K (2007) Indole-3-acetic acid and auxin herbicides up-regulate 9-cis-epoxycarotenoid dioxygenase gene expression and abscisic acid accumulation in cleavers (*Galium aparine*): interaction with ethylene. J. Exp. Bot. 58:1497-1503

Kubeš M, Yang H, Richter GL, Cheng Y, Młodzińska E, Wang X, Blakeslee JJ, Carraro N, Petrášek J, Zažímalová E (2012) The Arabidopsis concentration-dependent influx/efflux transporter ABCB4 regulates cellular auxin levels in the root epidermis. Plant J. 69:640-654

Kudsk P, Kristensen JL (1992) Effect of environmental factors on herbicide performance. Proc. First Int. Weed Control Congr., Melbourne, Australia:173-186

Kwak JM, Mori IC, Pei ZM, Leonhardt N, Torres MA, Dangl JL, Bloom RE, Bodde S, Jones JDG, Schroeder JI (2003) NADPH oxidase AtrbohD and AtrbohF genes function in ROS-dependent ABA signaling in Arabidopsis. EMBO J. 22:2623-2633

Lee SD, Oliver LR (1982) Efficacy of acifluorfen on broadleaf weeds - times and methods for application. Weed Sci. 30:520-526

Legleiter T, Johnson B (2013) Palmer amaranth biology, identification, and management. Purdue University Cooperative Extension Office WS-51

Leivar P, Monte E (2014) PIFs: Systems integrators in plant development. Plant Cell 26:56-78

Li KL, Yu RB, Fan LM, Wei N, Chen HD, Deng XW (2016) DELLA-mediated PIF degradation contributes to coordination of light and gibberellin signalling in Arabidopsis. Nat. Commun. 7

Lindgren LO, Stalberg KG, Hoglund AS (2003) Seed-specific overexpression of an endogenous Arabidopsis phytoene synthase gene results in delayed germination and increased levels of carotenoids, chlorophyll, and abscisic acid. Plant Physiol. 132:779-785

Lorrain S, Allen T, Duek PD, Whitelam GC, Fankhauser C (2008) Phytochrome-mediated inhibition of shade avoidance involves degradation of growth-promoting bHLH transcription factors. Plant J. 53:312-323

Luan S, Kudla J, Rodriguez-Concepcion M, Yalovsky S, Gruissem W (2002) Calmodulins and calcineurin B-like proteins: Calcium sensors for specific signal response coupling in plants. Plant Cell 14:S389-S400

Macdonald H (1997) Auxin perception and signal transduction. Physiol. Plantarum 100:423-430

Macháčková I, Chauvaux N, Dewitte W, van Onckelen H (1997) Diurnal fluctuations in ethylene formation in *Chenopodium rubrum*. Plant Physiol. 113:981-985

MacRae AW, Culpepper AS (2007) Managing glyphosate resistant Palmer amaranth in LibertyLink cotton. Proc. 2007 Beltwide Cotton Conf. Cordova, TN: National Cotton Council of America

Marin E, Nussaume L, Quesada A, Gonneau M, Sotta B, Hugueney P, Frey A, Marion-Poll A (1996) Molecular identification of zeaxanthin epoxidase of *Nicotiana plumbaginifolia*, a gene involved in abscisic acid biosynthesis and corresponding to the ABA locus of Arabidopsis thaliana. EMBO J. 15:2331-2342

Massinga RA, Currie RS, Horak MJ, Boyer J (2001) Interference of Palmer amaranth in corn. Weed Sci. 49:202-208

McAinsh MR, Pittman JK (2009) Shaping the calcium signature. New Phytol. 181:275-294

McCue KF, Conn EE (1990) Induction of shikimic acid pathway enzymes by light in suspension cultured-cells of parsley (*Petroselinum crispum*). Plant Physiol. 94:507-510

McGinnis KM, Thomas SG, Soule JD, Strader LC, Zale JM, Sun TP, Steber CM (2003) The Arabidopsis SLEEPY1 gene encodes a putative F-box subunit of an SCF E3 ubiquitin ligase. Plant Cell 15:1120-1130

McKeon TA, Fernández-Maculet JC, Yang SF (1995) Biosynthesis and metabolism of ethylene. *In* P. J. Davies ed. Plant Hormones: Physiology, Biochemistry and Molecular Biology. 2nd. Dordrecht, The Netherlands: Kluwer Academic Publishers. Pp. 118-139

Menges RM (1988) Allelopathic effects of Palmer amaranth (*Amaranthus palmeri*) on seedling growth. Weed Sci. 36:325-328

Miyazono K, Miyakawa T, Sawano Y, Kubota K, Kang HJ, Asano A, Miyauchi Y, Takahashi M, Zhi YH, Fujita Y, Yoshida T, Kodaira KS, Yamaguchi-Shinozaki K, Tanokura M (2009) Structural basis of abscisic acid signalling. Nature 462:609-614

Mockaitis K, Estelle M (2008) Auxin receptors and plant development: a new signaling paradigm. Ann. Rev. Cell Dev. Biol. 24:55-80

Møller SG, Ingles PJ, Whitelam GC (2002) The cell biology of phytochrome signalling. New Phytol. 154:553-590

Montgomery BL, Lagarias JC (2002) Phytochrome ancestry: sensors of bilins and light. Trends Plant Sci. 7:357-366

Montgomery GB, McClure AT, Hayes RM, Walker FR, Senseman SA, Steckel LE (2017) Dicamba-tolerant soybean combined cover crop to control Palmer amaranth. Weed Technol. 32:109-115

Morgan GD, Baumann PA, Chandler JM (2001) Competitive impact of Palmer amaranth (*Amaranthus palmeri*) on cotton (*Gossypium hirsutum*) development and yield. Weed Technol. 15:408-412

Müller K, Borsch T (2005) Phylogenetics of Amaranthaceae based on matK/trnK sequence data: Evidence from parsimony, likelihood, and Bayesian analyses. Ann. Mo. Bot. Gard. 92:66-102

Nagy F, Schäfer E (2002) Phytochromes control photomorphogenesis by differentially regulated, interacting signaling pathways in higher plants. Annu. Rev. Plant Biol. 53:329-355

Nambara E, Marion-Poll A (2005) Abscisic acid biosynthesis and catabolism. Annu. Rev. of Plant Biol. 56:165-185

Napier RM, David KM, Perrot-Rechenmann C (2002) A short history of auxin-binding proteins. *In* Perrot-Rechenmann C, Hagen G eds. Auxin Molecular Biology. The Netherlands: Kluwer Academic Publishers. Pp. 339-348

Nishimura N, Hitomi K, Arvai AS, Rambo RP, Hitomi C, Cutler SR, Schroeder JI, Getzoff ED (2009) Structural mechanism of abscisic acid binding and signaling by dimeric PYR1. Science 326:1373-1379

Norsworthy JK, Smith KL, Steckel LE, Koger CH (2009) Weed seed contamination of cotton gin trash. Weed Technol. 23:574-580

Nozue K, Harmer SL, Maloof JN (2011) Genomic analysis of circadian clock-, light-, and growth-correlated genes reveals PHYTOCHROME-INTERACTING FACTOR5 as a modulator of auxin signaling in *Arabidopsis*. Plant Physiol. 156:357-372

Nozue K, Maloof JN (2006) Diurnal regulation of plant growth. Plant Cell Environ. 29:396-408

Ortiz-Ribbing L, Williams MM (2006) Potential of *Phomopsis amaranthicola* and *Microsphaeropsis amaranthi*, as bioherbicides for several weedy *Amaranthus* species. Crop Prot. 25:39-46

Pandey S, Nelson DC, Assmann SM (2009) Two novel GPCR-type G proteins are abscisic acid receptors in Arabidopsis. Cell 136:136-148

Pazmino DM, Rodríguez-Serrano M, Romero-Puertas MC, Archilla-Ruiz A, Del Rio LA, Sandalio LM (2011) Differential response of young and adult leaves to herbicide 2, 4-dichlorophenoxyacetic acid in pea plants: role of reactive oxygen species. Plant Cell Environ. 34:1874-1889

Pech J-C, Latché A, Bouzayen M (2004) Ethylene Biosynthesis. *In* Davies PJ ed. Plant Hormones: Biosynthesis, Signal Transduction, Action. 3rd. Dordrecht, The Netherlands: Kluwer Academic Publishers. Pp. 115-136

Petruzzelli L, Coraggio I, Leubner-Metzger G (2000) Ethylene promotes ethylene biosynthesis during pea seed germination by positive feedback regulation of 1-aminocyclo-propane-1-carboxylic acid oxidase. Planta 211:144-149

Prasad R, Foy CL, Crafts AS (1967) Effects of relative humidity on absorption and translocation of foliarly applied dalapon. Weeds 15:149-156

Prigge MJ, Greenham K, Zhang Y, Santner A, Castillejo C, Mutka AM, O'Malley RC, Ecker JR, Kunkel BN, Estelle M (2016) The Arabidopsis auxin receptor F-box proteins AFB4 and AFB5 are required for response to the synthetic auxin picloram. G3-Genes Genom. Genet. 6:1383-1390

Quail PH, Boylan MT, Parks BM, Short TW, Xu Y, Wagner D (1995) Phytochromes - photosensory perception and signal-transduction. Science 268:675-680

Radosevich S, Holt J, Ghersa C (2007) Ecology of Weeds: Relationship to Agriculture and Natural Resource Management. 3rd. Hoboken, NJ: John Wiley & Sons

Reed JW (2001) Roles and activities of Aux/IAA proteins in Arabidopsis. Trends Plant Sci. 6:420-425

Romero-Puertas M, McCarthy I, Gómez M, Sandalio L, Corpas F, Del Rio L, Palma J (2004) Reactive oxygen species-mediated enzymatic systems involved in the oxidative action of 2, 4-dichlorophenoxyacetic acid. Plant Cell Environ. 27:1135-1148

Sage RF, Sage TL, Pearcy RW, Borsch T (2007) The taxonomic distribution of C_4 photosynthesis in Amaranthaceae sensu stricto. Am. J. Bot. 94:1992-2003

Sakamoto K, Nagatani A (1996) Nuclear localization activity of phytochrome B. Plant J. 10:859-868

Sanchez JP, Chua NH (2001) Arabidopsis PLC1 is required for secondary responses to abscisic acid signals. Plant Cell 13:1143-1154

Sanders GE, Pallett KE (1987) Physiological and ultrastructural changes in *Stellaria media* following treatment with fluroxypyr. Ann. Appl. Biol. 111:685-698

Sauer JD (1967) The grain amaranths and their relatives: a revised taxonomic and geographic survey. Ann. Mo. Bot. Gard. 54:103-137

Schäfer E, Bowler C (2002) Phytochrome-mediated photoperception and signal transduction in higher plants. Embo Reports 3:1042-1048

Scheltrup F, Grossmann K (1995) Abscisic-acid is a causative factor in the mode of action of the auxinic herbicide quinmerac in cleaver (*Galium aparine* L). J. Plant Physiol. 147:118-126

Schulz B, Segobye K (2016) 2,4-D transport and herbicide resistance in weeds. J. Exp. Bot. 67:3177-3179

Schwartz SH, Qin XQ, Zeevaart JAD (2003) Elucidation of the indirect pathway of abscisic acid biosynthesis by mutants, genes, and enzymes. Plant Physiol. 131:1591-1601

Sellers BA, Smeda RJ, Johnson WG (2003) Diurnal fluctuations and leaf angle reduce glufosinate efficacy. Weed Technol. 17:302-306

Sellers BA, Smeda RJ, Li JM (2004) Glutamine synthetase activity and ammonium accumulation is influenced by time of glufosinate application. Pestic. Biochem. Physiol. 78:9-20

Senseman SA (2007) Herbicide Handbook. 9th edn. Lawrence, KS: Weed Science Society of America

Sharkhuu A, Narasimhan ML, Merzaban JS, Bressan RA, Weller S, Gehring C (2014) A red and far-red light receptor mutation confers resistance to the herbicide glyphosate. Plant J. 78:916-926

Shen H, Moon J, Huq E (2005) PIF1 is regulated by light-mediated degradation through the ubiquitin-26S proteasome pathway to optimize photomorphogenesis of seedlings in Arabidopsis. Plant J. 44:1023-1035

Shen YY, Wang XF, Wu FQ, Du SY, Cao Z, Shang Y, Wang XL, Peng CC, Yu XC, Zhu SY, Fan RC, Xu YH, Zhang DP (2006) The Mg-chelatase H subunit is an abscisic acid receptor. Nature 443:823-826

Skelton JJ (2015) Uptake, translocation, and metabolism of 2,4-D in Enlist crops and control of drought-stressed waterhemp (*Amaranthus tuberculatus*) with 2,4-D and glyphosate (Doctoral dissertation). Illinois Digital Environment for Access to Learning and Scholarship. <http://hdl.handle.net/2142/88156>

Skuterud R, Bjugstad N, Tyldum A, Torresen KS (1998) Effect of herbicides applied at different times of the day. Crop Prot. 17:41-46

Smith H (2000) Phytochromes and light signal perception by plants - an emerging synthesis. Nature 407:585-591

Solano R, Stepanova A, Chao QM, Ecker JR (1998) Nuclear events in ethylene signaling: a transcriptional cascade mediated by ETHYLENE-INSENSITIVE3 and ETHYLENE-RESPONSE-FACTOR1. Gene Dev. 12:3703-3714

Song Y (2014) Insight into the mode of action of 2, 4-dichlorophenoxyacetic acid (2, 4-D) as an herbicide. J. Integr. Plant Biol. 56:106-113

Sosnoskie LM, Culpepper AS (2014) Glyphosate-resistant Palmer amaranth (*Amaranthus palmeri*) increases herbicide use, tillage, and hand-weeding in Georgia cotton. Weed Sci. 62:393-402

Sosnoskie LM, Culpepper AS, Grey TL, Webster TM (2012) Compensatory growth in Palmer amaranth: effects on weed seed production and crop yield. Proc. of the Western Soc. Weed Sci. Las Cruces, NM: Western Society of Weed Science p. 99

Sosnoskie LM, Culpepper AS, Webster TM (2011) Palmer amaranth seed mortality in response to burial depth and time. 2011 Proc. Beltwide Cotton Conf. Cordova, TN: National Cotton Council of America Pp. 1550-1552

Sosnoskie LM, Webster TM, Culpepper AS (2007) Palmer amaranth pollen viability. University of Georgia College of Agriculture and Environmental Sciences. <http://www.ugacotton.com/vault/rer/2007/p43.pdf>

Steckel LE, Sprague CL, Stoller EW, Wax LM (2004) Temperature effects on germination of nine *Amaranthus* species. Weed Sci. 52:217-221

Sterling TM (1994) Mechanisms of herbicide absorption across plant membranes and accumulation in plant cells. Weed Sci. 42:263-276

Sterling TM, Hall J (1997) Mechanism of action of natural auxins and the auxinic herbicides. Rev. Toxicol. 1:111-142

Stewart CL, Nurse RE, Sikkema PH (2009) Time of day impacts postemergence weed control in corn. Weed Technol. 23:346-355

Stopps GJ, Nurse RE, Sikkema PH (2013) The effect of time of day on the activity of postemergence soybean herbicides. Weed Technol. 27:690-695

Sun T (2008) Gibberellin metabolism, perception and signaling pathways in Arabidopsis. Arabidopsis Book 6:e0103

Swarup R, Péret B (2012) AUX/LAX family of auxin influx carriers—an overview. Front. Plant Sci. 3:225

Taiz L, Zeiger E (2010) Plant Physiology. 5th edn. Sunderland, MA: Sinauer Associates, Inc.

Thain SC, Vandenbussche F, Laarhoven LJJ, Dowson-Day MJ, Wang ZY, Tobin EM, Harren FJM, Millar AJ, Van Der Straeten D (2004) Circadian rhythms of ethylene emission in *Arabidopsis*. Plant Physiol. 136:3751-3761

Thompson CR, Peterson D, Lally NG (2012) Characterization of HPPD resistant Palmer amaranth. <http://wssaabstracts.cOm/public/9/abstract-4l3.htm>

Tranel PJ, Jiang WL, Patzoldt WL, Wright TR (2004) Intraspecific variability of the acetolactate synthase gene. Weed Sci. 52:236-241

Tranel PJ, Wright TR (2002) Resistance of weeds to ALS-inhibiting herbicides: what have we learned? Weed Sci. 50:700-712

Tsuchisaka A, Theologis A (2004) Unique and overlapping expression patterns among the arabidopsis 1-amino-cyclopropane-1-carboxylate synthase gene family members. Plant Physiol. 136:2982-3000

Umezawa T, Sugiyama N, Mizoguchi M, Hayashi S, Myouga F, Yamaguchi-Shinozaki K, Ishihama Y, Hirayama T, Shinozaki K (2009) Type 2C protein phosphatases directly regulate abscisic acid-activated protein kinases in Arabidopsis. Proc. Natl. Acad. Sci. 106:17588-17593

Vangronsveld J, Clijsters H, Vanpoucke M (1988) Phytochrome-controlled ethylene biosynthesis of intact etiolated bean seedlings. Planta 174:19-24

Vann RA, York AC, Cahoon CW, Buck TB, Askew MC, Seagroves RW (2017) Glufosinate plus dicamba for rescue Palmer amaranth control in XtendFlex™ cotton. Weed Technol. 31:666-674

Walkington DL (1960) Survey of the hay fever plants and important atmospheric allergens in the Phoenix, Arizona, metropolitan area. J. Allergy 31:25-41

Walsh TA, Neal R, Merlo AO, Honma M, Hicks GR, Wolff K, Matsumura W, Davies JP (2006) Mutations in an auxin receptor homolog AFB5 and in SGT1b confer resistance to synthetic picolinate auxins and not to 2, 4-dichlorophenoxyacetic acid or indole-3-acetic acid in Arabidopsis. Plant Physiol. 142:542-552

Wang JL, Long JJ, Hotchkiss T, Berry JO (1993) C_4 photosynthetic gene expression in light- and dark-grown amaranth cotyledons. Plant Physiol. 102:1085-1093

Ward SM, Webster TM, Steckel LE (2013) Palmer amaranth (*Amaranthus palmeri*): A review. Weed Technol. 27:12-27

Wassom JJ, Tranel PJ (2005) Amplified fragment length polymorphism-based genetic relationships among weedy *Amaranthus* species. J. Hered. 96:410-416

Weaver M, Nylund R (1963) Factors influencing the tolerance of peas to MCPA. Weeds 11:142-148

Webb SR, Hall JC (1995) Auxinic herbicide-resistant and-susceptible wild mustard (*Sinapis arvensis* L.) biotypes: effect of auxinic herbicides on seedling growth and auxin-binding activity. Pestic. Biochem. Physiol. 52:137-148

Wilson PB, Estavillo GM, Field KJ, Pornsiriwong W, Carroll AJ, Howell KA, Woo NS, Lake JA, Smith SM, Millar AH, von Caemmerer S, Pogson BJ (2009) The nucleotidase/phosphatase SAL1 is a negative regulator of drought tolerance in Arabidopsis. Plant J. 58:299-317

Wise AM, Grey TL, Prostko EP, Vencill WK, Webster TM (2009) Establishing the geographical distribution and level of acetolactate synthase resistance of Palmer amaranth (*Amaranthus palmeri*) accessions in Georgia. Weed Technol. 23:214-220

Wiśniewska J, Xu J, Seifertová D, Brewer PB, Růžička K, Blilou I, Rouquié D, Benková E, Scheres B, Friml J (2006) Polar PIN localization directs auxin flow in plants. Science 312:883-883

Woeste KE, Ye C, Kieber JJ (1999) Two Arabidopsis mutants that overproduce ethylene are affected in the posttranscriptional regulation of 1-aminocyclopropane-1-carboxylic acid synthase. Plant Physiol. 119:521-529

Xiong LM, Lee BH, Ishitani M, Lee H, Zhang CQ, Zhu JK (2001) FIERY1 encoding an inositol polyphosphate 1-phosphatase is a negative regulator of abscisic acid and stress signaling in *Arabidopsis*. Gene Dev. 15:1971-1984

Xiong LM, Zhu JK (2003) Regulation of abscisic acid biosynthesis. Plant Physiol. 133:29-36

Yamaguchi R, Nakamura M, Mochizuki N, Kay SA, Nagatani A (1999) Light-dependent translocation of a phytochrome B-GFP fusion protein to the nucleus in transgenic Arabidopsis. J. Cell Biol. 145:437-445

Yang H, Murphy AS (2009) Functional expression and characterization of Arabidopsis ABCB, AUX 1 and PIN auxin transporters in *Schizosaccharomyces pombe*. Plant J. 59:179-191

Yang SF, Hoffman NE (1984) Ethylene biosynthesis and its regulation in higher plants. Ann. Rev. Plant Physiol. 35:155-189

Yang Y, Hammes UZ, Taylor CG, Schachtman DP, Nielsen E (2006) High-affinity auxin transport by the AUX1 influx carrier protein. Curr. Biol. 16:1123-1127

Yeh KC, Lagarias JC (1998) Eukaryotic phytochromes: Light-regulated serine/threonine protein kinases with histidine kinase ancestry. Proc. Natl. Acad. Sci. 95:13976-13981

Zažímalová E, Křeček P, Skůpa P, Hoyerova K, Petrášek J (2007) Polar transport of the plant hormone auxin–the role of PIN-FORMED (PIN) proteins. Cell Mol. Life Sci. 64:1621-1637

Zažímalová E, Murphy AS, Yang H, Hoyerová K, Hošek P (2010) Auxin transporters—why so many? Cold Spring Harb. Perspect. Biol. 2:a001552

Zhang WH, Yu LJ, Zhang YY, Wang XM (2005) Phospholipase D in the signaling networks of plant response to abscisic acid and reactive oxygen species. Biochimica Et Biophysica Acta-Mol. Cell Biol. Lipids 1736:1-9

CHAPTER 2

TRANSLOCATION OF 2,4-D AND DICAMBA IN PALMER AMARANTH (*Amaranthus palmeri*) EXHIBIT DIFFERENTIAL SENSITIVITY TO AUXIN TRANSPORT INHIBITORS ACROSS APPLICATION TIMES[1]

[1]C. R. Johnston, W. K. Vencill, T. L. Grey, A. S. Culpepper, G. M. Henry, and M. A. Czarnota. To be submitted to *Plant Physiology*.

Abstract

Diurnal variation in auxinic herbicide efficacy has been reported in numerous field settings, displaying a classical trend of reduced efficacy at dawn and dusk. This has economic and resistance management implications, specifically with prolific weed species such as Palmer amaranth (*Amaranthus palmeri* S. Watson). The mechanisms conferring this phenomenon have yet to be fully elucidated, but differential translocation has been reported to play a potential role. Laboratory experiments were conducted under an LED light program designed to simulate early spring light intensity and spectral conditions. *Amaranthus palmeri* plants were treated with ^{14}C-2,4-D or ^{14}C-dicamba at two separate application times, corresponding to dawn and mid-day, along with translocation inhibitors that inhibited auxin movement via different transport proteins in order to determine if differential activity of any of these proteins at dawn and mid-day was a functional component of the time of day phenomenon. While absorption of ^{14}C-herbicides failed to display any consistent trend across transport inhibitor treatment, translocation responded to inhibitors differentially across application time within each herbicide. Dose response analysis revealed that the TI_{50} (concentration necessary for 50% inhibition of translocation) for N-1-napthylphthalamic acid (NPA) activity on ^{14}C-2,4-D movement with an 8 am application was achieved with a concentration many orders of magnitude higher than the TI_{50} at 1 pm of 1.02 µM. This observation coupled with a lack of differential sensitivity to 2,3,5-triiodobenzoic acid, a selective PIN transport inhibitor, suggests differential ATP-binding cassette subfamily B (ABCB) activity at dawn and mid-day was acted on by NPA. Consistently, the TI_{50} for verapamil, a selective ABCB transport inhibitor, was much higher with 8 am ^{14}C-dicamba applications than 1 pm applications in both studies. These findings suggest that should increased

translocation consistently present itself at dawn, it is potentially due to differential ABCB protein activity.

Introduction

Growers are frequently challenged by variation in herbicide efficacy across the time of day when an application is made. Reduced weed control resulting from this variation is not only detrimental from a financial standpoint, but also has serious implications on the development of resistance as reduced herbicide efficacy is consistently linked to selection for resistance-conferring traits (Norsworthy et al. 2012; Neve and Powles 2005; Manalil et al. 2011). Furthermore, each sequential herbicide application that is used to make up for reduced control of previous applications provides an additional selection event. Of particular concern in the southeastern United States is resistance in Palmer amaranth (*Amaranthus palmeri* S. Watson), a weed species that produces a large amount of genetic variability in offspring due to massive seed production and obligate outcrossing (Assad et al. 2017). This characteristic coupled with a high growth rate allows for accelerated evolution of herbicide resistance in the presence of overreliance on certain herbicide mechanisms of action (Horak and Loughin 2000; Heap 2014). Consistently, weeds in the *Amaranthus* genus have already evolved resistance to glyphosate, protoporphyrinogen oxidase inhibitors, acetolactate synthetase inhibitors, and herbicides of the triazine class (Culpepper et al. 2006; Shoup et al. 2003; Giacomini et al. 2017; Foes et al. 1998).

Auxinic herbicides were the first selective herbicides discovered, beginning with the advent of 2,4-D (Kreizinger and Rasmussen 1948; Peterson 1967). Dicamba has just recently received a magnitude of use not previously observed in the United States due to the advent of metabolically-resistant row crops such as cotton and soybean, as well as new formulations of dicamba aimed to reduce volatility (Johnston et al. 2018; Hartzler 2017; EPA 2017; Behrens et al. 2007). Metabolic resistance to 2,4-D has also been developed in crops utilizing low volatility formulations of the herbicide (Egan et al. 2011; Skelton 2015; Johnston et al. 2018). The

advances in herbicide-resistant crops thus warrants extensive study into application strategies that maximize efficacy. Variation in auxinic herbicide efficacy across time of application has been observed, displaying the classical trend of reduced phytotoxicity near dawn and/or dusk that has been reported with other herbicides (Culpepper 2014; Johnston et al. 2018; Stewart et al. 2009; Stopps et al. 2013). Coupled with the aforementioned growth and reproductive characteristics in *Amaranthus* spp., it can thus be conceived that it is only a matter of time until widespread selection for auxinic herbicide-resistant alleles are realized in *Amaranthus* spp. should application practices not be associated with maximized efficacy. Not surprisingly, metabolic resistance to 2,4-D has already been reported in waterhemp [*Amaranthus tuberculatus* (Moq.) J.D. Sauer] (Figueiredo et al. 2017). Thus, proper stewardship of these herbicides is highly warranted to prevent similar situations from occurring where weeds of the *Amaranthus* genus are widespread.

The causal mechanism(s) responsible for the diurnal variation in auxinic herbicide efficacy have yet to be conclusively established, but differential translocation has been observed to be at least part of the framework for this phenomenon. Increased translocation has been observed with dawn applications of 2,4-D and dicamba, and this association with reduced herbicidal activity contrasts the previously established understanding of the relationship between translocation and phytotoxicity, which classically couples reduced translocation with reduced herbicidal activity (Johnston et al. 2018; Riar et al. 2011; Goggin et al. 2016; Ge et al. 2010). The same recent research illustrates an increased rate of translocation associated with dawn applications of 2,4-D and dicamba, which may result in a decreased chance for absorbed herbicide molecules to interact with the target site (Johnston et al. 2018). This is consistent with reports that phytotoxicity inhibits sustenance of translocation; however, it is still currently

unclear whether increased auxinic herbicide translocation inhibits phytotoxic action, or conversely if reduced phytotoxic action allows for sustained translocation (Beriault et al. 1999; Hall and Devine 1993).

The framework for the translocation of auxinic herbicides is formed by the activity of auxin transport mechanisms, as structural similarities render auxinic herbicides substrates to many of the same proteins involved in both intra- and intercellular endogenous auxin movement. Some of the critical similarities between auxinic herbicides and native plant auxins are the presence of a free carboxyl group and the positioning of halogen groups (Cobb and Reade 2010). While protonated auxins can enter plant cells passively via the plasma membrane, dissociated auxins inside the cell are subject to cell-to-cell movement via auxin efflux carriers (Cobb and Reade 2010). Auxin influx into the cell, including IAA and 2,4-D occurs via the AUX1 carrier protein; however, dicamba is not a substrate for this carrier (Hoyerova et al. 2018). Identified auxin efflux carriers include proteins of the PIN family and ATP-binding cassette subfamily B (ABCB). The "short" PINs PIN5, PIN6 and PIN8 are known to mediate auxin movement between the endoplasmic reticulum and cytosol, whereas the "long" PINs PIN1-4 and PIN7 are known to function specifically as cell-to-cell efflux carriers operating at the plasma membrane (Mravec et al. 2008; Mravec et al. 2009; Petrášek et al. 2006; reviewed in Křeček et al. 2009). PIN proteins are strategically positioned in a unipolar fashion to maintain one-directional auxin movement from cell to cell (Petrášek and Friml 2009). The mechanism of PIN function has been established to be controlled by a proton gradient (Lomax et al. 1995). In contrast with PIN proteins, members of the ABCB family are mechanistically driven by ATP hydrolysis and are generally associated with the plasma membrane in a nonpolar orientation (Geisler et al. 2005; Cho and Cho 2013; reviewed in Titapiwatanakun and Murphy 2009). ABCB and PIN proteins

are known to act cooperatively in certain situations (Blakeslee et al. 2007; Yang and Murphy 2009).

To better understand what plant processes confer differential translocation across time of day, further investigation into the functional activity of the aforementioned transport proteins is warranted. Several inhibitors of auxin transport are available that inhibit different portions of the auxin transport framework. The compound N-1-naphthylphthalamic acid (NPA) is known to exhibit inhibitory activity on both PIN and ABCB protein function, potentially through competitive binding/inhibition with both proteins, although it has been noted that inhibition is stronger on PIN activity (Petrášek et al. 2006; Noh et al. 2001). The compound 2,3,5-triiodobenzoic acid (TIBA) has been shown to selectively block the trafficking of PIN proteins to the plasma membrane, resulting in a loss of unidirectional auxin flow (Dhonukshe et al. 2008; Goggin et al. 2016). In contrast, 5-[*N*-(3,4-dimethoxyphenylethyl)methylamino]-2-(3,4-dimethoxyphenyl)-2-isopropylvaleronitrile hydrochloride (verapamil), a calcium-channel blocker, interacts right at the substrate binding site of ABCB proteins resulting in selective inhibition of ABCB function (Shukla et al. 2011; Tsuruo et al. 1981; Cornwell et al. 1987; Foxwell et al. 1989; Goldberg et al. 1988). Use of these inhibitors of auxin transport at different times of auxinic herbicide application can potentially grant valuable insight into the functional differences in transport mechanisms across times of day. The objective of this study was to investigate the relationship of increasing concentrations of these auxin transport inhibitors with 2,4-D and dicamba translocation across both dawn and mid-day application times.

Materials and Methods

Separate experiments were conducted for 2,4-D and dicamba, with each herbicide experiment repeated twice. The experiments were a completely randomized design with four replications, using an herbicide-treated control and a factorial combination of one of three rates of either NPA, TIBA, or verapamil and an herbicide application at either 8 am coinciding with sunrise, or 1 pm coinciding with mid-day. Seed collected from a glyphosate-resistant *A. palmeri* population from Macon Co., GA was used for each study. Seeds were sown in a potting mix (Sun Gro Professional Growing Mix, Sun Gro Horticulture, Agawam, MA) and germinated in a growth chamber with day/night temperature of 30/20°C with light from 8 am to 12 am at 600 µmol m^{-2} s^{-1} and 50% relative humidity. Plants were allowed to grow in the growth chamber until reaching ~15 cm in height. Plants were then transplanted into 125 ml Nalgene bottles (Thermo Fisher Scientific, Waltham, MA) using deionized water as growth medium following a rinsing of roots with tap water. A 20-20-20 fertilizer was added at a rate required to deliver 1/6 the nitrogen content of a full-strength Hoagland solution (210 ppm). Plants were then acclimated to an LED light (Kind LED K5 Series, Kind LED Grow Lights, Santa Rosa, CA) program under laboratory conditions at 21°C, with LED spectrum and light intensity settings modified to be consistent with an early spring light schedule, and sunrise to sunset simulated by ramping of spectra and light intensities (Figure 1). Photosynthetic photon flux density and red/far-red light ratio was measured using a spectroradiometer (SS-110, Apogee Instruments, Logan, UT). Following a 48 h acclimation period, plants treated with translocation inhibitors had NPA, TIBA, or verapamil delivered 8 h prior to herbicide application in order to obtain a 1, 10, or 25 µM concentration of each inhibitor in respective bottles. Working stocks of inhibitors contained the inhibitor dissolved in dimethyl sulfoxide, and volumes of working stock were added to Nalgene

bottles so that the final concentration of dimethyl sulfoxide remained at 0.1% v/v across all inhibitor treatments. Following inhibitor treatment, the most recent fully expanded leaf of each plant was covered with plastic film and entire plants were broadcast with 0.28 kg a.i. ha^{-1} of the choline salt of 2,4-D for 2,4-D experiments, and 0.28 kg a.i. ha^{-1} of the diglycolamine salt of dicamba for dicamba experiments. Both herbicide spray solutions contained a nonionic surfactant at 0.25% v/v. Immediately following drying of spray droplets, plastic film was removed from the most recent fully expanded leaves which were then treated with ~1.79 kBq of the choline salt of ^{14}C-2,4-D (ring-labeled, specific activity 7.449 MBq mg^{-1}) for 2,4-D experiments, and ~1.05 kBq of the diglycolamine salt of ^{14}C-dicamba (ring-labeled, specific activity 1.658 MBq mg^{-1}) for dicamba experiments. Original concentrated stocks of radiolabeled herbicides were dissolved in acetonitrile and were then diluted with the same nonlabelled herbicide used for broadcast application to obtain the aforementioned radioactivity prior to application. Radiolabeled herbicides were applied to treated leaves in four 2.5 µl drops using a 0.5-10 µl pipettor (Research, Eppendorf, Hamburg, Germany).

Plants were removed from bottles 48 h after herbicide application and sectioned into treated leaves, stems, nontreated leaves, and roots. Treated leaves were then rinsed twice with 1 ml of a 10% aqueous methanol solution to remove unabsorbed radiolabeled herbicide. Treated leaves and stems were oxidized in a biological oxidizer (OX500, RJ Harvey Instrument Corp., Hillsdale, NJ). Radioactivity from treated leaves, stems, and leaf wash were measured using liquid scintillation spectrometry (Tri-Carb 2910 TR, PerkinElmer Inc., Waltham, MA). Percent recovery was calculated as the percentage of radioactivity applied that was obtained from treated leaves, stems, and leaf wash. Approximately 105 and 97% recovery of radioactivity was obtained from treated leaves, stems, and leaf wash for 2,4-D and dicamba experiments,

respectively, therefore roots and nontreated leaves were not included in the analysis. Percent absorption was calculated as the percentage of recovered radioactivity that was obtained from oxidized treated leaves and stems. The percentage of applied radioactivity contained in shoots was calculated as the sum of the radioactivity applied that was obtained from treated leaves and stems. Radioactivity translocated out of the treated leaf was calculated as the percentage of absorbed radioactivity that was obtained from the stem.

For absorption and percent of applied radioactivity obtained from shoots, data was subjected to the GLM procedure in JMP (JMP Pro 13, SAS Institute, Cary, NC) with means separated using pairwise t-tests at $\alpha = 0.05$. Nonlinear regression was used to determine the relationship of translocation out of the treated leaf with increasing inhibitor concentration. For nonlinear regression analyses, comparisons of this relationship were made across application times within each inhibitor treatment. Model selection and regression analyses were carried out using the 'drc' (Ritz et al. 2015) and 'qpcR' (Ritz and Spiess 2008) packages in R (R v. 3.4.4, R Foundation for Statistical Computing, Vienna, Austria). Models were selected using comparison of Akaike's information criterion corrected for small sample sizes (AICc). Models tested included a 3-parameter exponential decay function, a 4-parameter log-logistic function, a 3-parameter asymptotic regression function, and a linear function. Based on model selection, all models except for the linear model were used as indicated by AICc scores.

The exponential decay function is given by the formula:

$$y = T_{min} + (T_0 - T_{min})(exp(-x/e)) \quad [1]$$

where y is translocation out of the treated leaf, T_{min} is the lower limit, or minimum, of translocation, T_0 is y at $x = 0$, and e is the steepness of decay. The log-logistic function is given by the formula:

$$y = T_{min} + [(T_0 - T_{min})/(1 + exp(b(log(x) - log(I_{50}))))] \quad [2]$$

where y is translocation out of the treated leaf, T_{min} is the lower limit, or minimum, of translocation, T_0 is y at $x = 0$, b is the slope, and I_{50} is the inflection point or dose giving 50% response. The asymptotic regression function is given by the formula:

$$y = T_0 + (T_{max} - T_0)(1 - exp(-x/e)) \quad [3]$$

where y is translocation out of the treated leaf, T_0 is y at $x = 0$, T_{max} is upper limit of translocation, and e is the steepness of increase. For all models, the amount of translocation with no inhibitor was used as the 0 µM value for each inhibitor. Comparison of parameters across application times, within each inhibitor, was done via z-tests in accordance with Ritz et al. (2015). Inhibitor concentration giving 50% reduction in translocation (TI_{50}) was analyzed for inhibitors yielding a significant z-test for any parameter(s). Models were plotted using Sigmaplot (Sigmaplot 11, Systat Software, San Jose, CA).

Results and Discussion

Absorption and Shoot Radioactivity. For 2,4-D experiments, experiment by inhibitor interactions were detected for absorption data ($p = 0.0197$), therefore data is presented separately for each experiment (Table 1). Significant effects were only detected for one of two experiments. Experiment by inhibitor interactions were also detected for percent of radioactivity applied that was present in the shoot ($p = 0.0373$), therefore, data is presented separately for each experiment (Table 2). Similar to absorption data, significant effects were only detected for one of two experiments.

For dicamba experiments, no experiment by treatment interactions were detected for both absorption and percent of radioactivity applied that were present in the shoot, thus data is

combined over experiments. No significant effects were detected for application time, inhibitor, inhibitor by rate, or application time by inhibitor interactions for absorption data (Table 3). However, for percent of radioactivity applied that was present in the shoot, the effect of inhibitor was significant (Table 4). Significantly greater applied radioactivity was obtained from the shoot of plants receiving NPA and TIBA compared to those receiving verapamil or no inhibitor.

It is unclear as to the reason why a higher amount of applied radioactivity was recovered from shoots in the absence of consistently significant differences in absorption. Nonetheless, explanations as to why differences were observed are possible. Previous research suggests a correlation of ATPase activity with absorption of weak acid herbicides such as 2,4-D and dicamba. Metabolic inhibitors have been shown to reduce the rate of absorption of weak acid herbicides, primarily via inhibition of plasma membrane ATPase activity (Sterling 1994; Couderchet and Retzlaff 1991; Gronwald et al. 1993). Plasma membrane ATPase accumulation has been shown to increase with exposure to auxin transport inhibitors (Geldner et al. 2001). It is therefore suggested that increased dicamba absorption in plants treated with NPA and TIBA in our research is due to increased ATPase activity. The combination of diflufenzopyr, an auxin transport inhibitor, with dicamba has been reported to result in increased control of certain weed species (Wehtje 2008). As such, applying auxinic herbicides at times when transport would be low (i.e. mid-day) and in the presence of auxin transport inhibitors may prove to be a valuable strategy to growers in terms of obtaining maximal absorption in target weeds.

Translocation of 2,4-D. Experiment by rate or application time interactions were not detected for any inhibitor in 2,4-D experiments, therefore data is combined within each inhibitor. For all inhibitors, the exponential decay function was used. Steepness of decay, given by parameter *e*,

was significantly different across application times with NPA ($p < 0.0001$), therefore the null hypothesis that models were the same across application times was rejected (Table 5, Table 6, Figure 2, Figure 3). The TI_{50} for NPA was significantly lower with 2,4-D application at 1 pm at 1.02 µM, compared with 2.27×10^{10} µM for 2,4-D application at 8 am (Table 7). Relative potency of 2,4-D application at 1 pm with respect to 8 am was thus < 0.0001. No significant differences were detected for parameters across application times with TIBA or verapamil, thus resulting in a failure to reject the null hypothesis.

Increased sensitivity of 2,4-D translocation to NPA at 1 pm compared to 8 am is consistent with previous research that has suggested improved translocation of auxinic herbicides at dawn (Johnston et al. 2018). It would be assumed that if translocation is improved at dawn because a larger amount of critical NPA-sensitive transport proteins were active at this time, it would take a higher concentration of NPA to saturate this translocation complex at dawn than mid-day. *PIN3* expression is known to be upregulated by active phytochrome B (mid-day) via two genes encoding transcription factors that are members of a helix-loop-helix protein family, phytochrome-interacting factor 4 (*PIF4*) and phytochrome-interacting factor 5 (*PIF5*) (Nozue et al. 2011; Jonas 1981; Nomoto et al. 2012; Huq and Quail 2002; Khanna et al. 2004). Transcription of *PIF4* specifically is generally only present during the day, with peak transcript levels generally occurring at mid-day (Nomoto et al. 2012; Niwa et al. 2009). This fact coupled with a lack of differential activity of the PIN-specific inhibitor TIBA across application times suggests that PIN activity is not the limiting 2,4-D transport process inhibited by NPA in this research. Were that the case, it would be expected that TIBA sensitivity would be increased at 8 am when *PIF4*/*PIF5*, and consequently *PIN* expression, were at their lowest point. Covington and Harmer (2007) reported that 2,4-D transport is not dependent on PIN proteins, and thus the

findings in this research are consistent with these results. It can therefore be suggested that the critical NPA-sensitive 2,4-D transport function being inhibited in this research is the ABCB transporter complex. Long-distance transport of 2,4-D in wild radish (*Raphanus raphanistrum* L.) and *Arabidopsis* has been linked to ABCB transporters (Goggin et al. 2016; Schulz and Segobye 2016).

However, increasing the concentration of verapamil, a selective inhibitor of ABCB function, had no significantly different relationship with 2,4-D translocation across application times. As shown in Figure 3, inhibition of 2,4-D translocation did occur within the concentrations used for this study. This provides an interesting problem to the aforementioned interpretation of this paper's findings on NPA activity on 2,4-D translocation. Part of the differences in activity of NPA and verapamil in these findings may be due to the mechanism of action of both inhibitors. NPA has been demonstrated to bind directly with low affinity to not only ABCB1 and ABCB19, but also with high affinity to a regulatory protein TWD1 which is responsible for localization of several ABCB proteins to the plasma membrane, required for auxin transport functionality (Geisler et al. 2005; Nagashima et al. 2008; Rojas-Pierce et al. 2007; Bailly et al. 2008; Wu et al. 2010). In contrast, verapamil is a calcium channel blocker but also shows direct binding at the substrate site of ABCB proteins (Shukla et al. 2011; Cornwell et al. 1987). Consistent with this research, ABCB transport function has been shown to be less sensitive to verapamil than NPA (Geisler and Murphy 2005; Geisler et al. 2005; Terasaka et al. 2005). As such, this may be the reason behind reduced activity of verapamil on inhibition of 2,4-D transport compared to NPA, as well as a lack of significant differences in activity across 2,4-D application time seen with verapamil. Higher concentrations are thus potentially necessary to produce this effect with verapamil. This is inconsistent with results from Goggin et al. (2016),

where verapamil at a 10 µM concentration for root uptake demonstrated a significant degree of inhibition of 2,4-D transport in *R. raphanistrum*.

Based on the lack of sensitivity of 2,4-D transport to NPA with 8 am applications across concentrations tested, it appears that ABCB transport function may be improved at 8 am, leading to a highly-reduced sensitivity to NPA. This is however operating under the assumption that TWD1 and/or ABCB protein activity is the main difference between dawn and mid-day, according to which a highly-increased concentration of NPA would be necessary for saturation and inhibition of this complex at 8 am. Little diurnal variation in *TWD1*, *ABCB1*, *ABCB4*, and *ABCB19* expression is observed across long-day conditions similar to those used in this research, suggesting some other molecular mechanism for increased sensitivity to NPA of ABCB-mediated 2,4-D transport at dawn is at work (Winter et al. 2007). The previously reported increased 2,4-D translocation at dawn is consistent with the findings on decreased sensitivity to NPA at this time in this research (Johnston et al. 2018). It is important to note the lack of significant differences in T_{min} across application times with NPA, suggesting that despite the fact that a differential sensitivity to this inhibitor is present based on dose response analysis, sustained translocation is statistically similar across application times once NPA concentrations reach a level that presumably saturates the ABCB complex. This indicates that the NPA-sensitive translocation mechanism in this case is likely the factor involved in differential translocation across application time of 2,4-D; were this mechanism not the critical factor conferring differential translocation across application times, a significant difference in translocation at saturation of NPA would presumably be detected. Regardless, the fact that T_{min} is non-zero at these concentrations suggests another mechanism of 2,4-D movement may be at work even with inhibited ABCB-mediated active transport; this may potentially be passive

diffusion as this phenomenon has been suggested in previous literature (Carrier et al. 2008). Additionally, since TIBA did result in reductions of 2,4-D transport, some PIN-mediated 2,4-D transport is likely occurring, despite previous literature showing that 2,4-D movement is not reliant on PIN proteins (Covington and Harmer 2007). Nonetheless, it appears that differences in the magnitude of ABCB-mediated 2,4-D transport are at work across different times of day. Whether or not this is related to the differences in 2,4-D activity across both times of day requires further research, especially at the gene transcription, translational, and post-translational level.

Translocation of Dicamba. An experiment by rate interaction was detected for NPA in dicamba experiments ($p = 0.0124$), therefore comparisons of NPA models were carried out separately for each experiment. No experiment by treatment interactions were detected for TIBA or verapamil. Therefore, models for TIBA are combined over experiments; however, a model convergence failure for combined verapamil data resulted in separate model fitting for each experiment. The exponential decay function was used for both experiments for NPA models, the asymptotic regression function was used for TIBA models, and the log-logistic function was used for experiment 1 for verapamil whereas the exponential decay function was used for experiment 2. No significant parameter differences were detected across application times for NPA or TIBA, however for experiment 1 with verapamil, the I_{50} was significantly different across application times ($p < 0.0001$), and for experiment 2 with verapamil, both T_{min} and e were significantly different ($p < 0.0001$) (Table 8, Table 9, Figure 2, Figure 4). As a result, the null hypothesis was rejected for the effect of verapamil across application times in both studies. TI_{50} for verapamil, based on models for the rates used, was significantly higher at 8 am compared to 1

pm for both experiments (Table 10). In experiment 1, the TI_{50} with an 8 am application of dicamba was 3.32×10^{15} µM compared to 0.33 µM for the 1 pm application, and in experiment 2, the TI_{50} with the 8 am application was 2.75×10^{9} µM compared to 827 µM with the 1 pm application. Relative potency for 1 pm applications with respect to 8 am applications was < 0.0001 for both experiments.

Significant differences in the I_{50} and *e* parameters, and subsequently a higher TI_{50} for verapamil with dicamba application at dawn in studies 1 and 2, respectively, clearly indicate that a higher concentration of verapamil is necessary for dicamba transport to be inhibited at this time. Since verapamil is a selective ABCB transport inhibitor, it can be assumed that ABCB transport displays a differential activity on dicamba translocation across time of day. Previous work has illustrated that flavonol competition with dicamba for ABCB transport resulted in reduced dicamba translocation in kochia [*Bassia scoparia* (L.) A.J. Scott] (Pettinga et al. 2017). As such, it is well-substantiated, along with the results of this research, that dicamba is a substrate for ABCB transporters. Furthermore, the lack of differences in dicamba translocation with increasing TIBA concentrations suggests either a negligible amount or lack of PIN protein-mediated dicamba translocation. Interestingly, NPA, which as previously stated has activity on both PIN and ABCB transporters, failed to yield a significant difference in dicamba translocation across application times in both studies. This potentially may be due to the aforementioned reduced activity of NPA on ABCB activity compared PIN proteins, however it is then unclear why NPA activity would have a significantly different effect on 2,4-D movement across application times but not with dicamba. It took several orders of magnitude larger concentrations of verapamil to inhibit dicamba translocation at 8 am compared to 1 pm in both studies, suggesting an increased degree of ABCB activity at dawn compared to mid-day. This

may indeed be the critical difference across application times should differential dicamba translocation be a consistent phenomenon. As previously mentioned, since *ABCB* and *TWD1* genes display little variation in expression across time of day, a post-translational mechanism conferring differential ABCB activity may be at work. The fact that T_{min} was significantly different across application times in only one of two studies prevents any preliminary conclusions from being drawn about remaining translocation mechanisms existing at different times of day once saturating concentrations of verapamil are reached. It is unclear why translocation increased with increasing TIBA concentration. Further research is necessary to determine critical mechanisms of dicamba movement at the molecular level in general, as little literature is available on this topic (Fukui and Hayashi 2018).

Regardless of significant differences in regression parameters with verapamil across dicamba application time, concentrations indicating the TI_{50} were generally much greater than concentrations used for this study. This is somewhat consistent with findings from 2,4-D experiments, that sensitivity to verapamil was significantly reduced compared to NPA. Indeed, with dicamba experiments, notable reductions in translocation were observed with NPA well within the range of concentrations used for this study. Conversely, the fact that verapamil TI_{50} values generally fell well above the concentrations used for the study with dicamba, interpretations need to be taken in consideration of the fact that further research using increased verapamil concentrations may yield different results. Sensitivity of translocation to verapamil appears to be slightly higher with 2,4-D than with dicamba, but further research is needed to confirm this. The lack of saturable sensitivity of 2,4-D or dicamba to verapamil at concentrations up to 25 µM is inconsistent with previous research which demonstrated a significant reduction in translocation of 2,4-D out of treated leaves with 10 µM verapamil

concentrations compared to control 2,4-D application (Goggin et al. 2016). Regardless, it is consistent with the aforementioned previous research that a reduced sensitivity to verapamil compared to NPA was observed.

In summary, the diurnal variation in activity of ABCB-mediated 2,4-D and dicamba translocation appears to be at least partially responsible for any differential translocation across time of application. As this research demonstrates this suggestion at the functional level only, further molecular studies are necessary to determine mechanisms conferring this effect. While there is some evidence that ABCB protein abundance and/or functionality is differentially augmented across time of day, whether or not this occurs at the transcriptional level with *A. palmeri* (in contrast with *Arabidopsis*) or at the post-translational level remains to be elucidated. Identification of this mechanism may provide valuable information as to whether certain auxinic chemistries display a lesser degree of diurnal variation in translocation and/or activity. This knowledge would provide applicable implications for further development of auxinic herbicide-resistant crops, and ultimately further potential strategies for growers working with large acreage or in adverse environments that rely on herbicide applications to be made at different times of day.

References

Assad R, Reshi ZA, Snober J, Rashid I. (2017) Biology of Amaranths. Bot. Rev. 83:382-436

Bailly A, Sovero V, Vincenzetti V, Santelia D, Bartnik D, Koenig BW, Mancuso S, Martinoia E, Geisler M (2008) Modulation of P-glycoproteins by auxin transport inhibitors is mediated by interaction with immunophilins. J. Biol. Chem. 283:21817-21826

Behrens MR, Mutlu N, Chakraborty S, Dimitru R, Jiang WZ, LaVallee BJ, Herman PL, Clemente TE, Weeks DP (2007) Dicamba resistance: enlarging and preserving biotechnology-based weed management strategies. Science 216:1185-1188

Beriault JN, Horsman GP, Devine MD (1999) Phloem transport of D,L-glufosinate and acetyl-L-glufosinate in glufosinate-resistant and -susceptible *Brassica napus*. Plant Physiol. 121:619-627

Blakeslee JJ, Bandyopadhyay A, Lee OR, Mravec J, Titapiwatanakun B, Sauer M, Makam SN, Cheng Y, Bouchard R, Adamec J, Geisler M, Nagashima A, Sakai T, Martinoia E, Friml J, Peer WA, Murphy AS (2007) Interactions among PIN-FORMED and P-glycoprotein auxin transporters in *Arabidopsis*. The Plant Cell 19:131-147

Carrier DJ, Abu Bakar NT, Swarup R, Callaghan R, Napier RM, Bennett MJ, Kerr ID (2008) The binding of auxin to the Arabidopsis auxin influx transporter AUX1. Plant Physiol. 148:529-535

Cho M, Cho HT (2013) The function of ABCB transporters in auxin transport. Plant Signal. Behav. 8:2, e22990, doi:10.4161/psb.22990

Cobb AH, Reade JPH (2010) Herbicides and Plant Physiology. 2nd edn. West Sussex, United Kingdom: Wiley-Blackwell. Pp. 147-148

Cornwell MM, Pastan I, Gottesman MM (1987) Certain calcium channel blockers bind specifically to multidrug-resistant human KB carcinoma membrane vesicles and inhibit drug binding to P-glycoprotein. J. Biol. Chem. 262:2166-2170

Couderchet M, Retzlaff G (1991) The role of the plasma membrane ATPase in bentazone-sethoxydim antagonism. Pestic. Sci. 32:295-306

Covington MF, Harmer SL (2007) The circadian clock regulates auxin signaling and responses in Arabidopsis. PLoS Biol. 5:e222

Culpepper AS, Grey TL, Vencill WK, Kichler JM, T. M. Webster TM, Brown SM, York AC, Davis JW, Hanna WW (2006) Glyphosate-resistant Palmer amaranth (*Amaranthus palmeri*) confirmed in Georgia. Weed Sci. 54:620-626

Culpepper S (2014) Application time of day influence on Roundup, Reflex, and Clarity. Unpublished raw data

Dhonukshe P, Grigoriev I, Fischer R, Tominaga M, Robinson D, Hasek J, Paciorek T, Petrášek J, Seifertova D, Tejos R, Meisel L, Zazimalova E, Gadella T, Stierhof YD, Ueda T, Oiwa K, Akhmanova A, Brock R, Spang A, Friml J (2008) Auxin transport inhibitors impair vesicle motility and actin cytoskeleton dynamics in diverse eukaryotes. Proc. Natl. Acad. Sci. 105:4489-4494

Egan JF, Maxwell BD, Mortensen DA, Ryan MR, Smith RG (2011) 2,4-dichlorophenoxyacetic acid (2,4-D)-resistant crops and the potential for evolution of 2,4-D-resistant weeds. Proc. Natl. Acad. Sci. 108:E37

EPA (2017) Registration of dicamba for use on genetically engineered crops. United States Environmental Protection Agency. <https://www.epa.gov/ingredients-used-pesticide-products/registration-dicamba-use-genetically-engineered-crops>

Figueiredo MRA, Leibhart LJ, Reicher ZJ, Tranel PJ, Nissen SJ, Westra P, Bernards ML, Kruger GR, Gaines TA, Jugulam M (2017) Metabolism of 2,4-dichlorophenoxyacetic acid contributes to resistance in a common waterhemp (*Amaranthus tuberculatus*) population. Pest Manag. Sci. doi:10.1002/ps.4811

Foes MJ, Tranel PJ, Wax LM, Stoller EW (1998) A biotype of common waterhemp (*Amaranthus rudis*) resistant to triazine and ALS herbicides. Weed Sci. 46:514-520

Foxwell BM, Mackie A, Ling V, Ryffel B (1989) Identification of the multidrug resistance-related P-glycoprotein as a cyclosporine binding protein. Mol. Pharmacol. 36:543-546

Fukui K, Hayashi K (2018) Manipulation and sensing of auxin metabolism, transport and signaling. Plant Cell Physiol. 59:1500-1510

Ge X, d' Avignon DA, Ackerman JJH, Sammons RD (2010) Rapid vacuolar sequestration: the horseweed glyphosate resistance mechanism. Pest Manag. Sci. 66:345-348

Geisler M, Murphy AS (2005) The ABC of auxin transport: the role of P-glycoproteins in plant development. FEBS Letters 580:1094-1102

Geisler M, Blakeslee JJ, Bouchard R, Lee OR, Vincenzetti V, Bandyopadhyay A, Titapiwatanakun B, Peer WA, Bailly A, Richards EL, Ejendal KF, Smith AP, Baroux C, Grossniklaus U, Muller A, Hrycyna CA, Dudler R, Murphy AS, Martinoia E (2005) Cellular efflux of auxin catalyzed by the Arabidopsis MDR/PGP transporter AtPGP1. Plant J. 44:179-194

Geldner N, Friml J, Stierhof YD, Jürgens G, Palme K (2001) Auxin transport inhibitors block PIN1 cycling and vesicle trafficking. Nature 413:425-428

Giacomini DA, Umphres AM, Nie H, Mueller TC, Steckel LE, Young BG, Scott RC, Tranel PJ (2017) Two new *PPX2* mutations associated with resistance to PPO-inhibiting herbicides in *Amaranthus palmeri*. Pest Manag. Sci. 2017:10.1002/ps.4581

Goggin DE, Cawthray GR, Powles SB (2016) 2,4-D resistance in wild radish: reduced herbicide translocation via inhibition of cellular transport. J. Exp. Bot. 67:3223-3235

Goldberg H, Ling V, Wong PY, Skorecki K (1988) Reduced cyclosporin accumulation in multidrug-resistant cells. Biochem. Biophys. Res. Commun. 152:552-558

Gronwald JW, Jourdan SW, Wyse DL, Somers DA, Magnusson MU (1993) Effect of ammonium sulfate on absorption of imazethapyr by quackgrass (*Elytrigia repens*) and maize (*Zea mays*) cell suspension cultures. Weed Sci. 41:325-334

Hall LM, Devine MD (1993) Chlorsulfuron inhibition of phloem translocation in chlorsulfuron-resistant and susceptible *Arabidopsis thaliana*. Pestic. Biochem. Physiol. 45:81-90

Hartzler B (2017) Dicamba: Past, present, and future. Proc. Integ. Crop Manag. Conf. 12

Heap I (2014) Herbicide resistant weeds. *In* Pimentel D, Peshin R eds. Integrated Pest Management. Dordrecht, Netherlands: Springer Dordrecht. Pp. 281-301

Horak MJ, Loughin TM (2000) Growth analysis of four *Amaranthus* species. Weed Sci. 48:347-355

Hoyerova K, Hosek P, Quareshy M, Li J, Klima P, Kubes M, Yemm AA, Neve P, Tripathi A, Bennett MJ, Napier RM (2018) Auxin molecular field maps define AUX1 selectivity: many auxin herbicides are not substrates. New Phytol. 217:1625-1639

Huq E, Quail PH (2002) PIF4, a phytochrome-interacting bHLH factor, functions as a negative regulator of phytochrome B signaling in Arabidopsis. EMBO J. 21:2441-2450

Johnston CR, Eure PM, Grey TL, Culpepper AS, Vencill WK (2018) Time of application influences translocation of auxinic herbicides in Palmer amaranth (*Amaranthus palmeri*). Weed Sci. 66:4-14

Jonas H (1981) Responses of free running leaf movements to light, in particular to red and far red light during sunrise and sunset. Experientia 37:571-573

Khanna R, Huq E, Kikis EA, Al-Sady B, Lanzatella C, Quail PH (2004) A novel molecular recognition motif necessary for targeting photoactivated phytochrome signaling to specific basic helix-loop-helix transcription factors. Plant Cell 16:3033-3044

Křeček P, Skůpa P, Libus J, Naramoto S, Tejos R, Friml J, Zažímalová E (2009) The PIN-FORMED (PIN) protein family of auxin transporters. Genome Biol. 10:249

Kreizinger EJ, Rasmussen LW (1948) 2,4-D weed killer. Washington Cooperative Extension Mimeo 376

Lomax TL, Muday GK, Rubery PH (1995) Auxin transport. *In* Davies PJ ed. Plant Hormones: Physiology, Biochemistry, and Molecular Biology. 2nd edn. Norwell, MA: Kluwer Academic Publishers. Pp. 509-530

Manalil S, Busi R, Renton M, Powles SB (2011) Rapid evolution of herbicide resistance by low herbicide dosages. Weed Sci. 59:210-217

Mravec J, Kubeš M, Blelach A, Gaykova V, Petrášek J, Skůpa P, Chand S, Benková E, Zažímalová E, Friml J (2008) Interaction of PIN and PGP transport mechanisms in auxin distribution-dependent development. Development 135:3345-3354

Mravec J, Skůpa P, Bailly A, *Křeček P,* Hoyerová K, *Bielach A,* Petrášek J, Zhang J, Gaykova V, Stierhof YD, Schwarzerová K, Rol*čík J, Dobrev P, Seifertová D, Luschnig C, Benková E,* Zažímalová E, Markus G, Friml J (2009) ER-localized PIN5 auxin transporter mediates subcellular homeostasis of phytohormone auxin. Nature 439:1136-1140

Nagashima A, Uehara Y, Sakai T (2008) The ABC subfamily B auxin transporter AtABCB19 is involved in the inhibitory effects of *N*-1-naphthylphthalamic acid on the phototropic and gravitropic responses of *Arabidopsis* hypocotyls. Plant Cell Physiol. 49:1250-1255

Neve P, Powles S (2005) Recurrent selection with reduced herbicide rates results in the rapid evolution of herbicide resistance in *Lolium rigidum*. Theor. Appl. Genet. 110:1154-1166

Niwa Y, Yamashino T, Mizuno T (2009) The circadian clock regulates the photoperiodic response of hypocotyl elongation through a coincidence mechanism in *Arabidopsis thaliana*. Plant Cell Physiol. 50:838-854

Noh B, Murphy AS, Spalding EP (2001) *Multidrug resistance*-like genes of Arabidopsis required for auxin transport and auxin-mediated development. The Plant Cell 13:2441-2454

Nomoto Y, Kubozono S, Yamashino T, Nakamichi N, Mizuno T (2012) Circadian clock- and PIF4-controlled plant growth: a coincidence mechanism directly integrates a hormone signaling network into the photoperiodic control of plant architectures in *Arabidopsis thaliana*. Plant Cell Physiol. 53:1950-1964

Norsworthy JK, Ward SM, Shaw DR, Llewellyn RS, Nichols RL, Webster TM, Bradley KW, Frisvold G, Powles SB, Burgos NR, Witt WW, Barrett M (2012) Reducing the risks of herbicide resistance: best management practices and recommendations. Weed Sci. 60:31-62

Nozue K, Harmer SL, Maloof JN (2011) Genomic analysis of circadian clock-, light-, and growth-correlated genes reveals PHYTOCHROME-INTERACTING FACTOR5 as a modulator of auxin signaling in *Arabidopsis*. Plant Physiol. 156:357-372

Peterson GE (1967) The discovery and development of 2,4-D. Agr. Hist. 41:243-254

Pettinga DJ, Ou J, Patterson EL, Jugulam M, Westra P, Gaines TA (2017) Increased chalcone synthase (CHS) expression is associated with dicamba resistance in *Kochia scoparia*. Pest. Manag. Sci. doi:10.1002/ps.4778

Petrášek J, Mravec J, Bouchard R, Blakeslee JJ, Abas M, Seifertová D, Wisniewska J, Tadele Z, Kubes M, Covanová M, Dhonukshe P, Skupa P, Benková E, Perry L, Krecek P, Lee OR, Fink GR, Geisler M, Murphy AS, Luschnig C, Zazimalová E, Friml J (2006) PIN proteins perform a rate-limiting function in cellular auxin efflux. Science 312:914-918

Petrášek J, Friml J (2009) Auxin transport routes in plant development. Development 136:2675-2688

Riar DS, Burke IC, Yenish JP, Bell J, Gill K (2011) Inheritance and physiological basis for 2,4-D resistance in prickly lettuce (*Lactuca serriola* L.). J. Agric. Food Chem. 59:9417-9423

Ritz C, Spiess AN (2008) qpcR: an R package for sigmoidal model selection in quantitative real-time polymerase chain reaction analysis. Bioinformatics 24:1549-1551

Ritz C, Baty F, Streibig JC, Gerhard D (2015) Dose-response analysis using R. PLoS ONE 10:e0146021

Rojas-Pierce M, Titapiwatanakun B, Sohn EJ, Fang F, Larive CK, Blakeslee J, Cheng Y, Cuttler S, Peer WA, Murphy AS, Raikhel NV (2007) *Arabidopsis* P-glycoprotein19 participates in the inhibition of gravitropism by gravacin. Chem. Biol. 14:1366-1376

Schulz B, Segobye K (2016) 2,4-D transport and herbicide resistance in weeds. J. Exp. Bot. 67:3177-3179

Shoup DE, Al-Khatib K, Peterson DE (2003) Common waterhemp (*Amaranthus rudis*) resistance to protoporphyrinogen oxidase-inhibiting herbicides. Weed Sci. 51:145-150

Shukla S, Ohnuma S, Ambudkar SV (2011) Improving cancer chemotherapy with modulators of ABC drug transporters. Curr. Drug Targets 12:621–630

Skelton JJ (2015) Uptake, translocation, and metabolism of 2,4-D in Enlist crops and control of drought-stressed waterhemp (*Amaranthus tuberculatus*) with 2,4-D and glyphosate

(Doctoral dissertation. IL Digital Environment for Access to Learning and Scholarship. <http://hdl.handle.net/2142/88156>

Sterling TM (1994) Mechanisms of herbicide absorption across plant membranes and accumulation in plant cells. Weed Sci. 42:263-276

Stewart CL, Nurse RE, Sikkema PH (2009) Time of day impacts postemergence weed control in corn. Weed Technol. 23:346-355

Stopps GJ, Nurse RE, Sikkema PH (2013) The effect of time of day on the activity of postemergence soybean herbicides. Weed Technol. 27:690-695

Terasaka K, Blakeslee JJ, Titapiwatanakun B, Peer WA, Bandyopadhyaay A, Makam SN, Lee OR, Richards E, Murphy AS, Sato F, Yazaki K (2005) PGP4, an ATP-binding cassette p-glycoprotein, catalyzes auxin transport in *Arabidopsis thaliana* roots. Plant Cell 17:2922-2939

Titapiwatanakun B, Murphy AS (2009) Post-transcriptional regulation of auxin transport proteins: cellular trafficking, protein phosphorylation, protein maturation, ubiquitination, and membrane composition. J. Exp. Bot. 60:1093-1107

Tsuruo T, Iida H, Tsukagoshi S, Sakurai Y (1981) Overcoming of vincristine resistance in P388 leukemia in vivo and in vitro through enhanced cytotoxicity of vincristine and vinblastine by verapamil. Cancer Res. 41:1967-1972

Wehtje G (2008) Synergism of dicamba with diflufenzopyr with respect to turfgrass weed control. Weed Technol. 22:679-684

Winter D, Vinegar B, Nahal H, Ammar R, Wilson GV, Provart NJ (2007) An “electronic fluorescent pictograph” browser for exploring and analyzing large-scale biological data sets. PLoS ONE 2:e718

Wu G, Otegui MS, Spalding EP (2010) The ER-localized TWD1 immunophilin is necessary for localization of multidrug resistance-like proteins required for polar auxin transport in Arabidopsis roots. Plant Cell tpc-110

Yang H, Murphy AS (2009) Functional expression and characterization of *Arabidopsis* ABCB, AUX1, and PIN auxin transporters in *Schizosaccharomyces pombe*. The Plant J. 59:179-191

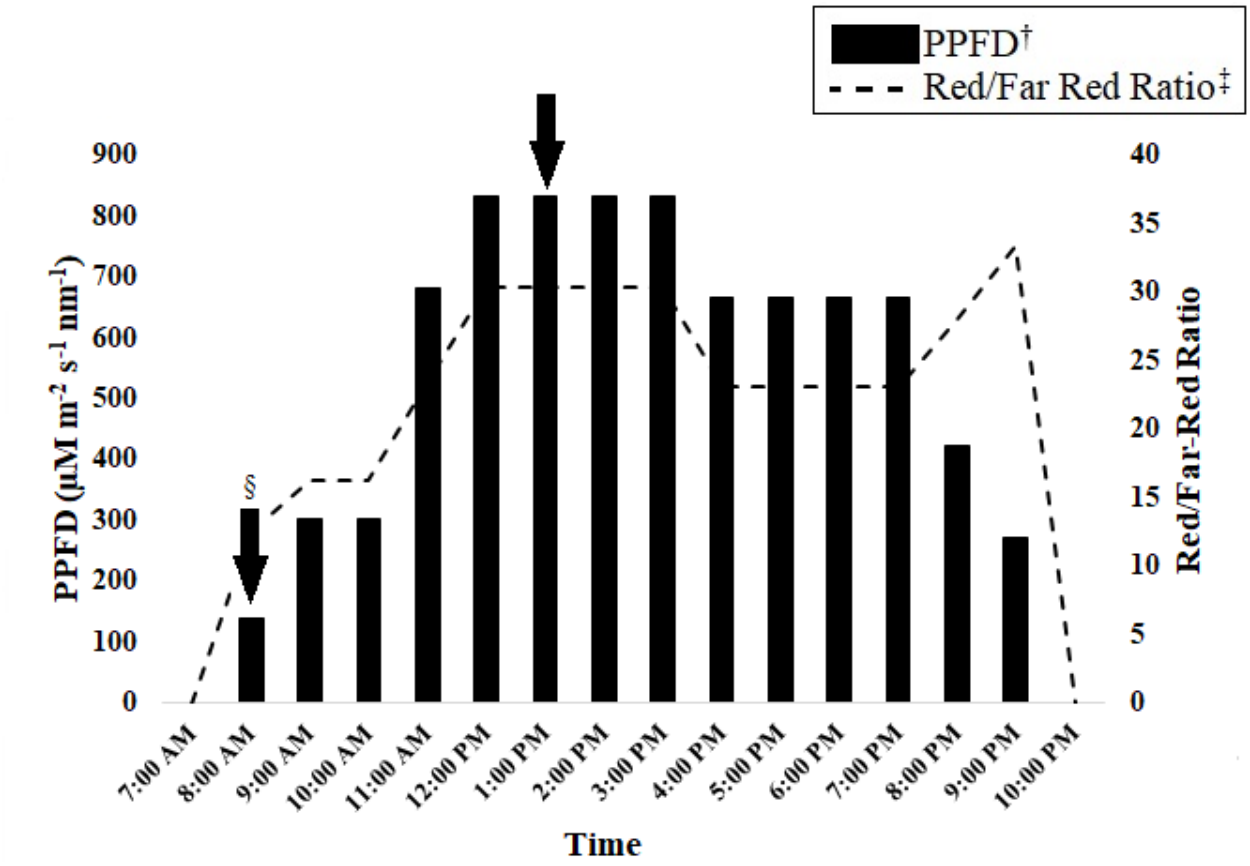

Figure 2.1. LED light program used for *A. palmeri* plants in laboratory for 2,4-D and dicamba applications, 2018.

†PPFD = Photosynthetic Photon Flux Density.

‡Red light range = 635 – 685 nm; Far-red light range = 710 – 760 nm.

§Black arrows represent both simulated dawn and mid-day application times of 2,4-D and dicamba.

2,4-D

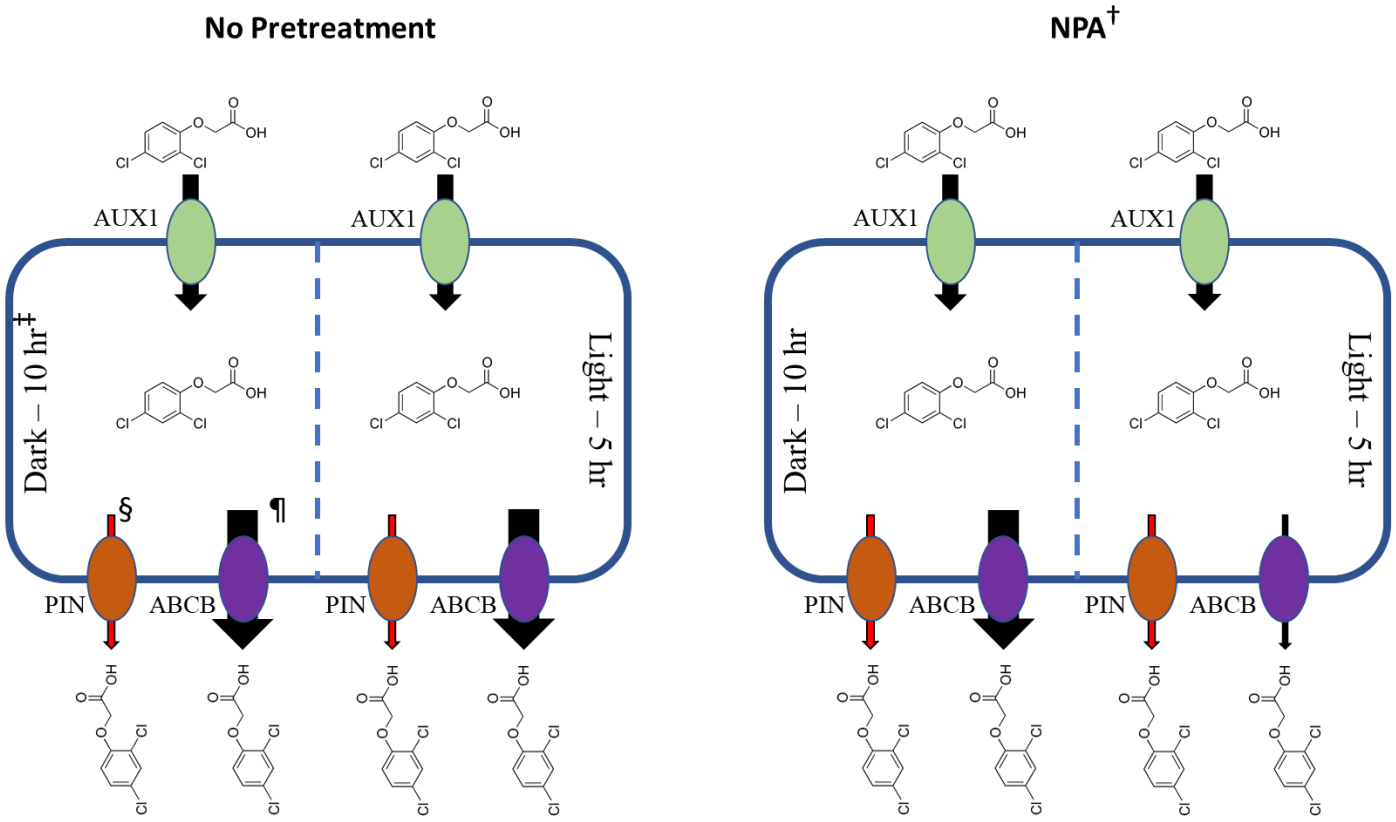
No Pretreatment
NPA†
AUX1
AUX1
AUX1
AUX1
Dark – 10 hr‡
Light – 5 hr
Dark – 10 hr
Light – 5 hr
§
¶
PIN
ABCB
PIN
ABCB
PIN
ABCB
PIN
ABCB

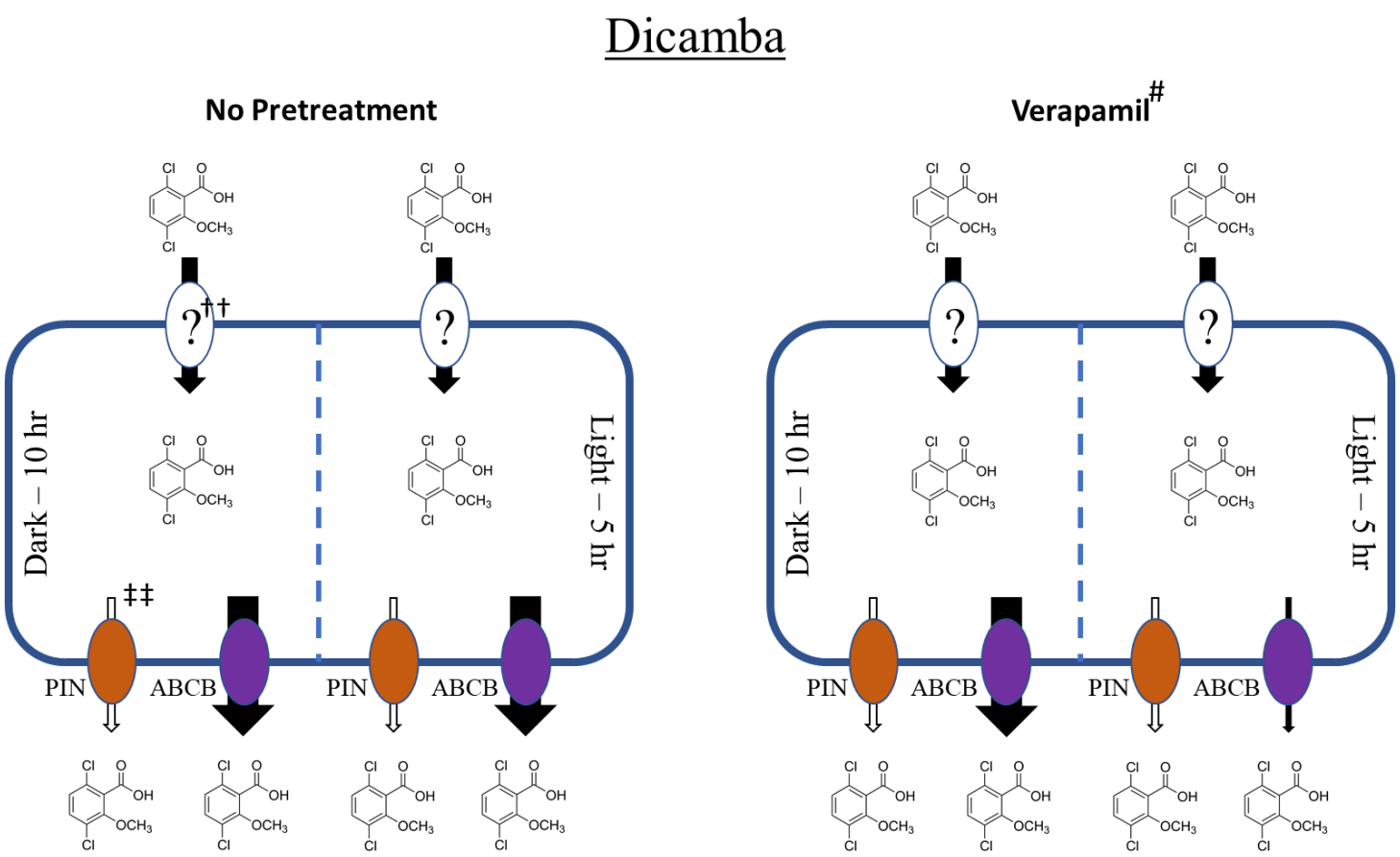

Figure 2.2. Diagrams illustrating differences in 2,4-D and dicamba efflux from plant cells across application times with no pretreatment and NPA and verapamil pretreatment, respectively, 2018.

†NPA = N-1-naphthylphthalamic acid.

‡Dark – 10 hr indicates the 8 am, simulated dawn application, as applications were made after 10 hours of darkness. Light – 5 hr indicates the 1 pm, simulated mid-day application, as applications were made after 5 hours of light.

§Red arrows indicate probable 2,4-D efflux via PIN transport proteins.

¶Size of black arrows indicate magnitude of efflux via ABCB proteins.

#Verapamil = 5-[*N*-(3,4-dimethoxyphenylethyl)methylamino]-2-(3,4-dimethoxyphenyl)-2-isopropylvaleronitrile hydrochloride.

††Question mark indicates unknown influx carrier, if any, of dicamba.

‡‡White arrows indicate unknown extent, if any, of dicamba efflux via PIN proteins.

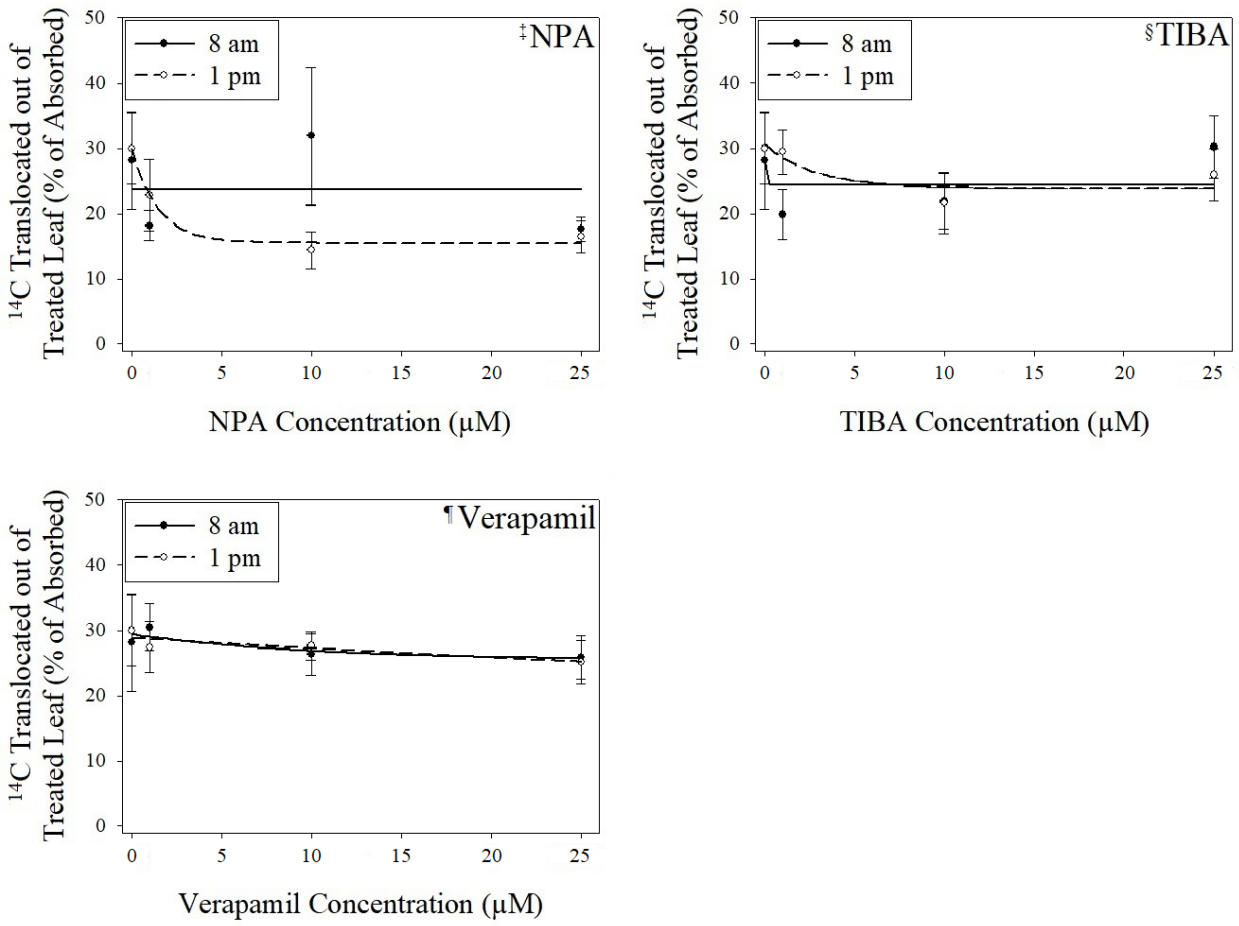

Figure 2.3. Effect of increasing translocation inhibitor concentrations on translocation of ^{14}C-2,4-D from treated leaves, 2018.

[†]Vertical bars represent standard error of the mean.

[‡]NPA = N-1-naphthylphthalamic acid.

[§]TIBA = 2,3,5-triiodobenzoic acid.

[¶]Verapamil = 5-[*N*-(3,4-dimethoxyphenylethyl)methylamino]-2-(3,4-dimethoxyphenyl)-2-isopropylvaleronitrile hydrochloride.

[#]NPA with 8 am ^{14}C-2,4-D application: Standard error of regression (SER) = 18.09; NPA with 1 pm ^{14}C-2,4-D application: SER = 11.58; TIBA with 8 am ^{14}C-2,4-D application: SER = 14.44;

TIBA with 1 pm ^{14}C-2,4-D application: SER = 11.81; Verapamil with 8 am ^{14}C-2,4-D application: SER = 12.28; Verapamil with 1 pm ^{14}C-2,4-D application: SER = 10.42.

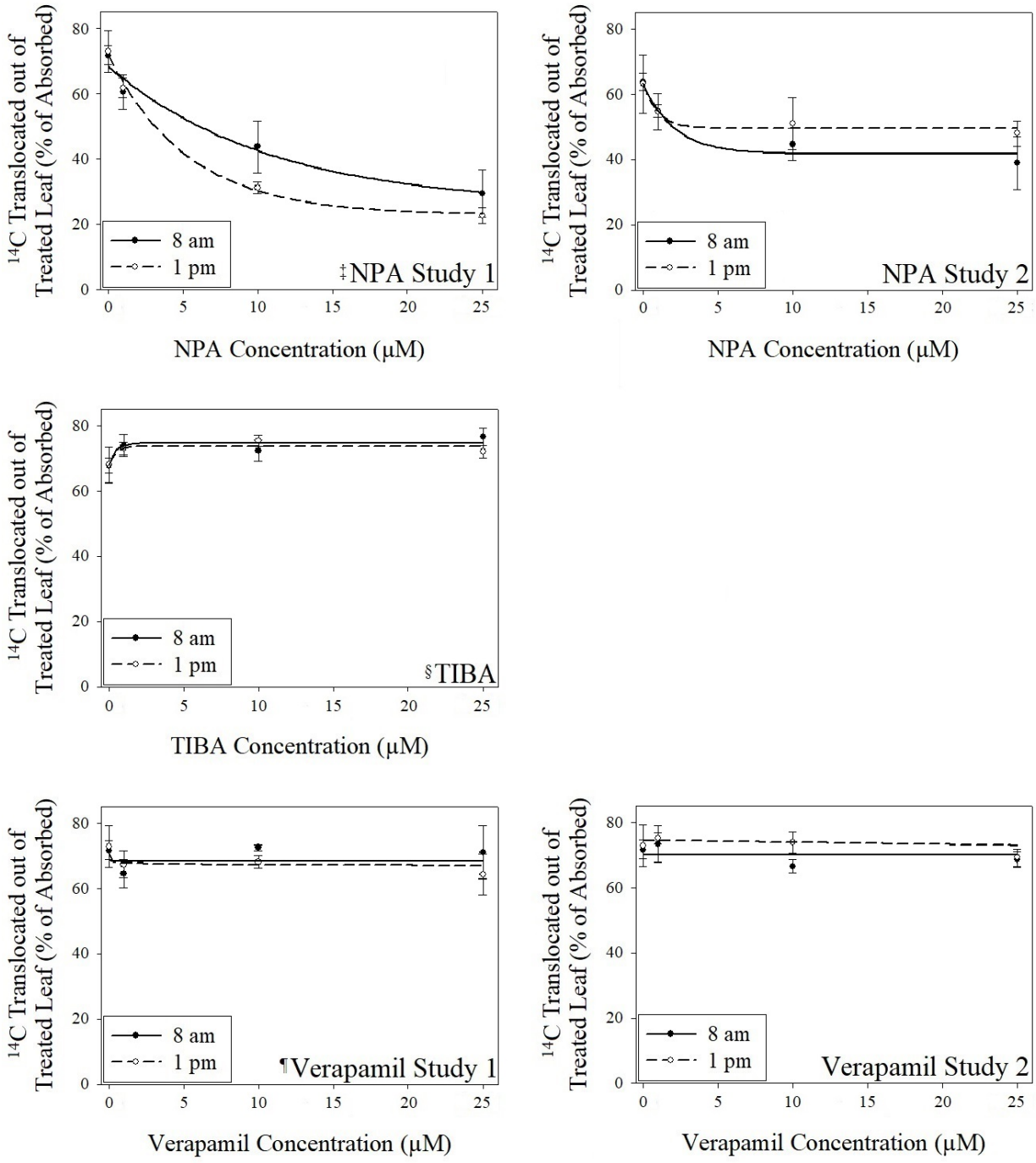

Figure 2.4. Effect of increasing translocation inhibitor concentrations on translocation of ^{14}C-dicamba from treated leaves, 2018.

[†]Vertical bars represent standard error of the mean.

[‡]NPA = N-1-naphthylphthalamic acid.

[§]TIBA = 2,3,5-triiodobenzoic acid.

[¶]Verapamil = 5-[*N*-(3,4-dimethoxyphenylethyl)methylamino]-2-(3,4-dimethoxyphenyl)-2-isopropylvaleronitrile hydrochloride.

[#]NPA with 8 am ^{14}C-dicamba application, study 1: Standard error of regression (SER) = 12.27; NPA with 1 pm ^{14}C-dicamba application, study 1: SER = 7.43; NPA with 8 am ^{14}C-dicamba application, study 2: SER = 9.91; NPA with 1 pm ^{14}C-dicamba application, study 2: SER = 13.30; TIBA with 8 am ^{14}C-dicamba application: SER = 8.20; TIBA with 1 pm ^{14}C-dicamba application: SER = 8.81; Verapamil with 8 am ^{14}C-dicamba application, study 1: SER = 13.32; Verapamil with 1 pm ^{14}C-dicamba application, study 1: SER = 10.14; Verapamil with 8 am ^{14}C-dicamba application, study 2: SER = 7.40; Verapamil with 1 pm ^{14}C-dicamba application, study 2: SER = 7.54.

Table 2.1. Absorption of ^{14}C-2,4-D in response to increasing rates of translocation inhibitors, 2018.

[†]NPA = N-1-naphthylphthalamic acid.

[‡]Parentheses represent standard error of the mean.

[§]Verapamil = 5-[*N*-(3,4-dimethoxyphenylethyl)methylamino]-2-(3,4-dimethoxyphenyl)-2-isopropylvaleronitrile hydrochloride.

[¶]TIBA = 2,3,5-triiodobenzoic acid.

Study	Inhibitor	Rate	Absorption	
			%	
1	[†]NPA	1 µM	68 [‡](3.33)	
		10 µM	77 (5.24)	
		25 µM	71 (2.69)	
	[§]Verapamil	1 µM	71 (4.44)	
		10 µM	70 (3.07)	
		25 µM	65 (1.47)	
	[¶]TIBA	1 µM	74 (1.97)	
		10 µM	71 (2.26)	
		25 µM	70 (2.06)	
	None		74 (1.77)	
		Application Time	0.4410	
		Inhibitor	0.6028	
		Application Time *Inhibitor	0.9890	
		Inhibitor*Rate	0.4804	
2	NPA	1 µM	60 (4.38)	BCD
		10 µM	57 (5.23)	BCD
		25 µM	75 (2.07)	A
	Verapamil	1 µM	64 (2.36)	ABC
		10 µM	68 (3.89)	AB

	25 µM	59 (2.98)	BCD
TIBA	1 µM	52 (4.74)	D
	10 µM	67 (5.21)	ABC
	25 µM	56 (5.76)	CD
None		53 (3.95)	D

Application Time	0.5181
Inhibitor	0.0059
Application Time*Inhibitor	0.1369
Inhibitor*Rate	0.0065

Table 2.2. Percent of applied radioactivity from ^{14}C-2,4-D application present in shoot of *A. palmeri*, 2018.

[†]Parentheses represent standard error of the mean.

[‡]NPA = N-1-naphthylphthalamic acid.

[§]Verapamil = 5-[*N*-(3,4-dimethoxyphenylethyl)methylamino]-2-(3,4-dimethoxyphenyl)-2-isopropylvaleronitrile hydrochloride.

[¶]TIBA = 2,3,5-triiodobenzoic acid.

Study	Application Time	Inhibitor	Rate	Percent Applied Radioactivity in Shoot
				%
1	8:00 AM			65 [†](2.12)
	1:00 PM			69 (1.61)
1		[‡]NPA	1 µM	71 (4.48)
			10 µM	66 (8.68)
			25 µM	69 (2.28)
		[§]Verapamil	1 µM	65 (4.56)
			10 µM	65 (2.39)
			25 µM	65 (2.37)
		[¶]TIBA	1 µM	70 (2.07)
			10 µM	72 (2.16)
			25 µM	67 (3.40)
		None		71 (4.60)
			Application Time	0.1693
			Inhibitor	0.9539

			Application Time*Inhibitor	0.7844	
			Inhibitor*Rate	0.9100	
2	8:00 AM			65 (2.27)	B
	1:00 PM			74 (2.55)	A
2		NPA	1 µM	67 (5.21)	BC
			10 µM	67 (6.55)	BC
			25 µM	87 (4.59)	A
		Verapamil	1 µM	74 (2.61)	B
			10 µM	76 (4.12)	AB
			25 µM	69 (3.28)	BC
		TIBA	1 µM	60 (6.32)	C
			10 µM	77 (6.98)	AB
			25 µM	59 (4.64)	C
		None		60 (4.31)	C
			Application Time	0.0050	
			Inhibitor	0.0009	
			Application Time*Inhibitor	0.1539	
			Inhibitor*Rate	0.0020	

Table 2.3. Absorption of ^{14}C-dicamba in response to increasing rates of translocation inhibitors, 2018.

[†]NPA = N-1-naphthylphthalamic acid.

[‡]Parentheses represent standard error of the mean.

[§]Verapamil = 5-[*N*-(3,4-dimethoxyphenylethyl)methylamino]-2-(3,4-dimethoxyphenyl)-2-isopropylvaleronitrile hydrochloride.

[¶]TIBA = 2,3,5-triiodobenzoic acid.

Inhibitor	Rate	Absorption
		%
[†]NPA	1 µM	56 [‡](3.71)
	10 µM	56 (3.49)
	25 µM	60 (3.03)
[§]Verapamil	1 µM	47 (3.29)
	10 µM	53 (4.39)
	25 µM	52 (3.09)
[¶]TIBA	1 µM	52 (3.58)
	10 µM	57 (4.46)
	25 µM	52 (3.01)
None		43 (4.51)
	Application Time	0.7334
	Inhibitor	0.2032
	Application Time*Inhibitor	0.8747
	Inhibitor*Rate	0.472

Table 2.4. Percent of applied radioactivity from ^{14}C-dicamba application present in shoot of *A. palmeri*, 2018.

[†]NPA = N-1-naphthylphthalamic acid.

[‡]Parentheses represent standard error of the mean.

[§]Verapamil = 5-[*N*-(3,4-dimethoxyphenylethyl)methylamino]-2-(3,4-dimethoxyphenyl)-2-isopropylvaleronitrile hydrochloride.

[¶]TIBA = 2,3,5-triiodobenzoic acid.

Inhibitor	Percent Applied Radioactivity in Shoot	
	%	
[†]NPA	56 [‡](1.97)	A
[§]Verapamil	47 (1.83)	B
[¶]TIBA	54 (2.30)	A
None	41 (4.06)	B
Application Time	0.2438	
Inhibitor	0.0001	
Application Time*Inhibitor	0.3501	
Inhibitor*Rate	0.2613	

Table 2.5. Equations and results of z-tests for comparing parameters between 8 am and 1 pm applications of ^{14}C-2,4-D on *A. palmeri* using different translocation inhibitors, 2018.

[†]p = p-value corresponding to z-test comparing respective parameters between 8 am and 1 pm application. Considered statistically significant at $p \leq 0.05$.

[‡]NPA = N-1-naphthylphthalamic acid.

[§]T_{min} = lower limit of translocation according to regression equation.

[¶]T_0 = translocation at $x = 0$.

[#]e = steepness of decay.

[††]TIBA = 2,3,5-triiodobenzoic acid.

[‡‡]Verapamil = 5-[*N*-(3,4-dimethoxyphenylethyl)methylamino]-2-(3,4-dimethoxyphenyl)-2-isopropylvaleronitrile hydrochloride.

Inhibitor	Equation	Parameter	[†]p
[‡]NPA	$y = T_{min} + (T_0 - T_{min})(exp(-x/e))$	[§]T_{min}	0.3505
		[¶]T_0	0.2704
		[#]e	<0.0001
[††]TIBA	$y = T_{min} + (T_0 - T_{min})(exp(-x/e))$	T_{min}	0.9244
		T_0	0.7023
		e	0.6548
[‡‡]Verapamil	$y = T_{min} + (T_0 - T_{min})(exp(-x/e))$	T_{min}	0.97
		T_0	0.8964
		e	0.9698

Table 2.6. Parameters associated with exponential decay functions used for regression of ^{14}C-2,4-D translocation in *A. palmeri* at two different application times and with different translocation inhibitors, 2018.

†NPA = N-1-naphthylphthalamic acid.

‡T_{min} = lower limit of translocation according to regression equation.

§T_0 = translocation at $x = 0$.

¶e = steepness of decay.

#TIBA = 2,3,5-triiodobenzoic acid.

††Verapamil = 5-[*N*-(3,4-dimethoxyphenylethyl)methylamino]-2-(3,4-dimethoxyphenyl)-2-isopropylvaleronitrile hydrochloride.

Inhibitor	Application Time	Parameter	Estimate
†NPA	8:00 AM	‡T_{min}	5.46
		§T_0	23.75
		¶e	3.27E+10
	1:00 PM	T_{min}	15.45
		T_0	30.03
		e	1.48
#TIBA	8:00 AM	T_{min}	24.31
		T_0	28.13
		e	0.091
	1:00 PM	T_{min}	23.86
		T_0	30.63
		e	2.81
††Verapamil	8:00 AM	T_{min}	25.40
		T_0	29.44
		e	9.70
	1:00 PM	T_{min}	15.54

	T_0	28.86
	e	77.37

Table 2.7. Dose response analysis comparing effect of increasing translocation inhibitor concentrations between two different application times of ^{14}C-2,4-D in *A. palmeri*, 2018.

[†]TI_{50} = Concentration of inhibitor required to achieve 50% inhibition of translocation.

[‡]Relative Potency = Relative index used for comparing TI_{50} across application times, corresponding to quotient of TI_{50} for 1 pm application divided by TI_{50} for 8 am application.

[§]NPA = N-1-naphthylphthalamic acid.

[¶]TIBA = 2,3,5-triiodobenzoic acid.

[#]NS = not significant. Dose response analysis was not carried out for inhibitors that failed to yield a significant ($p \leq 0.05$) difference in the z-test between application times with any parameter. Corresponds to a failure to reject the null hypothesis that curve functions were significantly different between application times.

[††]Verapamil = 5-[*N*-(3,4-dimethoxyphenylethyl)methylamino]-2-(3,4-dimethoxyphenyl)-2-isopropylvaleronitrile hydrochloride.

Inhibitor	Application Time	[†]TI_{50} (µM)	[‡]Relative Potency (1pm/8am)
[§]NPA	8:00 AM	>	
	1:00 PM	1.02	4.52E-11
[¶]TIBA	8:00 AM	[#]NS	
	1:00 PM	NS	NS
[††]Verapamil	8:00 AM	NS	
	1:00 PM	NS	NS

Table 2.8. Equations and results of z-tests for comparing parameters between 8 am and 1 pm applications of ^{14}C-dicamba on *A. palmeri* using different translocation inhibitors, 2018.

[†]p = p-value corresponding to z-test comparing respective parameters between 8 am and 1 pm application. Considered statistically significant at $p \leq 0.05$.

[‡]NPA = N-1-naphthylphthalamic acid.

[§]T_{min} = lower limit of translocation according to regression equation.

[¶]T_0 = translocation at $x = 0$.

[#]e = steepness of decay for exponential decay function, and steepness of increase for asymptotic regression function.

[††]TIBA = 2,3,5-triiodobenzoic acid.

[‡‡]T_{max} = Upper limit of translocation.

[§§]Verapamil = 5-[*N*-(3,4-dimethoxyphenylethyl)methylamino]-2-(3,4-dimethoxyphenyl)-2-isopropylvaleronitrile hydrochloride.

[¶¶]b = slope.

[##]I_{50} = inflection point, or dose giving 50% reduction in translocation.

Inhibitor	Study	Equation	Parameter	[†]p
[‡]NPA	1	$y = T_{min} + (T_0 - T_{min})(exp(-x/e))$	[§]T_{min}	0.8394
			[¶]T_0	0.5747
			[#]e	0.5249
	2	$y = T_{min} + (T_0 - T_{min})(exp(-x/e))$	T_{min}	0.2071
			T_0	0.9586
			e	0.7448
[††]TIBA	Combined	$y = T_0 + (T_{max} - T_0)(1 - exp(-x/e))$	T_0	0.9431
			[‡‡]T_{max}	0.768
			e	0.9785

§§Verapamil	1	$y = T_{min} + [(T_0 - T_{min})/ (1 + exp(b(log(x) - log(I_{50})))]$	¶¶b	0.5627
			T_{min}	0.3592
			T_0	0.4403
			##I_{50}	<0.0001
	2	$y = T_{min} + (T_0 - T_{min})(exp(-x/e))$	T_{min}	<0.0001
			T_0	0.1025
			e	<0.0001

Table 2.9. Parameters associated with exponential decay, asymptotic regression, or log-logistic functions used for regression of ^{14}C-dicamba translocation in *A. palmeri* at two different application times and with different translocation inhibitors, 2018.

[†]NPA = N-1-naphthylphthalamic acid.

[‡]T_{min} = lower limit of translocation according to regression equation.

[§]T_0 = translocation at $x = 0$.

[¶]e = steepness of decay for exponential decay function, and steepness of increase for asymptotic regression function.

[#]TIBA = 2,3,5-triiodobenzoic acid.

[††]T_{max} = Upper limit of translocation.

[‡‡]Verapamil = 5-[*N*-(3,4-dimethoxyphenylethyl)methylamino]-2-(3,4-dimethoxyphenyl)-2-isopropylvaleronitrile hydrochloride.

[§§]b = slope.

[¶¶]I_{50} = inflection point, or dose giving 50% reduction in translocation.

Inhibitor	Study	Application Time	Parameter	Estimate
[†]NPA	1	8:00 AM	[‡]T_{min}	25.41
			[§]T_0	68.35
			[¶]e	10.87
		1:00 PM	T_{min}	22.62
			T_0	71.75
			e	5.34
	2	8:00 AM	T_{min}	41.66
			T_0	63.61
			e	2.10
		1:00 PM	T_{min}	49.53

			T_0	63.16
			e	1.02
[#]TIBA	Combined	8:00 AM	T_0	67.75
			[††]T_{max}	74.62
			e	0.42
		1:00 PM	T_0	68.06
			T_{max}	73.71
			e	0.46
[‡‡]Verapamil	1	8:00 AM	[§§]b	0.0076
			T_{min}	47.42
			T_0	86.93
			[¶¶]I_{50}	3.32E+15
		1:00 PM	b	0.13
			T_{min}	59.78
			T_0	76.50
			I_{50}	0.33
	2	8:00 AM	T_{min}	56.74
			T_0	70.086
			e	3.96E9
		1:00 PM	T_{min}	-0.015
			T_0	74.52
			e	1193.10

Table 2.10. Dose response analysis comparing effect of increasing translocation inhibitor concentrations between two different application times of ^{14}C-2,4-D in *A. palmeri*, 2018.

[†]TI_{50} = Concentration of inhibitor required to achieve 50% inhibition of translocation.

[‡]Relative Potency = Relative index used for comparing TI_{50} across application times, corresponding to quotient of TI_{50} for 1 pm application divided by TI_{50} for 8 am application.

[§]NPA = N-1-naphthylphthalamic acid.

[¶]NS = not significant. Dose response analysis was not carried out for inhibitors that failed to yield a significant ($p \leq 0.05$) difference in the z-test between application times with any parameter. Corresponds to a failure to reject the null hypothesis that curve functions were significantly different between application times.

[#]TIBA = 2,3,5-triiodobenzoic acid.

[††]Verapamil = 5-[*N*-(3,4-dimethoxyphenylethyl)methylamino]-2-(3,4-dimethoxyphenyl)-2-isopropylvaleronitrile hydrochloride.

Inhibitor	Study	Application Time	[†]TI_{50} (µM)	[‡]Relative Potency (1pm/8am)
[§]NPA	1	8:00 AM	[¶]NS	
		1:00 PM	NS	NS
	2	8:00 AM	NS	
		1:00 PM	NS	NS
[#]TIBA	Combined	8:00 AM	NS	
		1:00 PM	NS	NS
[††]Verapamil	1	8:00 AM	>	
		1:00 PM	0.33	9.82E-17

2	8:00 AM	>		
	1:00 PM	827	3.01E-07	

CHAPTER 3

TIME OF APPLICATION AND TRANSLOCATION INHIBITION INFLUENCE 2,4-D AND DICAMBA-INDUCED ETHYLENE PRODUCTION IN PALMER AMARANTH[1]

[1]C. R. Johnston, A. Malladi, T. M. Randell, W. K. Vencill, T. L. Grey, A. S. Culpepper, G. M. Henry, and M. A. Czarnota. To be submitted to *Plant Physiology*.

Abstract

The efficacy of auxinic herbicide applications has been reported to vary across time of day. Mechanisms potentially involved in this phenomenon include translocation and phytochrome signaling, likely mediated by the variation in the red to far-red light ratio and light intensity seen across different times of day. Laboratory experiments were conducted under an early-spring simulated LED light program to determine the role of translocation and time of application on the production of ethylene resulting from 2,4-D and dicamba applications. Analysis of covariance on log-transformed ethylene production resulted in a lack of significant differences between 8 am and 1 pm application times of 2,4-D, ranging from 2.36 to 2.37 µL kg FW^{-1} h^{-1}. However, inhibition of translocation via pre-treatment of the 8 am application with 2,3,5-triiodobenzoic acid resulted in significantly increased ethylene production of 2.69 µL kg FW^{-1} h^{-1} in comparison with 8 am and 1 pm treatments alone. For dicamba studies, a significant difference in ethylene production from the 8 am application and 1 pm application was detected, yielding 2.75 and 3.07 µL kg FW^{-1} h^{-1}, respectively. Inhibition of translocation of the 8 am dicamba application via N-1-naphthylphthalamic acid pre-treatment resulted in a near-identical ethylene production to that observed with the 1 pm application, indicating a removal of the time of day effect via translocation inhibition. Together, these results suggest that for dicamba, ethylene production is altered across times of application and that translocation inhibition reverses part of the reduced herbicide activity associated with dawn applications. Consistently, inhibition of 2,4-D translocation, albeit likely by a different mechanism, also resulted in increased ethylene production.

Introduction

The efficacy of auxinic herbicides has been reported to be significantly influenced by the time of day in which an application is made. This phenomenon has been attributed to not only species-specific mechanisms, but also to physiological mechanisms potentially ranging over many weeds, resulting in reduced control with near-dawn and -dusk applications (Johnston et al. 2018; Stewart et al. 2009; Culpepper 2014). This presents a challenge for growers that must apply these herbicides at various times of day due to farm size, inclement weather, or other time constraints. Applications made too late or too early may cause reduced weed control resulting in the need for sequential applications, which incurs extra production costs. Furthermore, previous research has linked reduced herbicide efficacy to selection for resistance-conferring traits (Norsworthy et al. 2012; Neve and Powles 2005; Manalil et al. 2011). This risk is particularly daunting with weeds of the genus *Amaranthus*, as resistance has rapidly developed to several widely-used herbicide mechanisms of action (Culpepper et al. 2006; Giacomini et al. 2017; Shoup et al. 2003; Foes et al. 1998). This accelerated rate of resistance development is attributable to overreliance on certain mechanisms of action, obligate outcrossing of the species, and prolific seed production and high growth rates, which imparts a high level of genetic variability amongst offspring in a relatively short period of time (Horak and Loughin 2000; Heap 2014; Assad et al. 2017). Widespread use of auxinic herbicides has been on the rise due to the advent of resistant crops, which allows for postemergence use of 2,4-D and dicamba throughout the growing season (Bauerle et al. 2015; Johnston et al. 2018). The use of these herbicides presents an alternative mechanism of action that is especially valuable for glyphosate- and ALS-resistant *Amaranthus* spp. control; however, 2,4-D resistance has already been reported in waterhemp [*Amaranthus tuberculatus* (Moq.) J.D. Sauer] and sustained use will theoretically

cause further resistance (Figueiredo et al. 2017). Therefore, it is of great importance to maximize herbicide efficacy in all agricultural systems, and proper stewardship of auxinic herbicides is highly warranted to maintain its existence as a valuable weed control option.

Ethylene has been known to be a major contributor to the phytotoxic response observed from auxinic herbicide application for decades (Morgan and Hall 1962; Abeles 1968; Stacewicz-Sapuncakis et al. 1973; Cobb and Reade 2010). Ethylene is a trigger for many plant processes, including abscission and response to stress (Buchanan et al. 2000). Auxinic herbicides mimic endogenous auxins in plants and are known to upregulate the synthesis of 1-aminocyclopropane-1-carboxylic acid synthase (ACS) (Lin et al. 2009). The synthesis of ACS is the rate-limiting step in the biosynthesis of ethylene, as it is the enzyme responsible for formation of the intermediate 1-aminocyclopropane-1-carboxylic acid (ACC), which is further oxidized by ACC oxidases (ACOs) to produce ethylene (Thain et al. 2004; Kende 1993; Tsuchisaka and Theologis 2004; Gleason et al. 2011). Specifically, the ethylene biosynthesis genes *ACS4*, *ACS6*, and *ACS8* have been reported to be directly induced by auxins (Gleason et al. 2011; Thain et al. 2004). Ethylene itself is perceived in plants by binding to the N-terminal domain of several different receptors, likely initiating at least part of the classical epinastic response observed from auxinic herbicide treatment (Hua and Meyerowitz 1998; Bishopp et al. 2006; Wei et al. 2000; Hall et al. 1985). Ultimately, ethylene is reported to induce abscisic acid accumulation resulting in inhibition of growth (Hansen and Grossmann 2000).

The degree of translocation is perhaps associated and/or correlated with the role of ethylene in the phytotoxic response to auxinic herbicides. Previous research has indicated that increased herbicide translocation is potentially associated with reduced phytotoxicity in response to dawn applications of 2,4-D and dicamba (Johnston et al. 2018). This same research presents a

potential hypothesis that enhanced speed of translocation with dawn applications of these herbicides results in reduced saturation of the target site and thus a lesser degree of phytotoxicity, further leading to more herbicide translocation. This is supported by research that indicated that herbicide translocation is self-limited by phytotoxic action, however the causal relationship of these phenomenon with respect to one another is not established, particularly for auxinic herbicides (Beriault et al. 1999; Hall and Devine 1993). Such trends contrast the prevailing understanding of herbicide action, that reduced movement throughout the target plant results in a decrease in phytotoxic action (Riar et al. 2011; Goggin et al. 2016; Ge et al. 2010).

The red to far-red (R:FR) light spectrum is decreased at sunset and dawn (Jonas 1981). Phytochromes are photoreceptors responsive to differential R:FR light ratios and are known to have interactions with proteins responsible for auxin transport. Transcription factors known as Phytochrome Interacting Factors (PIFs) are rapidly accumulated in darkness in response to phytochrome reverting back to the inactive Pr state (Wang et al. 2013). PIFs have been shown to directly upregulate polar auxin transporter genes including PIN-FORMED3, which may account for improved translocation noted at dawn (Nozue et al. 2011; Johnston et al. 2018). Since *ACS* genes are directly induced by auxins at the target site, it can be hypothesized that reduced saturation of the target site with auxins (including auxinic herbicides) at dawn would result in suppressed ethylene production and thus reduced herbicidal activity. Interestingly, PIF4 and PIF5 have also been noted to modulate auxin sensitivity, which may also contribute to the time of day effect (Hersch et al. 2014).

Investigation into the mechanism and magnitude of the time of day effect is highly warranted to determine what popular auxinic herbicides are most prone to this phenomenon and to provide improved recommendations to growers on ideal application strategies using these

products. The objective of this research was 1) to investigate if ethylene formation differs across application times with 2,4-D and dicamba, using differential light intensities and R:FR found throughout the day in nature and 2) to determine the effect of translocation inhibition on ethylene production from these auxinic herbicides.

Materials and Methods

Laboratory experiments were conducted in Athens, GA from February to April 2016. Glyphosate-resistant Palmer amaranth seeds were collected from Macon Co., GA, sieved, and were sown in potting mix (Sun Gro Professional Growing Mix, Sun Gro Horticulture, Agawam, MA) and placed in a growth chamber with a day/night temperature of 30/20°C, with light from 8 am to 12 am (600 µmol m^{-2} s^{-1}) and an ambient relative humidity of 50%. Once plants reached ~15 cm in height they were transplanted into opaque amber 125 ml Nalgene bottles (Thermo Fisher Scientific, Waltham, MA) containing deionized water with 20-20-20 fertilizer added at a rate equivalent to 1/6 the nitrogen content of a full-strength Hoagland solution (210 ppm). Plants were then placed under an LED light (Kind LED K5 Series, Kind LED Grow Lights, Santa Rosa, CA) program consistent with an early spring red light spectrum and light intensity, scheduled to simulate sunrise to sunset via ramping of intensity and spectrum (Figure 1). Photosynthetic photon flux density and red/far-red light ratio was measured with a spectroradiometer (SS-110, Apogee Instruments, Logan, UT). The LED light program took place under laboratory conditions at 21°C. Plants were allowed to acclimate for 48 h and were then sprayed with the amine salt of 2,4-D or the diglycolamine salt of dicamba at 0.84 kg a.i. ha^{-1} and 0.56 kg a.i. ha^{-1}, respectively. Studies were performed separately for each herbicide. Herbicide was applied at either 8 am, coinciding with the beginning of the light schedule (dawn), or at 1 pm, coinciding

with one hour after the beginning of the mid-day stage. Some plants sprayed at 8 am were pre-treated with N-1-naphthylphthalamic acid (NPA), 2,3,5-triiodobenzoic acid (TIBA), or 5-[*N*-(3,4-dimethoxyphenylethyl)methylamino]-2-(3,4-dimethoxyphenyl)-2-isopropylvaleronitrile hydrochloride (verapamil) to inhibit translocation, presumably via interruption of subcellular dynamics involving auxin-efflux proteins of the PIN family in the case of TIBA, the ATP-binding cassette subfamily B in the case of verapamil, and both families of proteins in the case of NPA (Shukla et al. 2011; Geldner et al. 2001; Dhonukshe et al. 2008; Zhu and Geisler 2015; Noh et al. 2001; Petrášek et al. 2006). Pre-treatments were made 8 h prior to herbicide application and were delivered in 125 µL of dimethyl sulfoxide from separate working stock solutions. Final concentration of each inhibitor was 25 µM, a maximally-effective concentration based on preliminary research and previous reports, and final concentration of dimethyl sulfoxide in each bottle was 0.1% v/v (Goggin et al. 2016; Geldner et al. 2001). Preliminary experiments determined that the 0.1% concentration of dimethyl sulfoxide resulted in no phytotoxicity (data not shown). A completely randomized design was used with four replications. Each herbicide study was repeated.

Following administration of treatments, ethylene release was quantified via gas chromatography at separate time points. Plants were placed in 1,893 ml glass jars and sealed with metal lids 3 h prior to sampling to ensure that high-resolution, detectable concentrations of ethylene were collected. Each metal lid contained a rubber septa and AA battery pack connected to a 2.5 cm-diameter computer fan sealed with silicone. Fans were used to maintain adequate air mixing in the headspace of each jar for uniform sampling. Rubber septa were pierced with a 1 ml insulin syringe (BD U-100 Insulin Syringe Slip-Tip PrecisionGlide 25G 1cc; Beckton, Dickinson and Co., Franklin Lakes, NJ) and 1 ml of headspace gas was collected. Following

collection, gas samples were injected into a gas chromatograph (Shimadzu GC-17A, Shimadzu Corp., Kyoto, Japan) with a flame ionization detector. The system used helium as the carrier gas at a flow rate of 10 ml min^{-1} and a micro-packed HayeSep N column (Restek Corp., Bellefonte, PA). The temperature program was 60°C for 4 min followed by a 15°C min^{-1} increase to a hold at 150°C. Elution time of ethylene was determined to take place at 1.6 min using gas standards. For 2,4-D studies, samples were taken at 14, 20, 28, and 36 hours after treatment (HAT) and for dicamba studies samples were taken at 14, 20, and 28 HAT. Time points were established based on a preliminary study with 2,4-D applied at 1 pm (Figure 2), indicating an initial herbicide-induced pulse in ethylene production. The herbicide-induced pulse was thus targeted by the aforementioned sampling times. Final sampling of dicamba did not exceed 28 HAT due to faster release of ethylene following application (data not shown).

Analysis of covariance was performed on data using JMP (JMP Pro 13, SAS Institute, Cary, NC). Analysis used HAT as the covariate and ethylene production as the response variable. Ethylene concentration at sampling time was determined via a standard curve relating area under the 1.6 m peak to concentration in ppb, which was further converted to μL kg FW^{-1} h^{-1} using fresh plant weights, headspace volume, and the 3 h collection time. Ethylene production was log-transformed to allow for the application of linear functions to data, with equations following the formula

$$y = b + \beta x \quad [1]$$

where y is log(ethylene production), b is the intercept estimated by the prediction equation, β is the slope and x is HAT. Mean ethylene production was separated across treatments using pairwise t-tests. Graphs of ethylene production prediction equations were made using SigmaPlot (SigmaPlot 11, Systat Software, San Jose, CA) (Figure 3).

Results and Discussion

2,4-D. Treatment by study interactions were not detected for 2,4-D data ($p = 0.8486, 0.0977$), thus results were pooled over both studies. Covariate by treatment interactions were not detected indicating lack of significant differences in slope across treatments (Table 1, Figure 3). A highly significant effect of the covariate was detected along with a significant effect of treatment. No significant differences between the 1 pm application and 8 am application with no pre-treatment were detected. The 8 am application pre-treated with TIBA resulted in the highest ethylene production at 2.69 µL kg FW^{-1} h^{-1}, which was significantly greater than all treatments except for the 8 am application pre-treated with verapamil. The 8 am treatment pre-treated with NPA resulted in the least ethylene production at 2.35 µL kg FW^{-1} h^{-1}, significantly less than the 8 am application pre-treated with TIBA or verapamil.

The lack of a significant difference in ethylene production between the 8 am application with no pre-treatment and the 1 pm application suggest a potential lack of differential phytotoxicity across application times with 2,4-D. Alternatively, should a true difference in phytotoxicity occur across application times it may be due to a different mechanism than ethylene production, such as differential abscisic acid (ABA) accumulation or radical oxygen species (ROS) evolution. 2,4-D is known to upregulate the expression of *NCED* genes, responsible for the rate-limiting step in ABA biosynthesis (Nambara and Marion-Poll 2005). ROS production as a response to 2,4-D application is reported to take place via the activation of several enzymes associated with fatty acid metabolism, ureide metabolism, modification of peroxisomal proteins, and the biosynthesis of jasmonic acid (Pazmino et al. 2011; Ortega-Galisteo et al. 2012; reviewed in Song 2014). Further investigation is necessary to determine if a

time of day effect is attributable to such mechanisms, which if present may be due to differential 2,4-D perception at the target site across application times.

Nevertheless, the increased ethylene production following the 8 am 2,4-D application pre-treated with TIBA provides important insight into the relationship of translocation with phytotoxicity. Should the hypothesis hold true that reduced translocation results in increased saturation of the target site, it provides evidence that 2,4-D efflux from the cell is potentially reduced via the reported inhibition of PIN trafficking to the plasma membrane (Geldner et al. 2001). Therefore, a lack of the ability to export 2,4-D may result in an improved opportunity or increased duration for the herbicide to ultimately activate the auxin response factors associated with the signal cascade resulting from auxinic herbicide application (Ulmasov et al. 1999; reviewed in Bishopp et al. 2006). This may provide the mechanistic basis for the increased dicamba-induced phytotoxicity observed with certain weed species when the auxin transport inhibitor diflufenzopyr is added (Wehtje 2008). Should translocation play a significant role in the phytotoxicity of 2,4-D, the lack of significant differences between application times may be due to 2,4-D efflux relying on transport proteins not significantly affected by phytochrome regulation. Both PIF4 and PIF5 have been reported to upregulate the PIN3 transport protein which would conceivably lead to differential transport across dawn and mid-day (Nozue et al. 2011). The reported lack of dependence on PIN proteins for 2,4-D cellular efflux may explain the lack of differences in ethylene production between 1 pm and 8 am applications, however it does not explain why TIBA treatment resulted in a spike in ethylene production, particularly since TIBA has not been reported to have any significant activity on other transport mechanisms (Covington and Harmer 2007). Research aimed at the genetic regulation of transport proteins by PIFs and the function of knockout mutations on specific transport proteins may provide further

insight into limiting factors of 2,4-D cell efflux, particularly with respect to time of day. The fact that NPA pre-treatment did not result in similar ethylene production to that observed with TIBA further suggests specificity of 2,4-D to particular transport processes, regardless of the phytotoxic result. The degree of non-specificity of NPA makes drawing conclusions somewhat convoluted, as the spectrum of subcellular processes affected by this transport inhibitor is highly dose-dependent (Peer et al. 2009).

Dicamba. Treatment by study interactions were not detected for dicamba data ($p = 0.7669$, 0.6598), thus results are pooled across studies. The treatment by covariate interaction was statistically insignificant, yielding one slope for all treatments (Table 1). The greatest ethylene production was noted with the 1 pm application and 8 am application pretreated with NPA, both with a mean of 3.07 µL kg FW^{-1} h^{-1}. Significant differences were detected between the 1 pm treatment and 8 am treatment with no inhibitor. The 8 am application pre-treated with TIBA resulted in the least ethylene production at 2.66 µL kg FW^{-1} h^{-1}, significantly lower than both the 8 am application pre-treated with NPA and the 1 pm application.

The significant difference in ethylene production between dicamba applications at 8 am and 1 pm provides an interesting insight into the diurnal regulation of phytotoxicity. Whether or not this effect is due to differential signaling or translocation requires further research for confirmation, but it nonetheless confirms that ethylene production is at least one of the defining factors in the time of day effect with this herbicide. It is highly noteworthy that the 8 am application pre-treated with NPA resulted in nearly the same amount of ethylene production that was observed with the 1 pm application. This directly suggests that the reduced translocation previously reported with mid-day dicamba applications is one of the major factors in differential

phytotoxicity, as shutting down of cellular dicamba efflux via NPA resulted in a statistically significant increase in ethylene production compared to the 8 am treatment with no inhibitor (Johnston et al. 2018).

Little research is available on the specificity of dicamba for certain transport proteins or protein families, however certain trends in comparison with 2,4-D have been made. In particular, cellular influx of dicamba potentially suggests reliance on a different membrane-localized protein than 2,4-D (Gleason et al. 2011). Should dicamba exhibit differential affinities for influx mechanisms compared to 2,4-D, it could be conceived that the same holds true for efflux mechanisms. Pre-treatment with TIBA or verapamil failed to cause any significant increase in ethylene concentration from 8 am alone; however, addition of verapamil resulted in a statistically similar degree of ethylene production compared to NPA. This, paired with the fact that verapamil is highly specific for interrupting ATP-binding cassette subfamily B (ABCB) transporters alone, suggests that dicamba may have a higher preference for this efflux mechanism than PIN proteins. Further work on the translocation of 2,4-D and dicamba in response to these compounds is necessary to determine to what extent translocation plays a role in the differential phytotoxic responses reported with these herbicides.

Inhibition of auxin efflux has been shown in previous research to enhance the defoliation induced by exogenously applied ethylene, presumably in accordance with a hormone balance model (Morgan 1985; Burton et al. 2008). Specifically, the inhibitory effect of ethylene itself on auxin supply to cells is coupled with an ethylene-induced increase in hydrolases that aid in the cell separation responsible for abscission (Sexton and Roberts 1982; reviewed in Morgan 1976). The pre-treatment of plants with auxin has been reported to reverse the defoliation activity of ethylene (Morgan 1985). Since a lack of auxinic herbicide translocation would thus limit the

balance of auxin and ethylene at the whole-plant level, phytotoxic responses in addition to defoliation may indeed be enhanced via this hormone balance model.

In summary, this research provides important insights into the relationship of both time of application and translocation with ethylene production resulting from 2,4-D and dicamba applications. This is an economically critical area of research due to the increased use of these herbicides with the advent of transgenic crops, as well as the rapid spread of herbicide resistance in one of the worst weeds in the southeastern United States. A fully-elucidated mechanism behind diurnal variation in herbicide efficacy and the processes underlying differential translocation will aid in the stewardship of these herbicide chemistries required for optimal weed control and thus crop productivity. The aforementioned involvement of ethylene in this phenomenon provides an important part of this investigation.

References

Abeles FB (1968) Herbicide-induced ethylene production: role of the gas in sublethal doses of 2,4-D. Weed Sci. 16:498-500

Assad R, Reshi ZA, Snober J, Rashid I (2017) Biology of Amaranths. Bot. Rev. 83:382-436

Bauerle MJ, Griffin JL, Alford JL, Curry AB, Kenty MM (2015) Field evaluation of auxin herbicide volatility using cotton and tomato as bioassay crops. Weed Technol. 29:185-197

Beriault JN, Horsman GP, Devine MD (1999) Phloem transport of D,L-glufosinate and acetyl-L-glufosinate in glufosinate-resistant and -susceptible *Brassica napus*. Plant Physiol. 121:619-627

Bishopp A, Mähönen AP, Helariutta Y (2006) Signs of change: hormone receptors that regulate plant development. Development 133:1857-1869

Buchanan BB, Gruissem W, Jones RL (2000) Biochemistry and molecular biology of plants. Rockville, MD: The American Society of Plant Biologists. Pp. 895-901

Burton JD, Pedersen MK, Coble HD (2008) Effect of cyclanilide on auxin activity. J. Plant Growth Regul. 27:342-352

Cobb AH, Reade JPH (2010) Herbicides and Plant Physiology. 2nd edn. West Sussex, United Kingdom: Wiley-Blackwell. Pp. 149-150

Covington MF, Harmer SL (2007) The circadian clock regulates auxin signaling and responses in *Arabidopsis*. PLoS Biol. 5:e222

Culpepper AS, Grey TL, Vencill WK, Kichler JM, Webster TM, Brown SM, York AC, Davis JW, Hanna WW (2006) Glyphosate-resistant Palmer amaranth (*Amaranthus palmeri*) confirmed in Georgia. Weed Sci. 54:620-626

Culpepper S (2014) Application time of day influence on Roundup, Reflex, and Clarity. Unpublished raw data

Dhonukshe P, Grigoriev I, Fischer R, Tominaga M, Robinson D, Hasek J, Paciorek T, Petrášek J, Seifertova D, Tejos R, Meisel L, Zazimalova E, Gadella T, Stierhof YD, Ueda T, Oiwa K, Akhmanova A, Brock R, Spang A, Friml J (2008) Auxin transport inhibitors impair vesicle motility and actin cytoskeleton dynamics in diverse eukaryotes. Proc. Natl. Acad. Sci. 105:4489-4494

Figueiredo MRA, Leibhart LJ, Reicher ZJ, Tranel PJ, Nissen SJ, Westra P, Bernards ML, Kruger GR, Gaines TA, Jugulam M (2017) Metabolism of 2,4-dichlorophenoxyacetic acid

contributes to resistance in a common waterhemp (*Amaranthus tuberculatus*) population. Pest Manag. Sci. doi:10.1002/ps.4811

Foes MJ, Tranel PJ, Wax LM, Stoller EW (1998) A biotype of common waterhemp (*Amaranthus rudis*) resistant to triazine and ALS herbicides. Weed Sci. 46:514-520

Ge X, d' Avignon DA, Ackerman JJH, Sammons RD (2010) Rapid vacuolar sequestration: the horseweed glyphosate resistance mechanism. Pest Manag. Sci. 66:345-348

Geldner N, Friml J, Stierhof YD, Jürgens G, Palme K (2001) Polar auxin transport inhibitors block PIN1 cycling and vesicle trafficking. Nature 413:425-428

Giacomini DA, Umphres AM, Nie H, Mueller TC, Steckel LE, Young BG, Scott RC, Tranel PJ (2017) Two new *PPX2* mutations associated with resistance to PPO-inhibiting herbicides in *Amaranthus palmeri*. Pest Manag. Sci. 2017:10.1002/ps.4581

Gleason C, Foley RC, Singh KB (2011) Mutant analysis in Arabidopsis provides insight into the molecular mode of action of the auxinic herbicide dicamba. PLoS ONE 6:e17245 doi:10.1371/journal.pone.0017245

Goggin DE, Cawthray GR, Powles SB (2016) 2,4-D resistance in wild radish: reduced herbicide translocation via inhibition of cellular transport. J. Exp. Bot. 67:3223-3235

Hall JC, Bassi PK, Spencer MS, Vanden Born WH (1985) An evaluation of the role of ethylene in herbicidal injury induced by picloram or clopyralid in rapeseed and sunflower plants. Plant Physiol. 79:18-23

Hall LM, Devine MD (1993) Chlorsulfuron inhibition of phloem translocation in chlorsulfuron-resistant and susceptible *Arabidopsis thaliana*. Pestic. Biochem. Physiol. 45:81-90

Hansen H, Grossmann K (2000) Auxin-induced ethylene triggers abscisic acid biosynthesis and growth inhibition. Plant Physiol. 124:1437-1448

Heap I (2014) Herbicide resistant weeds. *In* Pimentel D, Peshin R eds. Integrated Pest Management. Dordrecht, Netherlands: Springer Dordrecht. Pp. 281-301

Hersch M, Lorrain S, de Wit M, Trevisan M, Ljung K, Bergmann S, Fankhauser C (2014) Light intensity modulates the regulatory network of the shade avoidance response in *Arabidopsis*. Proc. Natl. Acad. Sci. 111:6515-6520

Horak MJ, Loughin TM (2000) Growth analysis of four *Amaranthus* species. Weed Sci. 48:347-355

Hua J, Meyerowitz EM (1998) Ethylene responses are negatively regulated by a receptor gene family in *Arabidopsis thaliana*. Cell 94:261-271

Johnston CR, Eure PM, Grey TL, Culpepper AS, Vencill WK (2018) Time of application influences translocation of auxinic herbicides in Palmer amaranth (*Amaranthus palmeri*). Weed Sci. 66:4-14

Jonas H (1981) Responses of free running leaf movements to light, in particular to red and far red light during sunrise and sunset. Experientia 37:571-573

Kende H (1993) *Ethylene biosynthesis. Annu. Rev. Plant Physiol. Plant Mol. Biol. 44:293-307*

Lin Z, Zhong S, Grierson D (2009) Recent advances in ethylene research. J. Exp. Bot. 60:3311-3336

Manalil S, Busi R, Renton M, Powles SB (2011) Rapid evolution of herbicide resistance by low herbicide dosages. Weed Sci. 59:210-217

Morgan PW, Hall WC (1962) Effect of 2,4-dichlorophenoxyacetic acid on the production of ethylene by cotton and grain sorghum. Physiol. Plantarum 15:420-427

Morgan PW (1976) Effects on ethylene physiology. *In* Audus, L. J. ed. Herbicides: physiology, biochemistry, ecology. 2nd edn. Academic Press, London. Pp. 255-280

Morgan PW (1985) Chemical manipulation of abscission and desiccation. *In* Rowman & Allanheld eds. BARC Sym. No. 8, Totowa. Pp. 16-19

Nambara E, Marion-Poll A (2005) Abscisic acid biosynthesis and catabolism. Annu. Rev. Plant Biol. 56:165-185

Neve P, Powles S (2005) Recurrent selection with reduced herbicide rates results in the rapid evolution of herbicide resistance in *Lolium rigidum*. Theor. Appl. Genet. 110:1154-1166

Noh B, Murphy AS, Spalding EP (2001) *Multidrug resistance*-like genes of Arabidopsis required for auxin transport and auxin-mediated development. The Plant Cell 13:2441-2454

Norsworthy JK, Ward SM, Shaw DR, Llewellyn RS, Nichols RL, Webster TM, Bradley KW, Frisvold G, Powles SB, Burgos NR, Witt WW, Barrett M (2012) Reducing the risks of herbicide resistance: best management practices and recommendations. Weed Sci. 60:31-62

Nozue K, Harmer SL, Maloof JN (2011) Genomic analysis of circadian clock-, light-, and growth-correlated genes reveals PHYTOCHROME-INTERACTING FACTOR5 as a modulator of auxin signaling in *Arabidopsis*. Plant Physiol. 156:357-372

Ortega-Galisteo AP, Rodriguez-Serrano M, Pazmino DM, Gupta DK, Sandalio LM, Romero-Puertas MC (2012) S-nitrosylated proteins in pea (*Pisum sativum* L.) leaf peroxisomes: Changes under abiotic stress. J. Exp. Bot. 63:2089-2103

Pazmino DM, Rodriguez-Serrano M, Romero-Puertas MC, Archilla-Ruiz A, Del Rio LA, Sandalio LM (2011) Differential response of young and adult leaves to herbicide 2,4-dichlorophenoxyacetic acid in pea plants: Role of reactive oxygen species. Plant Cell Environ. 34:1874-1889

Peer WA, Hosein FN, Bandyopadhyay A, Makam SN, Otegui MS, Lee GJ, Blakeslee JJ, Cheng Y, Titapiwatanakun B, Yakubov B, Bangari B, Murphy AS (2009) Mutation of the membrane-associated M1 protease APM1 results in distinct embryonic and seedling developmental defects in *Arabidopsis*. The Plant Cell 21:1693-1721

Petrášek J, Mravec J, Bouchard R, Blakeslee JJ, Abas M, Seifertová D, Wisniewska J, Tadele Z, Kubes M, Covanová M, Dhonukshe P, Skupa P, Benková E, Perry L, Krecek P, Lee OR, Fink GR, Geisler M, Murphy AS, Luschnig C, Zazimalová E, Friml J (2006) PIN proteins perform a rate-limiting function in cellular auxin efflux. Science 312:914-918

Riar DS, Burke IC, Yenish JP, Bell J, Gill K (2011) Inheritance and physiological basis for 2,4-D resistance in prickly lettuce (*Lactuca serriola* L.). J. Agric. Food Chem. 59:9417-9423

Sexton R, Roberts JA (1982) Cell biology of abscission. Ann. Rev. Plant Physiol. 33:133-162

Shoup DE, Al-Khatib K, Peterson DE (2003) Common waterhemp (*Amaranthus rudis*) resistance to protoporphyrinogen oxidase-inhibiting herbicides. Weed Sci. 51:145-150

Shukla S, Ohnuma S, Ambudkar SV (2011) Improving cancer chemotherapy with modulators of ABC drug transporters. Curr. Drug Targets 12:621–630

Song Y (2014) Insight into the mode of action of 2,4-dichlorophenoxyacetic acid (2,4-D) as an herbicide. J. Integr. Plant Biol. 56:106-113

Stacewicz-Sapuncakis M, Marsh HV, Vengris J, Jennings PH, Robinson T (1973) Participation of ethylene in common purslane response to dicamba. Plant Physiol. 52:466-471

Stewart CL, Nurse RE, Sikkema PH (2009) Time of day impacts postemergence weed control in corn. Weed Technol. 23:346-355

Thain SC, Vandenbussche F, Laarhoven LJJ, Dowson-Day MJ, Wang ZY, Tobin EM, Harren FJM, Millar AJ, van der Straeten D (2004) Circadian rhythms of ethylene emission in *Arabidopsis*. Plant Physiol. 136:3751-3761

Tsuchisaka A, Theologis A (2004) Unique and overlapping expression patterns among the *Arabidopsis* 1-amino-cyclopropane-1-carboxylate synthase gene family members. Plant Physiol. 136:2982-3000

Ulmasov T, Hagen G, Guilfoyle TJ (1999) Activation and repression of transcription by auxin-response factors. Proc. Natl. Acad. Sci. 96:5844-5849

Wang KC, Liu X, Chen CY, Wu K (2013) Roles of phytochrome-interacting factors in light signaling. J. Plant Biochem. Physiol. 1:e114. doi: 10.4172/2329-9029.1000e114

Wehtje G (2008) Synergism of dicamba with diflufenzopyr with respect to turfgrass weed control. Weed Technol. 22:679-684

Wei YD, Zheng HG, Hall JC (2000) Role of auxinic herbicide-induced ethylene on hypocotyl elongation and root/hypocotyl radial expansion. Pest Manag. Sci. 56:377-387

Zhu J, Geisler M (2015) Keeping it all together: auxin-actin crosstalk in plant development. J. Exp. Bot. 66:4983-4998

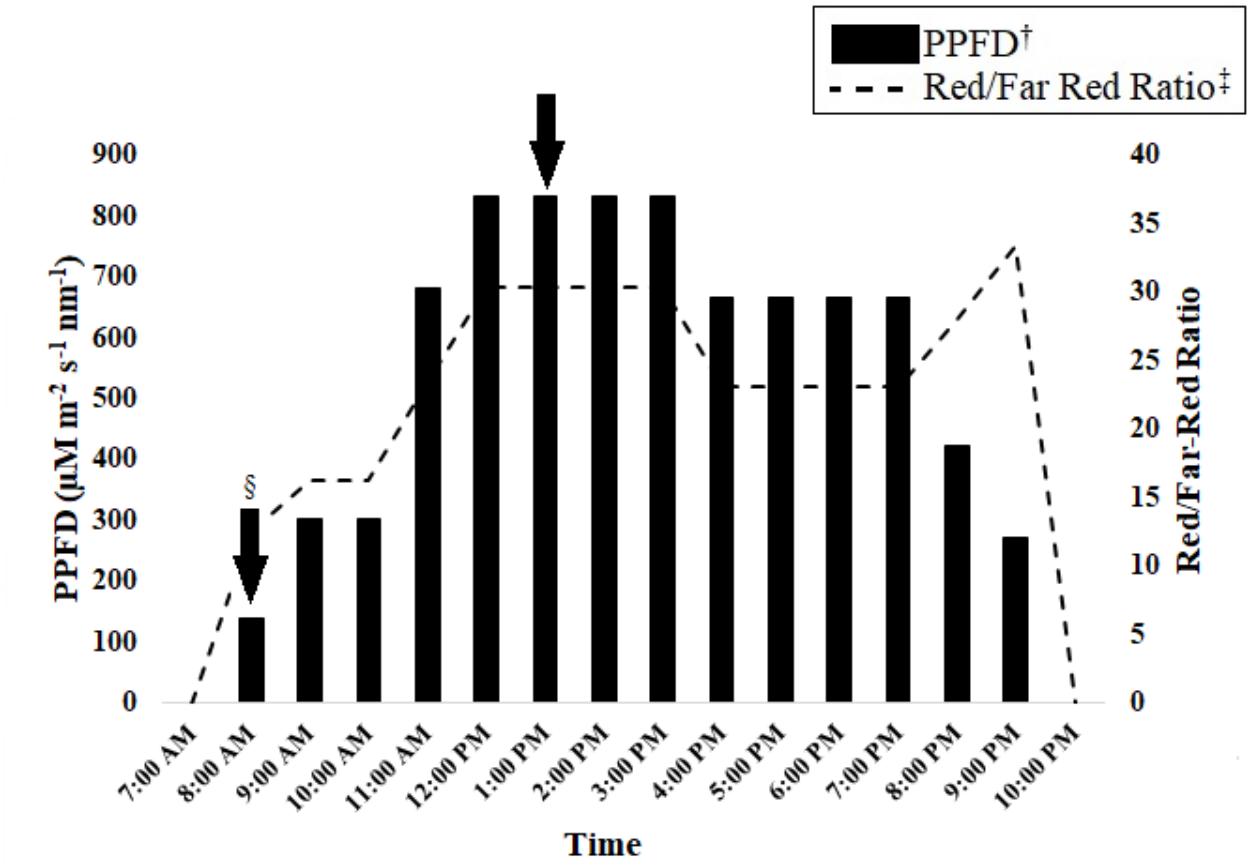

Figure 3.1. LED light program used for *A. palmeri* plants in laboratory for 2,4-D and dicamba applications, 2018.

†PPFD = Photosynthetic Photon Flux Density.

‡Red light range = 635 – 685 nm; Far-red light range = 710 – 760 nm.

§Black arrows represent both simulated dawn and mid-day application times of 2,4-D and dicamba.

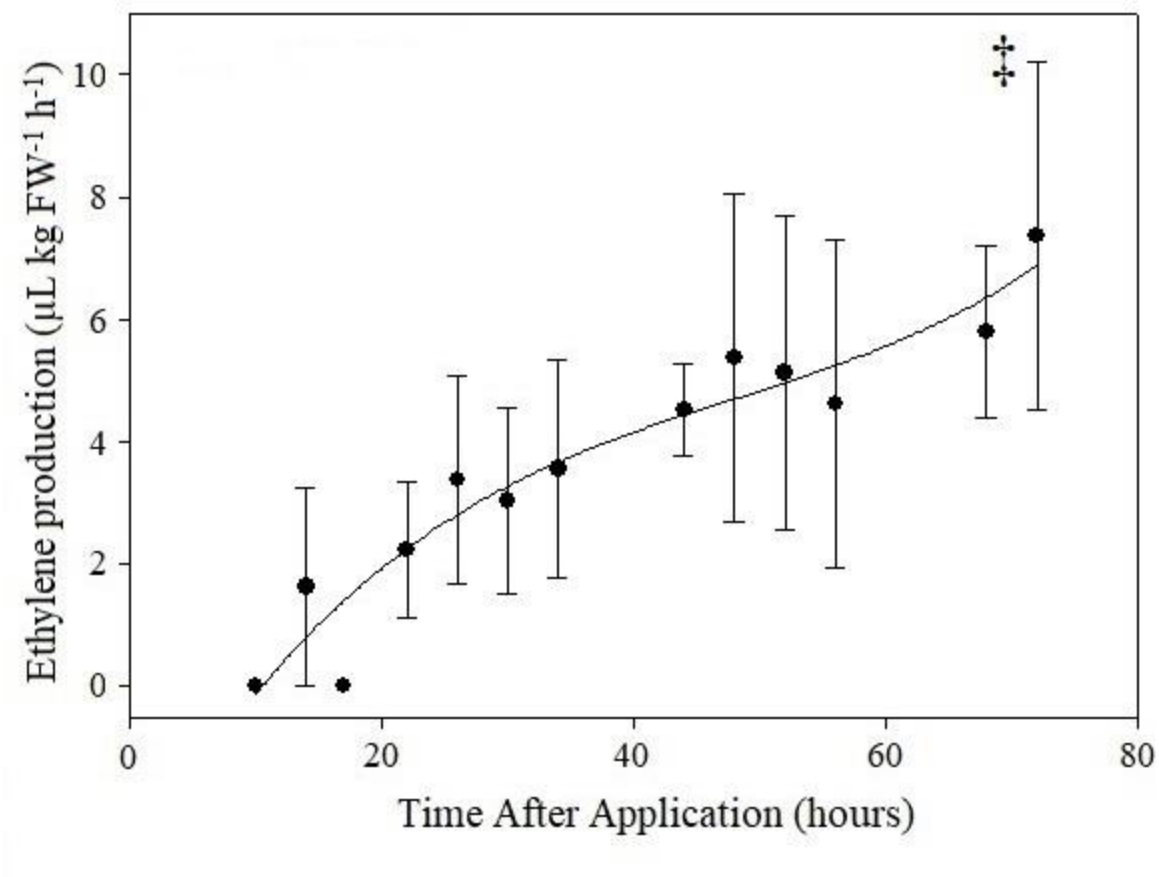

Figure 3.2. Ethylene production resulting from 0.56 kg ha^{-1} 2,4-D application at 1 pm, determined from preliminary study to evaluate initial peak rate of herbicide-induced ethylene production, 2018.

†Cubic polynomial function fit to data, following the formula:

$$y = -3.15 + 0.36x + -0.0061x^2 + 0.000042x^3 \quad [2]$$

SE = 2.81, $r^2 = 0.37$.

‡Vertical bars represent standard error of the mean.

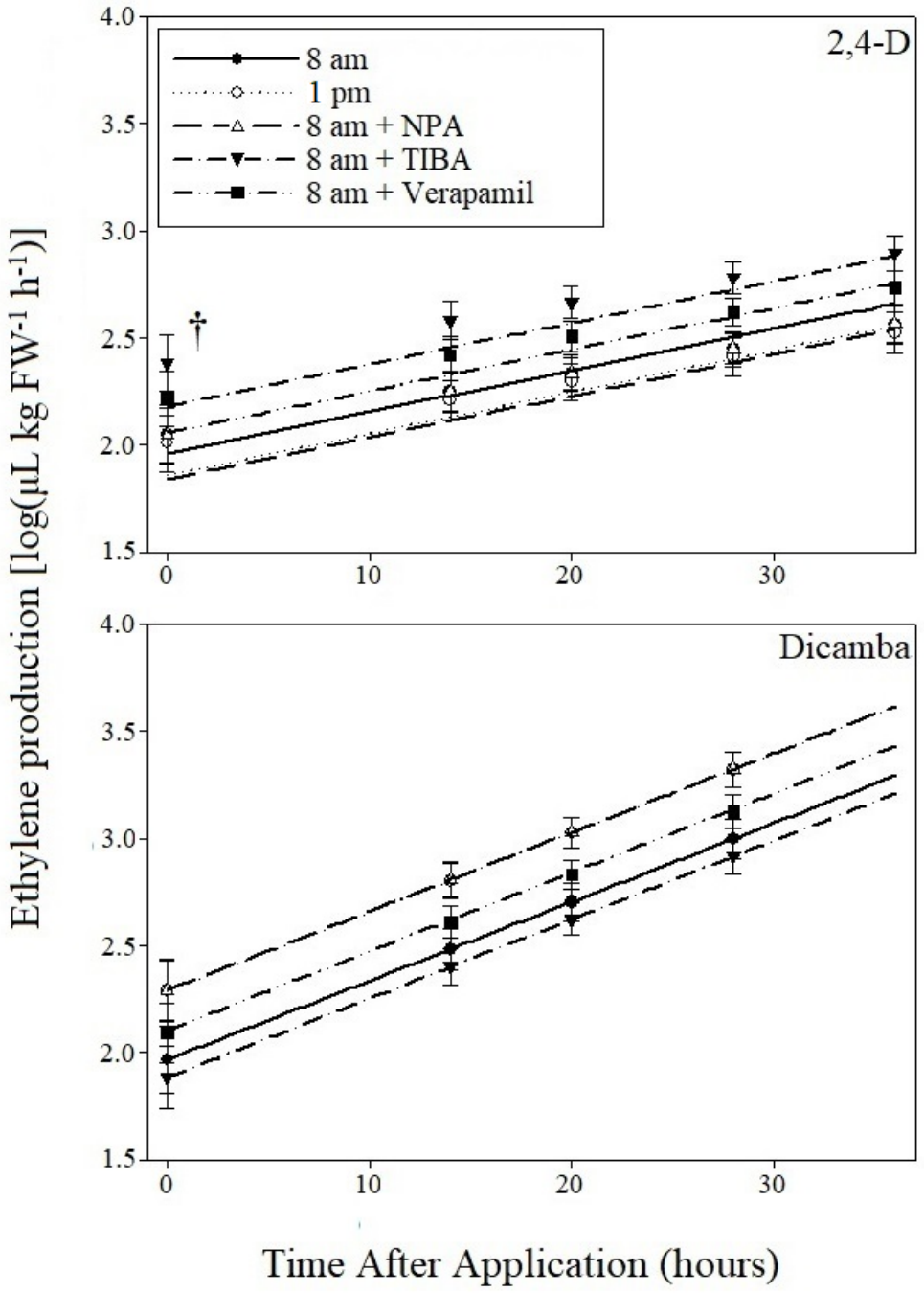

Figure 3.3. Prediction equations of ethylene production resulting from 2,4-D and dicamba applications at a rate of 0.84 and 0.56 kg ha^{-1}, respectively, applied at two timings and with three translocation inhibitors, 2018.

[†]Vertical bars represent standard error of the mean. Bars at zero hours after application represent standard error of the predicted intercept.

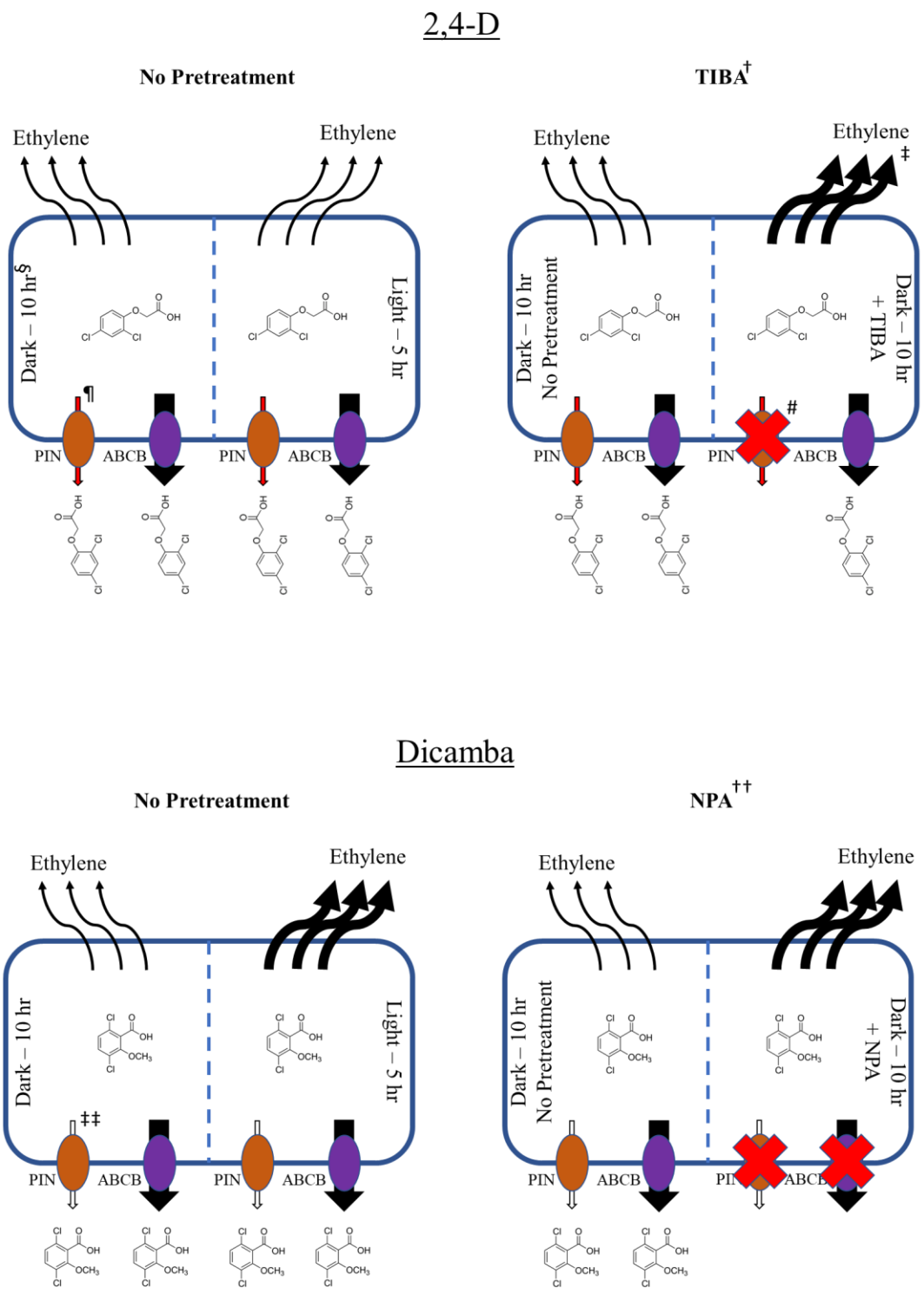

Figure 3.4. Diagrams illustrating differences in 2,4-D and dicamba-induced ethylene production from plant cells across application times, and across 8 am applications with no pretreatment and TIBA and NPA pretreatment, respectively, 2018.

[†]TIBA = 2,3,5-triiodobenzoic acid.

[‡]Size of black arrows indicate magnitude of ethylene production.

[§] Dark – 10 hr indicates the 8 am, simulated dawn application, as applications were made after 10 hours of darkness. Light – 5 hr indicates the 1 pm, simulated mid-day application, as applications were made after 5 hours of light.

[¶] Red arrows indicate probable 2,4-D efflux via PIN transport proteins.

[#]Red "X" indicates likely total inhibition of efflux via respective transport protein.

[††] NPA = N-1-naphthylphthalamic acid.

[‡‡]White arrows indicate unknown extent, if any, of dicamba efflux via PIN proteins.

Table 3.1. Analysis of covariance results from 2,4-D and dicamba applications at a rate of 0.84 and 0.56 kg ha^{-1}, respectively, applied at two timings and with three translocation inhibitors, 2018.

[†]Covariate by treatment interactions were not detected, therefore one slope is used for all treatments.

[‡]Means followed by different letters are significantly ($p \leq 0.05$) different. Means separations are based on pairwise t-tests.

[§]HAT = hours after treatment.

2,4-D

Treatment	Mean (SE)		Equation	Slope[†] (SE)
	log(µL kg FW^{-1} h^{-1})			
1:00 PM	2.36 (0.15)	CD[‡]	y = 1.86 + 0.019x	0.0194 (0.0044)
8:00 AM	2.37 (0.14)	BCD	y = 1.96 + 0.019x	__
8 am + TIBA	2.69 (0.14)	A	y = 2.18 + 0.019x	__
8 am + NPA	2.35 (0.14)	D	y = 1.84 + 0.019x	__
8 am + Verapamil	2.56 (0.14)	ABC	y = 2.06 + 0.019x	__
[§]HAT	<.0001			
Treatment	0.0019			
HAT*Treatment	0.3806			

Dicamba

Treatment	Mean (SE)		Equation	Slope (SE)
	log(µL kg FW^{-1} h^{-1})			
1:00 PM	3.07 (0.07)	A	y = 2.29 + 0.037x	0.0368 (0.0059)
8:00 AM	2.75 (0.09)	B	y = 1.97 + 0.037x	__

8 am + TIBA	2.66 (0.07)	B	y = 1.88 + 0.037x	__
8 am + NPA	3.07 (0.07)	A	y = 2.29 + 0.037x	__
8 am + Verapamil	2.87 (0.07)	AB	y = 2.10 + 0.037x	__

HAT	<.0001
Treatment	0.0004
HAT*Treatment	0.6661

CHAPTER 4

TIME OF 2,4-D AND DICAMBA APPLICATION AFFECTS HERBICIDE-INDUCIBLE GENE EXPRESSION[1]

[1]C. R. Johnston, A. Malladi, W. K. Vencill, T. L. Grey, A. S. Culpepper, G. M. Henry, and M. A. Czarnota. To be submitted to *Plant Physiology*.

Abstract

Auxinic herbicides are well-known to induce an upregulation in genes encoding abscisic acid and ethylene biosynthesis, namely those encoding 9-*cis*-epoxycarotenoid dioxygenase (*NCED*) and 1-aminocyclopropane-1-carboxylic acid synthase (*ACS*), respectively. Experiments were carried out to determine how the expression of both *NCED1* and *ACS1* in Palmer amaranth (*Amaranthus palmeri* S. Watson) were affected by time of application and the herbicides 2,4-D and dicamba. The sequence for *NCED1* was obtained via multiple scaffold sequence alignment of prince's-feather (*Amaranthus hypochondriacus* L.), while the sequence for *ACS1* was known in *A. palmeri*. The use of qPCR indicated a significant increase in relative *NCED1* expression with herbicide applications at 8 am (1.842) compared to 1 pm (0.699) in relation to untreated plants, while no consistent trends were observed with *ACS1* expression across treatments. It appears that the use of auxinic herbicides at a time coinciding with an increased ability of plants to express *NCED1* results in reduced herbicide efficacy, potentially through an ABA-mediated reduction in plant biochemical processes due to decreases in carbon fixation and overall photosynthesis. As ABA is known to antagonize the effects of auxin, it appears that applying auxinic herbicides may result in reduced phytotoxicity when plants are under stressors that induce ABA biosynthesis. Whether or not the increased expression of *NCED1* is directly correlated with ABA concentrations in the plant cell requires further investigation.

Introduction

A diurnal variation in the efficacy and translocation of auxinic herbicides such as 2,4-D and dicamba has been reported in field and laboratory settings, with reductions in activity being noted around dawn and dusk (Culpepper 2014; Stewart et al. 2009; Johnston et al. 2018). This is of concern today due to the introduction of 2,4-D- and dicamba-resistant crops, which have resulted in a sharp increase in the use of dicamba and an expected increase in the use of 2,4-D (Johnston et al. 2018; Hartzler 2017; EPA 2017; Behrens et al. 2007; Egan et al. 2011; Skelton 2015). In situations where growers are forced to make dawn or dusk applications due to such issues as large acreages and adverse weather events, a notable reduction in weed control could confer a necessity for sequential herbicide applications. An additional negative effect of reduced herbicide efficacy is an acceleration in the rate of selection for alleles contributing to resistance (Norsworthy et al. 2012; Neve and Powles 2005; Manalil et al. 2011).

Herbicide resistance has become a specifically dire concern in the case of weedy *Amaranthus* spp., partly due to fast growth rate and the high degree of genetic variability granted to offspring (Assad et al. 2017). These characteristics in the presence of sustained reliance on specific herbicide mechanisms of action have resulted in the heavy selection pressure necessary for the proliferation of herbicide-resistant traits in *Amaranthus* (Horak and Loughin 2000; Heap 2014). While glyphosate-resistant Palmer amaranth (*Amaranthus palmeri* S. Watson) is the most problematic case of resistance in *Amaranthus* spp., resistance to acetolactate synthase-inhibiting herbicides and triazines has been reported in other species of the genus (Culpepper et al. 2006; Foes et al. 1998). Resistance to protoporphyrinogen oxidase inhibitors, once the preferred herbicide option for managing resistant *Amaranthus* spp. in the United States, has now been reported as well, resulting in a great necessity for new and effective POST herbicide options

(Shoup et al. 2003; Giacomini et al. 2017). With the recent report of a metabolic resistance mechanism occurring in tall waterhemp [*Amaranthus tuberculatus* (Moq.) J.D. Sauer], maintaining stewardship of auxinic herbicides is of paramount importance (Figueiredo et al. 2017). As such, determination of which biochemical and molecular processes confer the diurnal variation in the efficacy of 2,4-D and dicamba is necessary in order to evaluate what kind of future strategies can be implemented with these herbicides, as well as other members of the auxinic mechanism of action (WSSA Group 4).

The ethylene and abscisic acid (ABA) biosynthesis genes encoding 1-aminocyclopropane-1-carboxylic acid synthase (ACS) and 9-*cis*-epoxycarotenoid dioxygenase (NCED), respectively, have been reported to be upregulated mere hours after treatment with auxinic herbicides (Yang and Hoffmann 1984; Grossmann 2009; Grossmann 2003; Hansen and Grossmann 2000; Song 2014). Upregulation of ethylene biosynthesis is noted to be a key contributor to the epinasty and eventual growth inhibition that leads to a full realized phytotoxic response (Sterling and Hall 1997; Grossmann 1998). While the ABA-induced upregulation of NADPH-oxidases has been reported to stimulate the formation of radical oxygen species, the classical stomatal closure and photosynthesis inhibition granted by this hormone are believed to be among the chief herbicidal processes resulting from auxinic herbicide application (Romero-Puertas et al. 2004; Grossmann 2009; Dat et al. 2000; Grossmann et al. 1996; Scheltrup and Grossmann 1995; Buchanan et al. 2000). Interestingly, ethylene itself has been suggested to stimulate the formation of ABA precursors, illustrating interplay between the pathways associated with both of these hormones (Hansen and Grossmann 2000). While substantial research has investigated the overall roles of ethylene and abscisic acid in the herbicidal response

to auxinic materials, none have examined the degree of gene expression corresponding to applications at different times of day.

Differences in ethylene production have been reported between dawn and mid-day applications of dicamba (Johnston et al. 2019). This may be due to phytochrome-mediation of diurnal rhythms of ethylene production, which has been reported in *Sorghum* (Finlayson et al. 1999). Phytochrome B specifically is a photoreceptor responsible for perception of the red to far-red light ratio (R:FR), which changes across times of day (Taiz and Zeiger 2010; Jonas 1981). Biosynthesis of ethylene has been closely correlated with a part of the pathway responsive to different R:FR ratios (Finlayson et al. 1999). The activity of ACS2 has been reported to act downstream of phytochrome B; however, whether this occurs at the transcriptional level requires further research (Bours et al. 2013). Should differential gene expression across time of application be reported with such chemistries, it may serve as a further basis for selection of alternative herbicide options where around-the-clock applications must be made. The objective of this study was to investigate the effect of application time of 2,4-D and dicamba on *ACS1* and *NCED1* transcript levels in *A. palmeri*.

Materials and Methods

Plant Materials and Experimental Design. Sieved seed from a population of glyphosate-resistant *A. palmeri* collected from Macon Co., GA was used for study. Seeds were germinated in potting mix (Sun Gro Professional Growing Mix, Sun Gro Horticulture, Agawam, MA) in 111 cm^3 containers where they remained throughout the experiment. Seeds were germinated in a growth chamber set to a day/night temperature of 30/20°C, with light at 600 µmol m^{-2} s^{-1} from 8 am to 12 am. Ambient relative humidity was 50%. Plants were then brought to a laboratory held

at 21°C and placed under an LED light (Kind LED K5 Series, Kind LED Grow Lights, Santa Rosa, CA) program designed to simulate a light intensity and R:FR consistent with early spring (Figure 1). Plants were acclimated for 48 hours then treated with herbicides. Treatments included an untreated check, 2,4-D amine at 0.25 kg a.i. ha^{-1} at 8 am or 1 pm, and dicamba diglycolamine at 0.25 kg a.i. ha^{-1} at 8 am or 1 pm. Treatments were made using a 0.5-10 µl pipettor (Research, Eppendorf, Hamburg, Germany), with herbicide being applied in seven 10 µl drops corresponding to the aforementioned rate and a simulated coverage of 281 L ha^{-1}. Spray coverage was determined using the average leaf area of 4 plants (~26 cm^2), with droplets placed on one side of each leaf midrib. Experimental design was completely randomized with four replications. Studies were repeated in time.

RNA Extraction and Purification. Plants were harvested 3 hours after treatment, consistent with the time reported by Kraft et al. (2007) that was required to maximize upregulation of *NCED* genes. Leaf tissue was then frozen in liquid nitrogen and ground into a fine powder in a sterilized and pre-cooled mortar and pestle. Powdered leaf tissue was placed in a 15 ml centrifuge tube and stored at -80°C prior to extraction. Approximately 0.4 g of ground frozen leaf tissue was added to 3 ml of a 2% cetyl trimethylammonium bromide (CTAB) buffer solution containing a 2 M concentration of NaCl, 100 mM tris HCl (pH = 7.5), 25 mM EDTA (pH = 8), 3.44 mM spermidine, 2% β-mercaptoethanol, and 2% PVP dissolved in DEPC-treated water. The CTAB buffer was heated to 65°C in a water bath prior to adding frozen leaf powder. The leaf powder-buffer mixture was vortexed and incubated at 65°C for 10 min, then vortexed again and incubated at 23°C for 5 min. One volume of a 24:1 chloroform:isoamyl alcohol solution was added to the mixture and immediately centrifuged (Centrific, Fisher Scientific, Hampton, NH) at

5,000 g at 4°C for 15 min. Supernatant was extracted and another volume of chloroform:isoamyl solution was added prior to another 15 min centrifuging. This final supernatant was added to a 2.5 ml centrifuge tube and 0.25 volumes of LiCl were added. The supernatant was then inverted twice and precipitated at 4°C for approximately 16 h.

The supernatant was then centrifuged (Marathon 26KMR, Fisher Scientific, Hampton, NH) at 12,000 g for 20 min at 4°C to collect an RNA pellet on the bottom of the tube. Supernatant was discarded and 500 µl of cold 70% ethanol in DEPC-treated water was added prior to centrifuging at 12,000 g for 20 min at 4°C. The 70% ethanol solution was then completely removed using a pipettor, and 100 µl of 1X SSTE buffer in DEPC-treated water was added prior to adding 2.5 volumes of cold absolute ethanol. This mixture was precipitated at 20°C for 2 h prior to centrifuging at 12,000 g at 4°C for 20 min. Supernatant was discarded and the RNA pellet was washed once more with 700 µl of the cold 70% ethanol solution prior to centrifuging at 4°C at 12,000 g for 10 min. Tubes containing RNA were then placed on ice and allowed to air dry at 4°C. RNA was suspended in 20 µl of DEPC-treated water and concentration and quality (260/280 nm ratio ~2.0) was quantified using a NanoDrop (NanoDrop 8000, Thermo Fisher Scientific, Waltham, MA), followed by confirmation of purity using 1.2% agarose gel electrophoresis in TBE buffer at 80V for 25 min to identify the 18S and 28S ribosomal RNA bands (Figure 2). Each RNA extract tested contained 1.5 µl RNA extract, 2.4 µl formamide, 0.9 µl of loading dye (DNA Gel Loading Dye (6X), Thermo Fisher Scientific, Waltham, MA), and 0.6 µl of DEPC-treated water. Each extract mixture was incubated at 65°C prior to loading into the gel. Original RNA extract was then stored in a -80°C freezer (Symphony Ultra-Low Temperature Freezer, VWR International, Radnor, PA).

cDNA Synthesis. RNA samples were subjected to a DNase cycle first. Samples were removed from the -80°C freezer and thawed prior to light mixing and briefly running in a mini centrifuge (MiniStar, VWR International, Radnor, PA). RNA samples were placed in a rack on ice and a 1 µg 2 μl^{-1} concentration of each RNA sample was created in a 200 µl PCR tube. A 2 µl aliquot of the 1 µg 2 μl^{-1} concentration of each RNA sample was added to a separate PCR tube. To each aliquot was added 1 µl of DNase buffer (RQ1 DNase 10X Reaction Buffer, Promega Corp., Madison, WI), 0.5 µl DNase (RQ1 RNase-free DNase, Promega Corp., Madison, WI), and 6.5 µl of autoclaved distilled water. The mixtures were mixed in a pipette tip prior to spinning in a mini centrifuge, and were then placed in a thermal cycler (2720 Thermal Cycler, Applied Biosystems, Foster City, CA) at 37°C for 34 min then held at 4°C. Samples were then placed back on ice and 1 µl of DNase stop solution (RQ1 DNase Stop Solution, Promega Corp., Madison, WI) was added to each sample prior to spinning down in a mini centrifuge. Samples were then incubated at 23°C for 2 min.

Samples were then carried through the reverse transcriptase cycle. Tubes containing RNA samples were placed back on ice and each sample received 1 µl of 0.5 µg μl^{-1} oligo dTs, 1 µl of 10 mM dNTPs, and 1.3 µl of autoclaved distilled water. Samples were mixed in a pipette tip and spun down in a mini centrifuge prior to running in a thermal cycler at 70°C for 10 min, then brought down to 4°C. Samples were immediately removed prior to adding 4 µl 5X reverse transcriptase buffer (ImProm-II 5X Reaction Buffer, Promega Corp., Madison, WI), 1.2 µl of 25 mM $MgCl_2$, and 0.5 µl reverse transcriptase (ImProm-II Reverse Transcriptase, Promega Corp., Madison, WI). The samples were then placed back in the thermal cycler and run at 4°C for 3 min, 42°C for 75 min, and finally 75°C for 15 min followed by holding at 4°C. The cDNA samples were diluted six-fold with 100 µl of autoclaved distilled water and stored at -20°C.

Identification and Sequencing of NCED1. The known sequence for *NCED3* in thale cress [*Arabidopsis thaliana* (L.) Heynh.] was run against the prince's-feather (*Amaranthus hypochondriacus* L.) genome using Phytozome (Phytozome 12, The Regents of the University of California, Oakland, CA). The resulting *A. hypochondriacus* scaffolds with the lowest E value (and thus greatest match) between the two species were aligned using Clustal Omega (Multiple Sequence Alignment Tool, European Molecular Biology Laboratory—European Bioinformatics Institute, Cambridgeshire, UK), and initial primers were designed at areas of significant scaffold matching at the 5' and 3' end (Figure 3, Table 1). Primers were tested with a 1X reaction mixture containing 2 µl of cDNA of 2,4-D-treated plants, 2 µl of 5X DNA polymerase buffer (5X Colorless GoTaq Flexi Buffer, Promega Corp., Madison, WI), 0.2 µl of 10 mM dNTPs, 0.6 µl of 25 mM $MgCl_2$, 0.05 µl Taq polymerase (GoTaq Flexi DNA Polymerase, Promega Corp., Madison, WI), and 3.15 µl of autoclaved distilled water such that the final concentration of each primer in the tube was 0.2 µM. Samples were run in a thermal cycler at 95°C for 5 min, followed by 40 cycles of a 30 s 95°C, 30 s 55°C, then 1 min 72°C program. Following the 40 cycles, the samples were brought to 72°C for 10 min before holding at 4°C.

A 1.2% agarose gel electrophoresis in TBE buffer at 80V for 25 min was performed, and it was found that the initial *NCED3F* 5'-GGTCATCATTTCTTTGACGGTGA-3' and *NCED3R* 5'-AATCCAGACACCTTTGGCCA-3' primer pair yielded a ~1,000 bp product (Figure 4). Twelve samples of the initial *NCED3* primer pair were run each in a 2X strength, 20 µl PCR mixture such that each primer was at a 0.4 µM concentration. Gel electrophoresis was then performed as described above and resulting bands were excised from the gel under UV light using a razor blade (Figure 5). The excised DNA products were extracted from the gel using a gel extraction kit (E.Z.N.A. Gel Extraction Kit, Omega Bio-Tek, Norcross, GA) and sent to the

Georgia Genomics Facility (Georgia Genomics and Bioinformatics Core, Athens, GA) for Sanger capillary sequencing using a 96-capillary DNA analyzer (3730xl, Applied Biosystems, Foster City, CA). Each reaction submitted for sequencing contained a reaction mixture of 20 ng of template DNA extracted from the gel, and 1 µl of a 3.3 µM working solution of each sequencing primer. Sequencing primers were the same sequences used to amplify the product(s) excised from the gel. The resulting sequence was then run in Sequence Manipulation Suite Translate Tool (Stothard 2000) and the reverse strand at reading frame 3 was found to produce a single protein product (Figure 6). This nucleotide sequence was run using BLASTx (National Center for Biotechnology Information, U.S. National Library of Medicine, Bethesda, MD) and found to have 86% amino acid identity with *NCED1* in *Chenopodium quinoa*, which shares the Amaranthaceae family with *A. palmeri* (query cover = 99%, E-value = 0.0). Three sets of specific qPCR primers were then designed using the resulting Sanger capillary-derived sequence described above (Table 2).

qPCR. A 2X SYBR Green master mix (PowerUp SYBR Green Master Mix, Applied Biosystems, Foster City, CA) with a ROX reference was used to perform qPCR. The reaction mixture contained a 0.2 µM concentration of both forward and reverse primers, 2.0 µl cDNA (1 µg 120 μl^{-1}), and 6 µl of the 2X master mix. The reaction was carried out in a qPCR system (Mx3005P, Stratagene, San Diego, CA) to determine amplification in real-time. The program for the reaction consisted of 2 min at 50°C, 3 min at 95°C, 40 cycles of 95°C for 30 sec and 60°C for 1 min, followed by a final cycle of 1 min at 95°C, 30 sec at 55°C, and 30 sec at 95°C. A dissociation profile was examined following amplification to ensure specificity of primer pairs. The 18S ribosomal RNA gene (*18SRibo*) of *A. palmeri* (Accession No.: MG685258.1) was used

as a reference gene, utilizing the 2nd qPCR primer set tested (*18SRiboF* 5'-AGTGGATGCACCCAGTATT-3' and *18SRiboR* 5'-TCGATGGTTCACGGGATT-3'). The primers *NCED1F* 5'-GATCGTCGTAATCGGATCTTG-3' and *NCED1R* 5'-TCTCTCCGGGTTGAAACT-3' were selected for *NCED1* amplification. respectively. *ACS1* qPCR primers used consisted of *ACS1F* 5'-AAGCTGGATGGTTTAGAGTATG-3' and *ACS1R* 5'-GATGCCAACATTTCCTCTTTG-3', which were designed based on the *A. palmeri ACS1* sequence determined by Giacomini et al. (2019) (Figure 7).

Data Analysis. The fluorescence threshold for calculating Ct values was 0.1, with fluorescence (dRn) log-transformed using MxPro (Agilent Technologies, Santa Clara, CA). Amplification efficiency was calculated by converting fluorescence data to the Rn format to correct baseline for noise. Efficiency was determined by finding the window of linearity of each sample's fluorescence curve using LinRegPCR (Ruijter et al. 2009), with the overall efficiency averaged within genes and studies being used for calculation of respective relative quantity of transcript (RQ) values. Values for RQ, normalized relative quantity of transcript (NRQ), $\log_2$-transformed NRQ data (Cq`) and standard errors of relative transcript expression (RE) were calculated according to Rieu and Powers (2009). The values for RQ were calculated using the formula:

$$RQ = 1 / E^{Ct} \quad [1]$$

where *E* is amplification efficiency and *Ct* is the threshold cycle used for quantification. Values for NRQ (normalized against the reference gene) were then calculated according to the formula:

$$NRQ = GOI_{RQ} / Ref_{RQ} \quad [2]$$

where GOI_{RQ} is the RQ value for the gene of interest (*NCED1* or *ACS1*), and Ref_{RQ} is the RQ value of the reference gene (*18SRibo*) corresponding to the same sample used for calculating the RQ value of the gene of interest. The values for Cq` were used for statistical analysis to determine treatment effects at the p = 0.05 significance level according to the PROC GLM procedure in SAS (SAS Institute, Cary, NC). Values for Cq` were calculated as follows:

$$Cq` = log_2(NRQ + 1) \quad [3]$$

where *NRQ* is the normalized relative quantity for the respective treatment, with one added to all NRQ values to allow for inclusion of samples with zero amplification. The reported mean values for RE of each herbicide treatment were calculated as follows:

$$RE = NRQ / Unt_{NRQavg} \quad [4]$$

where *NRQ* is the normalized relative quantity for each respective treatment and Unt_{NRQavg} is the mean NRQ for the untreated control. As such, the mean RE for the untreated control was one in all cases and all treatment means were reported in relation to the untreated control. The standard error for the RE values was calculated according to the following:

$$SE\left(\frac{NRQ}{NRQunt}\right) = \left[\frac{NRQ\text{^}2}{NRQunt\text{^}2}\left(\frac{SE(NRQ)\text{^}2}{NRQ\text{^}2} + \frac{SE(NRQunt)\text{^}2}{NRQunt\text{^}2}\right)\right]^{1/2} \quad [5]$$

where *SE* is the standard error of corresponding terms, *NRQ* is the mean normalized relative quantity for each respective treatment, and *NRQunt* is the mean normalized relative quantity for the untreated control.

Results and Discussion

Treatment by study interactions were not detected for *NCED1* expression (p = 0.2329, p = 0.5642), therefore results from both studies were combined prior to analysis. No significant herbicide effects were detected for *NCED1* data (p = 0.3696), however relative expression was

significantly affected by time of application ($p = 0.0494$) (Table 3, Figure 8). Relative expression of *NCED1* was increased approximately three-fold when herbicide applications were made at 8 am compared to 1 pm, at 1.842 and 0.699, respectively. Study by herbicide interactions were detected for *ACS1* expression, therefore studies were analyzed and are presented separately. In study one, relative expression of *ACS1* was significantly higher with 2,4-D compared to dicamba, at 0.827 and 0.225, respectively (Table 4, Figure 9). In contrast, with study two relative expression of *ACS1* was similar to that observed with study one at 0.852, however relative expression from dicamba application was significantly higher at 10.027, and nearly 45 times higher than observed with dicamba in study one.

Interestingly, despite the fact that improved auxinic herbicide efficacy has been reported at mid-day, the relative expression of *NCED1* was much higher with simulated dawn applications compared to those at mid-day (Culpepper 2014). Intuitively, it would be expected that due to the negative effects on plant growth imparted by increased ABA production, higher *NCED1* expression would be detected with mid-day applications when these herbicides are more active (Song 2014; Grossmann 2009). Several reasons may be behind this observation. ABA promotes stomatal closure, partially due to increasing cytosolic calcium levels and partially due to the increase in cytosolic pH which induces potassium efflux (Taiz and Zeiger 2010; Allan et al. 1994; Allen et al. 1999). This results in a reduction in carbon fixation and a potential overall reduction in photosynthesis which may negatively affect general biochemical activity (Taiz and Zeiger 2010; Downton et al. 1988; Schroeder et al. 2001). This reduction may reduce the perception of auxinic herbicides when applied at dawn, as well as decrease the degree of signal transduction caused by this perception. Consistently, previous research has illustrated that auxin activity, specifically by inhibiting lateral root formation, is antagonized by ABA (De Smet et al.

2003). This may be only one of potentially a whole suite of auxin-inducible process affected by ABA. Furthermore, ABA has been shown to increase auxin conjugation, thus reducing overall free concentrations of auxin in the cell (Dunlap and Robacker 1990). In contrast, when plants are attacked by auxinic herbicides at a time with lower ABA activity (i.e. mid-day), a full degree of perception and therefore signal transduction may be allowed to occur. However, this hypothesis relies on the assumption that increased *NCED1* expression does indeed cause a direct increase in ABA, disregarding the potential activity of post-translational regulation mechanisms and metabolic manipulation of ABA concentrations in plant cells. Further research is necessary to confirm this phenomenon. Regardless, the fact that improved translocation of auxinic herbicides may take place at dawn shows that even if plant biochemical activity is reduced with dawn applications, this does not affect the ability of the plant to move auxinic herbicides (Johnston et al. 2018).

Why increased *NCED1* expression does occur at dawn requires further investigation. The carotenoid biosynthetic pathway is closely tied with ABA biosynthesis, and light has been shown to repress genes directly involved in carotenoid biosynthetic pathways in carrot (*Daucus carota* L.) (Parry et al. 1990; Fuentes et al. 2012). Whether or not this also results in a reduction in auxin-inducible ABA concentrations demands further research. Interestingly and to the contrary, the same research by Parry et al. (1990) illustrated that the production of ABA in etiolated common bean (*Phaseolus vulgaris* L.) seedlings is maintained despite reductions in carotenoid concentrations compared to light-grown seedlings. This suggests that the role of light in ABA and/or carotenoid production is either species-specific or that some other mechanism(s) may be involved in this relationship. How the production of carotenoids correlates with *NCED1*

expression (and ABA concentrations overall) in *A. palmeri* would provide valuable insights into the regulation of auxinic herbicide activity across times of day.

The lack of consistent trends in *ACS1* expression across studies convolutes the ability to draw any direct conclusions concerning the role of ethylene biosynthesis in auxinic herbicide efficacy. Since no significant time of application effects were detected, there may another mechanism (in addition to there still being a possibility of differential *ACS1* expression not picked up by this research) that causes the reported increase in ethylene production with dicamba applications at mid-day compared to dawn (Johnston et al. 2019). Regardless, that lack of a significant time of application effect suggests that of *ACS1* expression via 2,4-D may be constant across both application times. This may involve differential auxinic herbicide conjugation, metabolism, or ethylene signaling across times of day. Further research is necessary to investigate this phenomenon.

Overall, it appears that reductions in auxinic herbicide activity at dawn coincides with an increase in *NCED1* expression and potentially increased ABA concentrations in the plant cell. For this reason, the increase in *NCED1* activity not only at dawn but also potentially under other conditions imparting plant stress (due to higher ABA concentrations) may result in a reduction of efficacy for growers. As such, it may be recommended that auxinic herbicides be applied not only to plants between an hour after dawn and an hour before dusk, but also to *A. palmeri* plants under a negligible amount of stress.

References

Allan AC, Fricker MD, Ward JL, Beale MH, Trewavas AJ (1994) Two transduction pathways mediate rapid effects of abscisic acid in *Commelina* guard cells. Plant Cell 6:1319-1328

Allen GJ, Kwak JM, Chu SP, Llopis J, Tsien RY, Harper JF, Schroeder JI (1999) Cameleon calcium indicator reports cytoplasmic calcium dynamics in *Arabidopsis* guard cells. Plant J. 19:735-747

Assad R, Reshi ZA, Snober J, Rashid I. (2017) Biology of Amaranths. Bot. Rev. 83:382-436

Behrens MR, Mutlu N, Chakraborty S, Dimitru R, Jiang WZ, LaVallee BJ, Herman PL, Clemente TE, Weeks DP (2007) Dicamba resistance: enlarging and preserving biotechnology-based weed management strategies. Science 216:1185-1188

Bours R, van Zanten M, Pierik R, Bouwmeester H, van der Krol A (2013) Antiphase light and temperature cycles affect PHYTOCHROME B-controlled ethylene sensitivity and biosynthesis, limiting leaf movement and growth of Arabidopsis. Plant Physiol. 163:882-895

Buchanan BB, Gruissem W, Jones RL (2000) Biochemistry and molecular biology of plants. Rockville, MD: The American Society of Plant Biologists. Pp. 895-901

Culpepper AS, Grey TL, Vencill WK, Kichler JM, Webster TM, Brown SM, York AC, Davis JW, Hanna WW (2006) Glyphosate-resistant Palmer amaranth (*Amaranthus palmeri*) confirmed in Georgia. Weed Sci. 54:620-626

Culpepper S (2014) Application time of day influence on Roundup, Reflex, and Clarity. Unpublished raw data

Dat J, Vandenabeele S, Vranová E, Van Montagu M, Inzé D, Van Breusegem F (2000) Dual action of the active oxygen species during plant stress responses. Cell Mol. Life Sci. 57:779-795

De Smet I, Signora L, Beeckman T, Inzé D, Foyer CH, Zhang H (2003) An abscisic acid-sensitive checkpoint in lateral root development of *Arabidopsis*. Plant J. 33:543-555

Downton WJS, Loveys BR, Grant WJR (1988) Stomatal closure fully accounts for the inhibition of photosynthesis by abscisic acid. New Phytol. 108:263-266

Dunlap JR, Robacker KM (1990) Abscisic acid alters the metabolism of indole-3-acetic acid in senescing flowers of *Cucumis melo* L. Plant Physiol. 94:870-874

Egan JF, Maxwell BD, Mortensen DA, Ryan MR, Smith RG (2011) 2,4-dichlorophenoxyacetic acid (2,4-D)-resistant crops and the potential for evolution of 2,4-D-resistant weeds. Proc. Natl. Acad. Sci. 108:E37

EPA (2017) Registration of dicamba for use on genetically engineered crops. United States Environmental Protection Agency. <https://www.epa.gov/ingredients-used-pesticide-products/registration-dicamba-use-genetically-engineered-crops>

Figueiredo MRA, Leibhart LJ, Reicher ZJ, Tranel PJ, Nissen SJ, Westra P, Bernards ML, Kruger GR, Gaines TA, Jugulam M (2017) Metabolism of 2,4-dichlorophenoxyacetic acid contributes to resistance in a common waterhemp (*Amaranthus tuberculatus*) population. Pest Manag. Sci. doi:10.1002/ps.4811

Finlayson SA, Lee IJ, Mullet JE, Morgan PW (1999) The mechanism of rhythmic ethylene production in sorghum. The role of phytochrome B and simulated shading. Plant Physiol. 119:1083-1089

Foes MJ, Tranel PJ, Wax LM, Stoller EW (1998) A biotype of common waterhemp (*Amaranthus rudis*) resistant to triazine and ALS herbicides. Weed Sci. 46:514-520

Fuentes P, Pizarro L, Moreno JC, Handford M, Rodriguez-Concepcion M, Stange C (2012) Light-dependent changes in plastid differentiation influence carotenoid gene expression and accumulation in carrot roots. Plant Mol. Biol. 79:47-59

Giacomini DA, Umphres AM, Nie H, Mueller TC, Steckel LE, Young BG, Scott RC, Tranel PJ (2017) Two new *PPX2* mutations associated with resistance to PPO-inhibiting herbicides in *Amaranthus palmeri*. Pest Manag. Sci. 2017:10.1002/ps.4581

Giacomini DA, Sammons RD, Tao N, Xiang B, Zhou X, Yang S-P, Du Z, Kerstetter RA, Ward S, Westra P, Tranel PJ (2019) A *de novo* draft assembly of Palmer amaranth (*Amaranthus palmeri* S. Watson) using Illumina short and long read technology. In prep

Godar AS, Varanasi VK, Nakka S, Vara Prasad PV, Thompson CR, Jugulam M (2015) Physiological and molecular mechanisms of differential sensitivity of Palmer amaranth (*Amaranthus palmeri*) to mesotrione at varying growth temperatures. PLoS One 10:e0126731

Grossmann K, Scheltrup F, Kwiatkowski J, Caspar G (1996) Induction of abscisic acid is a common effect of auxin herbicides in susceptible plants. J. Plant Physiol. 149:475-478

Grossmann K (1998) Quinclorac belongs to a new class of highly selective auxin herbicides. Weed Sci. 46:707-716

Grossmann K (2003) Mediation of herbicide effects by hormone interactions. J. Plant Growth Regul. 22:109-122

Grossmann K (2009) Auxin herbicides: current status of mechanism and mode of action. Pest Manag. Sci. 66:113-120

Hansen H, Grossmann K (2000) Auxin-induced ethylene triggers abscisic acid biosynthesis and growth inhibition. Plant Physiol. 124:1437-1448

Hartzler B (2017) Dicamba: Past, present, and future. Proc. Integ. Crop Manag. Conf. 12

Heap I (2014) Herbicide resistant weeds. *In* Pimentel D, Peshin R eds. Integrated Pest Management. Dordrecht, Netherlands: Springer Dordrecht. Pp. 281-301

Horak MJ, Loughin TM (2000) Growth analysis of four *Amaranthus* species. Weed Sci. 48:347-355

Johnston CR, Eure PM, Grey TL, Culpepper AS, Vencill WK (2018) Time of application influences translocation of auxinic herbicides in Palmer amaranth (*Amaranthus palmeri*). Weed Sci. 66:4-14

Johnston CR, Malladi A, Randell TM, Vencill WK, Grey TL, Culpepper AS, Czarnota MA, Henry GM (2019) Time of application and translocation inhibition influence 2,4-D and dicamba-induced ethylene production in Palmer amaranth. Unpublished manuscript

Jonas H (1981) Responses of free running leaf movements to light, in particular to red and far red light during sunrise and sunset. Experientia 37:571-573

Kraft M, Kuglitsch R, Kwiatkowski J, Frank M, Grossmann K (2007) Indole-3-acetic acid and auxin herbicides up-regulate 9-cis-epoxycarotenoid dioxygenase gene expression and abscisic acid accumulation in cleavers (*Galium aparine*): interaction with ethylene. J. Exp. Bot. 58:1497-1503

Manalil S, Busi R, Renton M, Powles SB (2011) Rapid evolution of herbicide resistance by low herbicide dosages. Weed Sci. 59:210-217

Neve P, Powles S (2005) Recurrent selection with reduced herbicide rates results in the rapid evolution of herbicide resistance in *Lolium rigidum*. Theor. Appl. Genet. 110:1154-1166

Norsworthy JK, Ward SM, Shaw DR, Llewellyn RS, Nichols RL, Webster TM, Bradley KW, Frisvold G, Powles SB, Burgos NR, Witt WW, Barrett M (2012) Reducing the risks of herbicide resistance: best management practices and recommendations. Weed Sci. 60:31-62

Parry AD, Babiano MJ, Horgan R (1990) The role of cis-carotenoids in abscisic acid biosynthesis. Planta 182:118-128

Rieu I, Powers SJ (2009) Real-time quantitative RT-PCR: Design, calculations, and statistics. Plant Cell 21:1031-1033

Romero-Puertas M, McCarthy I, Gómez M, Sandalio L, Corpas F, Del Rio L, Palma J (2004) Reactive oxygen species-mediated enzymatic systems involved in the oxidative action of 2,4-dichlorophenoxyacetic acid. Plant Cell Environ. 27:1135-1148

Ruijter JM, Ramakers C, Hoogaars WMH, Karlen Y, Bakker O, van den Hoff MJB, Moorman AFM (2009) Amplification efficiency: linking baseline and bias in the analysis of quantitative PCR data. Nucleic Acids Res. 37:e45

Scheltrup F, Grossmann K (1995) Abscisic-acid is a causative factor in the mode of action of the auxinic herbicide quinmerac in cleaver (*Galium aparine* L.). J. Plant Physiol. 147:118-126

Schroeder JI, Kwak JM, Allen GJ (2001) Guard cell abscisic acid signaling and engineering drought hardiness in plants. Nature 410:327-330

Shoup DE, Al-Khatib K, Peterson DE (2003) Common waterhemp (*Amaranthus rudis*) resistance to protoporphyrinogen oxidase-inhibiting herbicides. Weed Sci. 51:145-150

Skelton JJ (2015) Uptake, translocation, and metabolism of 2,4-D in Enlist crops and control of drought-stressed waterhemp (*Amaranthus tuberculatus*) with 2,4-D and glyphosate (Doctoral dissertation. IL Digital Environment for Access to Learning and Scholarship. <http://hdl.handle.net/2142/88156>

Song Y (2014) Insight into the mode of action of 2,4-dichlorophenoxyacetic acid (2,4-D) as an herbicide. J. Integr. Plant Biol. 56:106-113

Sterling TM, Hall J (1997) Mechanism of action of natural auxins and the auxinic herbicides. Rev. Toxicol. 1:111-142

Stewart CL, Nurse RE, Sikkema PH (2009) Time of day impacts postemergence weed control in corn. Weed Technol. 23:346-355

Stothard P (2000) The Sequence Manipulation Suite: JavaScript programs for analyzing and formatting protein and DNA sequences. Biotechniques 28:1102-1104

Taiz L, Zeiger E (2010) Plant Physiology. 5th edn. Sunderland, MA: Sinauer Associates, Inc.

Yang SF, Hoffman NE (1984) Ethylene biosynthesis and its regulation in higher plants. Ann. Rev. Plant Physiol. 35:155-189

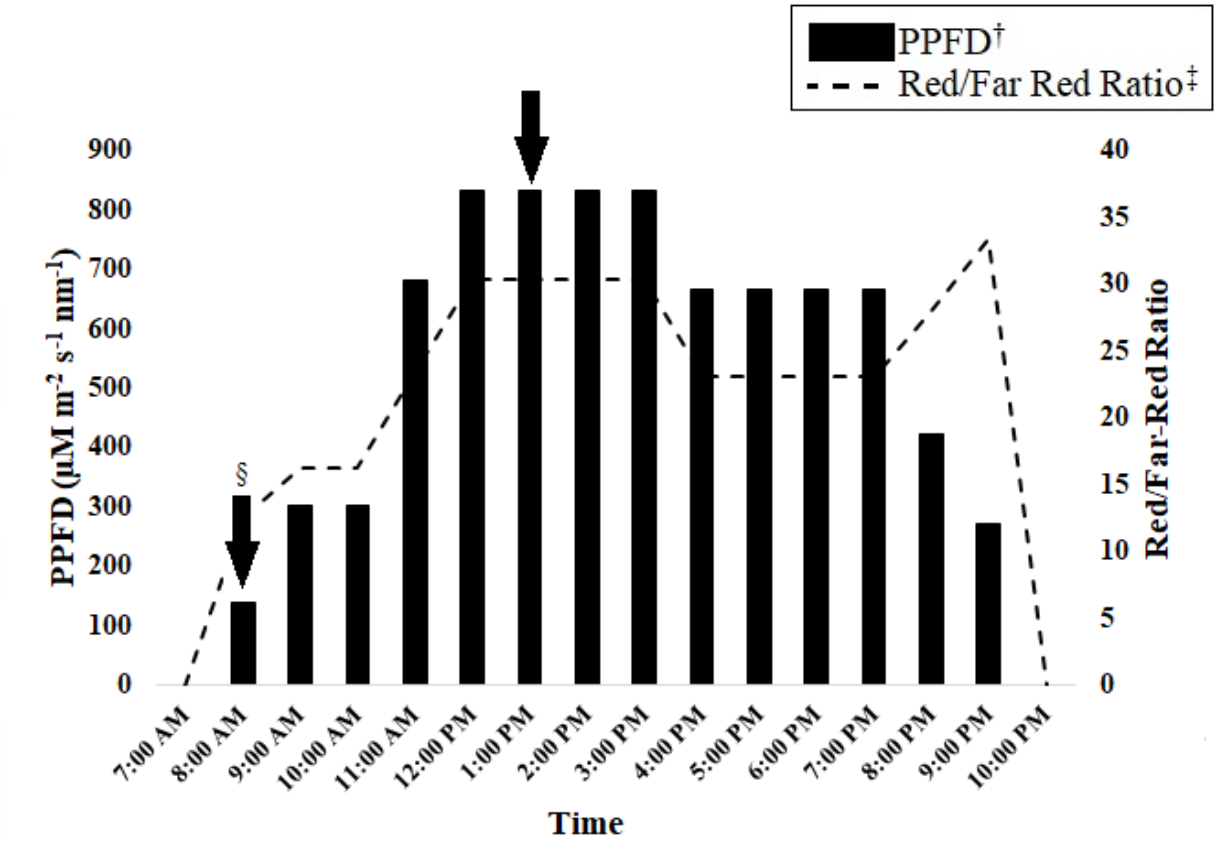

Figure 4.1. LED light program used for *A. palmeri* plants in laboratory for 2,4-D and dicamba applications, 2018.

†PPFD = Photosynthetic Photon Flux Density.

‡Red light range = 635 – 685 nm; Far-red light range = 710 – 760 nm.

§Black arrows represent both simulated dawn and mid-day application times of 2,4-D and dicamba.

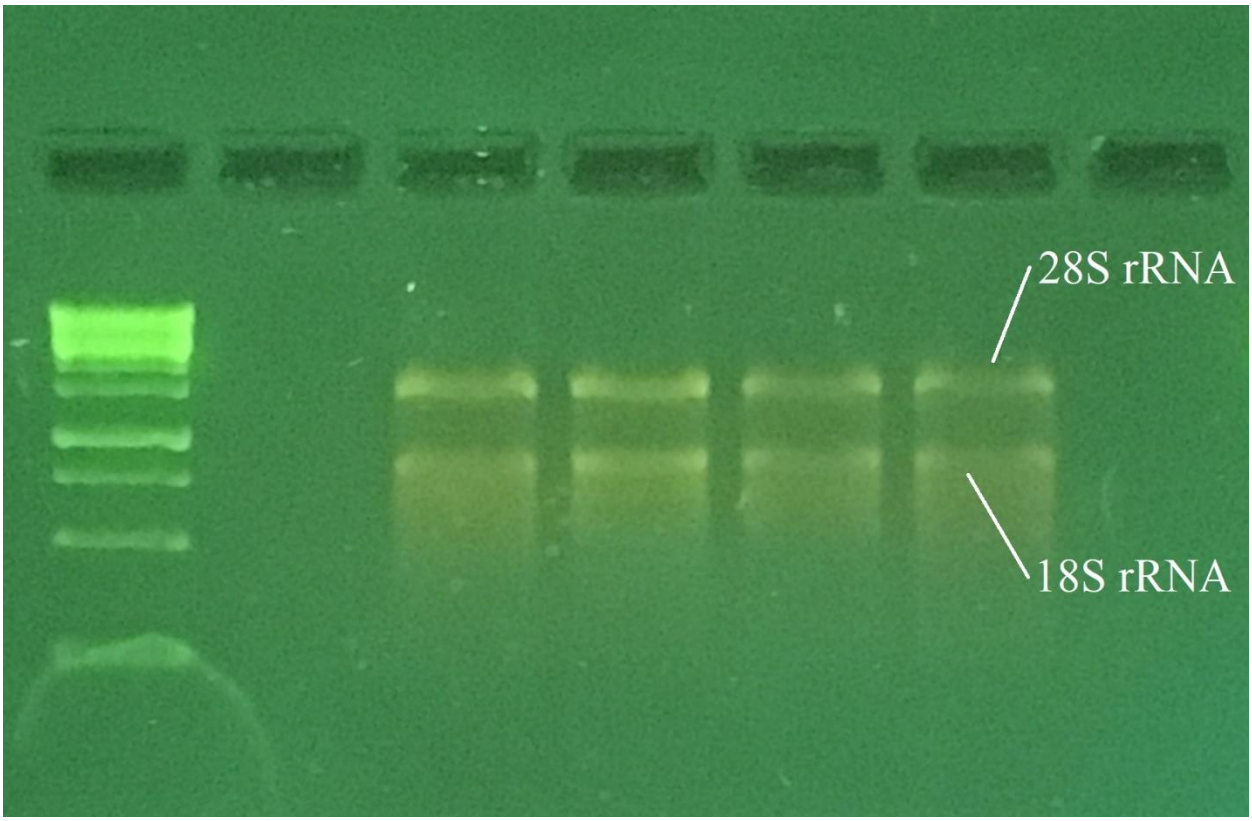

Figure 4.2. Gel electrophoresis of RNA samples used to confirm quality of rRNA. 1.2% agarose in TBE buffer, 2018.

[†]Intact, quality RNA confirmed by clear presence of rRNA bands from the large subunit (28S) and small subunit (18S).

[‡]Middle four lanes represent test of final extraction procedure used for study. All further samples subjected to same criteria for determining presence of intact, quality RNA.

```
AHYPO_017265-RA      ------------------------------------------------------------      0
AHYPO_008268-RA      ----------ATGA----------TCATCATGAATCCTACAATAACTCCTACATCAACC      39
AHYPO_004405-RA      ATGGCATCAATTAGTAATACTAATTGGGTAATTAAACCCCAAATTACCTCTAAATCAAAG      60


AHYPO_017265-RA      ------------------------------------------------------------      0
AHYPO_008268-RA      A------------ATACAACTACAATAAATATAC--------CCTACAAAGCCCATTTAC      79
AHYPO_004405-RA      CTTCATTTGGGTTCTAATCCTACCCTTAAGTGGCCTAAAAAAGCTACCCATTCTATTAAC      120


AHYPO_017265-RA      ------------------------------------------------------------      0
AHYPO_008268-RA      CCATCTCTTCTAAGCCCAT-----TTTCAGCCCGAAAAAGCCCATTACCATTCATTGTGC      134
AHYPO_004405-RA      TCTGTTCTTCAATTACCTTTACTTGATTCTCCTAAAAAATCCAATATCCAACCC------      174


AHYPO_017265-RA      ------------------------------------------------------------      0
AHYPO_008268-RA      TCTTCACTCAGCAGCCCCTCCTTCCATTTTCCATTT---CCCAAACCATGAATCATCACC      191
AHYPO_004405-RA      -------AAATCCCCACCTACTAAAAATTTCCCTACAAATCCTTCTACTCTTAATCCCCC      227


AHYPO_017265-RA      ------------------------------------------------------------      0
AHYPO_008268-RA      CAAATCTTCTCCTCCTCATCATCTTCCTCAATGGAACCTTTTCCAAAAAGCTGCTGCATC      251
AHYPO_004405-RA      CAAAAAATCATCGAATCCTCTACCTCATCAATGGAACCCAATTCAAAAAGCTGCTTCAAT      287


AHYPO_017265-RA      ------------------------------------------------------------      0
AHYPO_008268-RA      AACCTTTGACTTCATTGAAAACACCCTTACAACCCGAGAACGTGCCCACCCGTTTCCCAA      311
AHYPO_004405-RA      TGCTTTAGACATGGTGGAAAATGCCATAAATTCCTTTGAAAACCAACACCCACTTCCAAA      347


AHYPO_017265-RA      ------------------------------------------------------------      0
AHYPO_008268-RA      AACATCCGACCCGAAAATCCAAATATCCGGTAACTTCGCCCCAGTACAAGAAACCCCCGT      371
AHYPO_004405-RA      AACATCCGACCCGAGGGTCCAAATATCCGGTAATTTCGCCCCGGTACCTGAACAACCCGT      407


AHYPO_017265-RA      ------------------------------------------------------------      0
AHYPO_008268-RA      CAAACAATCTCTCCCTATCATAGGAGAAATACCATCTTGCATTGACGGCGTTTACGTACG      431
AHYPO_004405-RA      TAAAAAGAACCTTCCAGTTATCGGGTCTATCCCAGAATGTATCCGTGGAGTGTACGTTAG      467


AHYPO_017265-RA      ----------------ATGCTACCACCCTCTGGTGCCCATCACTTGTTTGACGGTGATGG      44
AHYPO_008268-RA      AAACGGCGCTAACCCTTTATTCAAACCAACCGCCGGCCACCATTTATTTGACGGTGACGG      491
AHYPO_004405-RA      AAACGGAGCTAACCCACTTTACGAACCCGTAGCCGGTCATCATTTCTTTGACGGTGACGG      527
                                      *      ***    *  *  ** ** ** ********** **

AHYPO_017265-RA      GATGATCCACGCCGTTAAACTTGGACCGGGAAATAAAGCCTCTTACTGCTGCCGGTTTAC      104
AHYPO_008268-RA      CATGGTTCACGCCGTTACCATCCACAACGG---GGTAGCAAGTTACGCCTGTAGATTCAC      548
AHYPO_004405-RA      AATGATTCACGCCGTTCAGTTTAACTCCGATGGGTCTGTGAATTACTGTTGCCGGTTCAC      587
                      *** * *********    *       *        *    ****   **  * ** **

AHYPO_017265-RA      TAAAACAAACCGGTTTGTTCAAGAAAAAGCAGCCGGGAGACAGTTATTCCCTAAACCGGT      164
AHYPO_008268-RA      TGAAACCAACAGATTAACGCAAGAACGGGATCTGGGTCGAGCTGTTTTCCCTAAATCTAT      608
AHYPO_004405-RA      TGAAACCCACCGGTTTAAACAAGAACGGGAGTTGGGTCGACCCATTTTCCCTAAAGCAAT      647
                     * ****  ** * **    ******   *     **  **    * ********* *  *

AHYPO_017265-RA      TAGTGAATTGCACGGTCAAACCGGATTGCTTAGGCTGGGTTTATTTTATGCACGTGTCGC      224
AHYPO_008268-RA      CGGTGAACTCCATGGTCATTCAGGAATTGCTAGATTGTTTTTGTTTTACGCTCGTGGGTT      668
AHYPO_004405-RA      CGGTGAATTACATGGGCATTCGGGTATCGCCCGTCTTCTTTTGTTCTACTCCCGTGCTCT      707
                       ***** * ** ** **  * **  *     *  *   *** ** **  * ****

AHYPO_017265-RA      TGTTGGGTTAATTAATCCGTCACGTGGGACAGGTGTCGCTAATGCTGGGTTAGTTTATTT      284
```

```
AHYPO_008268-RA      GTTTGGGCTTTTGAATCATGAAAATGGTATGGGTGTTGCTAATGCTGGTTTAGTTTATTT      728
AHYPO_004405-RA      GTTCGGTCTACTAGATCAAAACAATGGTATAGGAGTAGCAAACGCTGGAGTAGTTTATTT      767
                       * **  *  *  ***       *** *  ** ** ** ** *****  **********

AHYPO_017265-RA      TAACGGAAGATTGCTTGCTATGTCCGAGGACGACTTGCCATATCATGTTAAAATCAACGG      344
AHYPO_008268-RA      TAATGGAAGGTTGTTAGCTATGTCAGAAGATGATATACCTTACCATGTAAAAGTTACCTC      788
AHYPO_004405-RA      CAATAACAGATTATTAGCTATGTCGGAAGATGATTTACCTTATCAAATTCAAATTACTCC      827
                      **    ** **  * ******** ** ** **  * ** ** **  *  ** * *

AHYPO_017265-RA      CGATGGTGATTTGATTACGATCGGACGGTTTAATTTTAACGAGCAGGTAAACTGCCCTTT      404
AHYPO_008268-RA      TAATGGCGATTTAAAAACTGTGGGAAGGTTTGATTTCAATGGGCAGTTAAATTCCTCCAT      848
AHYPO_004405-RA      TTCAGGTGATCTGAAAACTGTTGGTAGATATGGATTTAATGGCGAATTGAAATCAACAAT      887
                         ** *** * *  **  * **  * * *   ** ** *   *  * ** *   *  *

AHYPO_017265-RA      GATAGCACACCCTAAGGTGGACCCTATCACAGGGGATTTTCATACGTTAAGCTACGACGT      464
AHYPO_008268-RA      GATTGCTCACCCAAAACTTGATCCACAATCCAAAGAATTATTTGCTTTAAGTTACGATGT      908
AHYPO_004405-RA      GATTGCGCATCCAAAAATCGATCCGGTTAGTCATGAAATGTTCGCTTTAAGCTACGATGT      947
                     *** ** ** ** **  * ** **          **  *     * ***** ***** **

AHYPO_017265-RA      CTTACGTAGACCGTATCTTAAATACTTCAGGTTCGATAAGAAGGGCCAGAAATCTCGTGA      524
AHYPO_008268-RA      TATTAAACCTCCATTTCTTAAATACTTTAAATTTTCACGGGATGGTGAGAAATCTGAAGA      968
AHYPO_004405-RA      TGTGAAGAAACCCTATTTGAAATACTTCTATTTCAAAGAAAATGGTACGAAATCTGCTGA     1007
                       *       ** * * * ********    **        * **   *******   **

AHYPO_017265-RA      GGTACACGTGCCTCTTACAAAGCCTACTATGATTCATGACTTTGCTATAACTAAAAACTA      584
AHYPO_008268-RA      TGTTGAAATCCCATTAAAGGAACCTACAATGATGCATGATTTCGCTATTACCCAGAATTT     1028
AHYPO_004405-RA      TGTTGAAATTGATCTTAAATCACCAACTATGATGCATGATTTCGCAATTTCGGAGAATTT     1067
                      **  *  *     * *     ** ** ***** ***** ** ** **  *  * ** *

AHYPO_017265-RA      CGTAATCATCCCGGATAATCAAGTTGTATTCAAGCTATCCGAAATGGTTTGGGGCGGGTC      644
AHYPO_008268-RA      TGTAGTTATCCCAGATCAACAGGTGGTGTTTAAGATGAAGGAAATGATTACCGGAGGATC     1088
AHYPO_004405-RA      CGTTATAATTCCTGATTCACAAGTTGTGTTTAAGCTTCAAGAAATGATCCATGGCGGTTC     1127
                      **  * ** ** ***   ** ** ** ** *** *    ****** *    ** ** **

AHYPO_017265-RA      ACCTCTCGGGTTTGACCCAAATAAAAAGGCCCGATTTGGGATTCTTTCAAAGGAGGATAC      704
AHYPO_008268-RA      TCCCGTTGTTTTTGACAAGAACAAAACGTCGCGTTTTGGGGTTATGAGAAAAGACGCTAA     1148
AHYPO_004405-RA      ACCTGTTGTTTTCGATAAAGAGAAGGTTTCTCGATTCGGAATTCTCCCTAAATATTCAAA     1187
                      **  * *  ** **     * **     * ** ** **  ** *    **  *    *

AHYPO_017265-RA      AAATGGGTTGAAGATAAAATGGGTTGAAGTTCCGAATAGCTTTTGCTTTCATTTTATAAA      764
AHYPO_008268-RA      AAAAGCGTCGGAAATTGTATGGGTTGATTCTCCTGACACTTTTTGCTTCCATGTTTGGAA     1208
AHYPO_004405-RA      ATCTTCCGATGAAATTCAATGGATTGATGTTCCAGATTGTTTTTGCTTTCATTTATGGAA     1247
                     *          * **   **** ****   ***  *    ******** *** *    **

AHYPO_017265-RA      TGCATGGGAAGAAAATGAAGGTAGAAATATAGTTATTATCGGGTCATGCATGAGCCCACC      824
AHYPO_008268-RA      CGCTTGGGAAGAATCTCAAAGCGACGAGATTGTGGTTATTGGGTCTTGTATGACTCCTCC     1268
AHYPO_004405-RA      TGCTTGGGAAGAATCTGACTCCGATGAGATCGTCGTAATTGGATCTTGTATGACTCCGGC     1307
                      ** *********  * *       * ** **  * ** ** ** ** ****  **  *

AHYPO_017265-RA      CGATTCAATATTTACCGAGAGTGATGAACCGGCCCGAATAGAGCTTTGTGAAATCGGGTT      884
AHYPO_008268-RA      TGATTCTATTTTTAATGAATGTGATGAAAATTTAAAGAGTGTTTTATCTGAAATCCGGCT     1328
AHYPO_004405-RA      CGACTCCATTTTCAACGAATGTGACGAGAATCTCTCTAGTGTGTTGTCCGAAATCCGATT     1367
                      ** ** ** ** *  **  **** **          *  *   * *  ****** *  *

AHYPO_017265-RA      GGATGTCGAAACGGGTAAATCAACCCGACGGGTGATAGTTTT---------------GGG      929
AHYPO_008268-RA      TAATTTAAGGACGGGTCAGTCAACCCGACGACCCATTATTGACCCGGCCCTGTATGATCA     1388
AHYPO_004405-RA      AAACCGTAAAACCGGAGTTTCAACCCGGAGAGAAATCCTTCCG------AATTCGGAGAA     1421
                       *       ** **    ********  *    **  **

AHYPO_017265-RA      TATGAATTTAGAAGTAGGGCAAGTAAATAAAAAGCTCTTAGGAAGAAAGACAAGGTACGT      989
AHYPO_008268-RA      TTTTAATCTTGAAGCGGGTATGGTAAACCGTAATTTACTTGGGAGAAAAACCCGGTTTGC     1448
```

Figure 4.3. Multiple *NCED3* sequence alignment for scaffolds 71, 28, and 373, made using Clustal Omega 0(1.2.4), 2018.

†Scaffold sequences obtained from running *NCED3* sequence of *A. thaliana* (Locus tag: AT3G14440) against the *A. hypochondriacus* genome in Phytozome 12.

‡Underlined green sequences indicate initial forward primers and underlined red sequences indicate initial reverse primers that were used to amplify the preliminary PCR product from *A. palmeri* to be sequenced at the Georgia Genomics Facility. Reverse complement of underlined red sequences were used for primers.

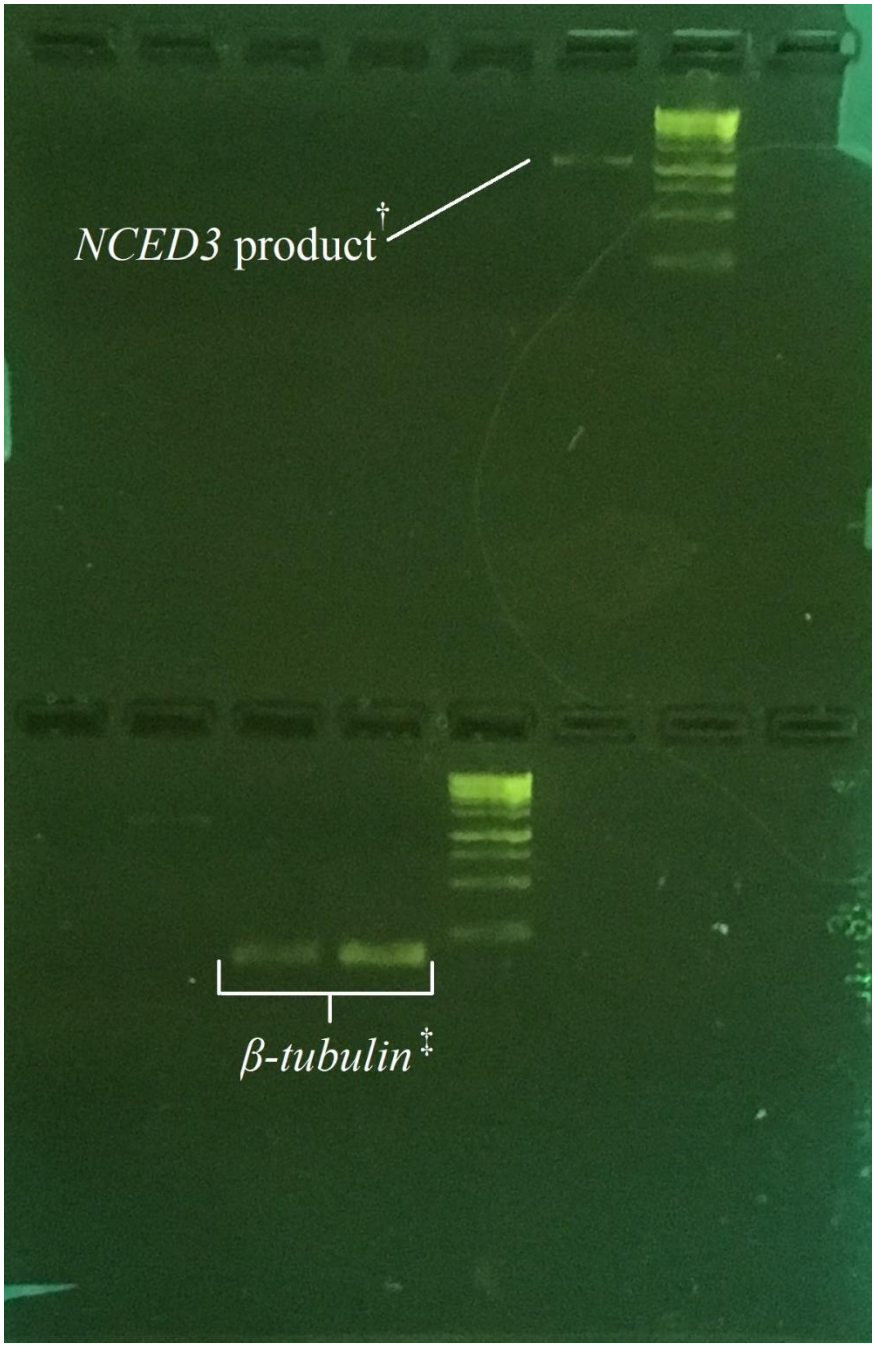

Figure 4.4. Initial amplification of potential *NCED1* gene product using gel electrophoresis. 1.2% agarose in TBE buffer, 2018.

†Potential *NCED1* product amplified using a 1X strength PCR reaction mixture, ~1,000 bp. Primer sequences: F 5'-GGTCATCATTTCTTTGACGGTGA-3' and R 5'-AATCCAGACACCTTTGGCCA-3'.

‡*β-tubulin* PCR primers used for reference gene. Primer sequences: F 5'-ATGTGGGATGCCAAGAACATGATGTG-3' and R 5'-TCCACTCCACAAAGTAGGAAGAGTTCT-3'.

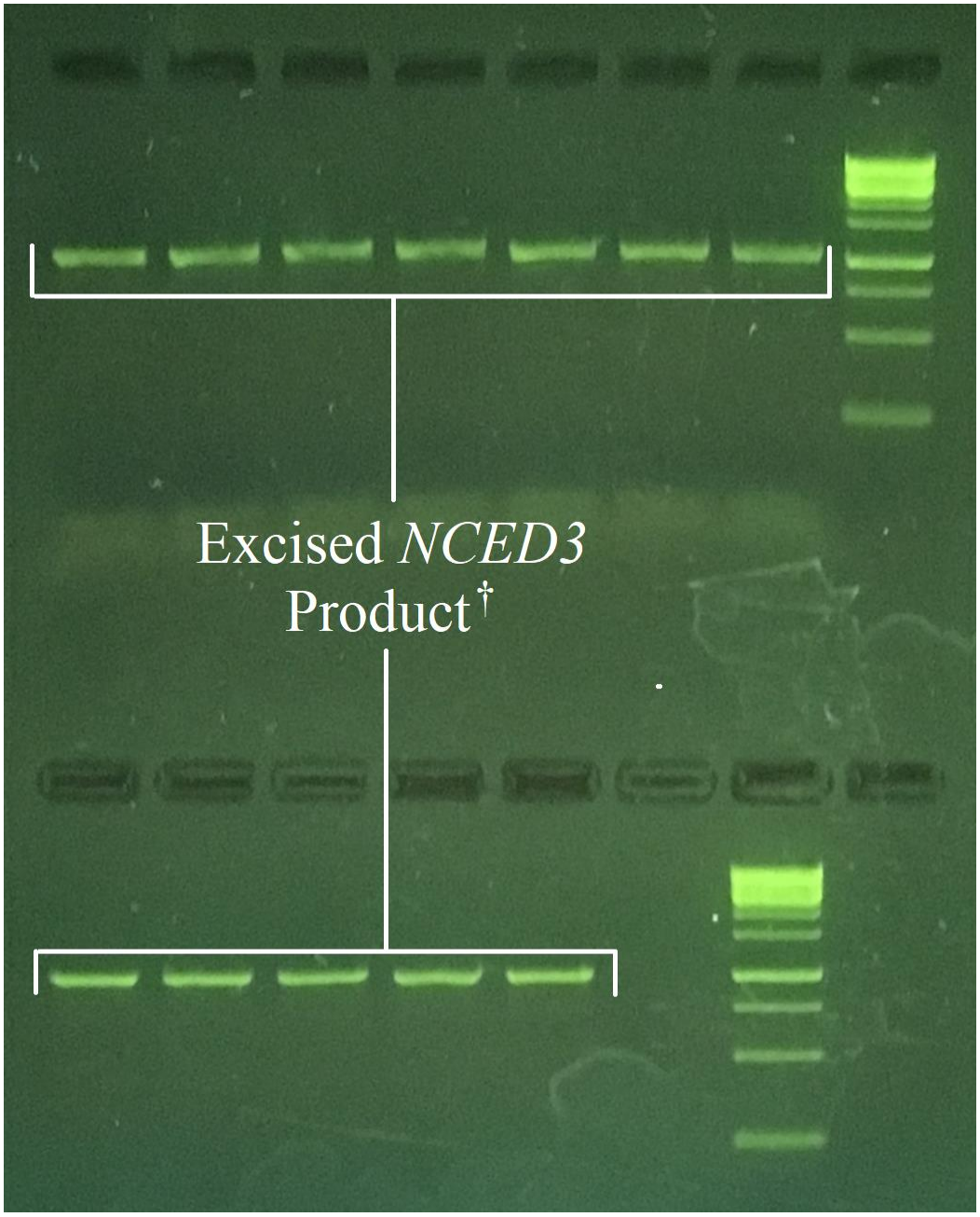

Figure 4.5. Potential *NCED1* gene used for DNA extraction, isolated using gel electrophoresis. 1.2% agarose in TBE buffer, 2018.

†Potential *NCED1* product amplified using a 2X strength PCR reaction mixture, ~1,000 bp. Primer sequences: F 5'-GGTCATCATTTCTTTGACGGTGA-3' and R 5'-AATCCAGACACCTTTGGCCA-3'.

A)
GTGACGGAATGATTCACGCCGTTCAGTTTAANTNGGATGGGTCTGTGAATTACTGTT
GCCGGTTCACGGAAACCCACCGGTTTAAACAAGAACGGGAGTTGGGCCGACCCATT
TTCCCTAAAGCAATTGGTGAATTACATGGGCATTCGGGTATTGCCCGTCTACTATTGT
TCTACTCCCGTGCTCTGTTCGGTCTGCTAGATCAAAACAATGGTATAGGAGTAGCAA
ACGCTGGAGTAGTTTATTTCAATAACAGATTATTAGCTATGTCGGAAGATGATTTAC
CTTATCAAATTCAAATTACTCCGTCAGGTGATCTGAAAACTGTTGGTAGATATGGAT
TTAATGGAGAATTGAAATCGACAATGATTGCGCATCCGAAAATCGATCCGGTTAGTC
ATGAAATGTTCGCTTTAAGCTACGATGTTGTGAAGAAACCCTATCTGAAATACTTTT
ATTTCAAAGAAAATGGTACGAAATCTGCTGATGTTGAAATTGATCTTAAATCACCAA
CTATGATGCATGATTTCGCAATTTCGGAGAATTTCGTTATAATTCCTGATTCACAAGT
TGTGTTTAAGCTTCAAGAAATGATCCATGGCGGTTCCCCTGTAGTTTTCGATAAAGA
GAAGGTTTCGCGATTCGGAATTCTCCCTAAATATTCAAAATCTTCCGATGAAATTCA
ATGGATTGATGTTCCAGATTGTTTTTGCTTTCATTTGTGGAATGCTTGGGAAGAATCC
GACTCCGATGAGATCGTCGTAATCGGATCTTGTATGACTCCGGCCGACTCCATTTTC
AACGAATGTGACGAGAATCTCTCTAGTGTGTTGTCCGAAATCCGATTAAACCGTAAA
ACCGGAGTTTCAACCCGGAGAGAAATCCTTCCGAATTCGGAGAAAATGAATTTAGA
AGCAGGAATGGTGAACAAGAACAAACTCGGAAGAAAAACACAATC

B)
DGMIHAVQFXXDGSVNYCCRFTETHRFKQERELGRPIFPKAIGELHGHSGIARLLLFYSR
ALFGLLDQNNGIGVANAGVVYFNNRLLAMSEDDLPYQIQITPSGDLKTVGRYGFNGELK
STMIAHPKIDPVSHEMFALSYDVVKKPYLKYFYFKENGTKSADVEIDLKSPTMMHDFAI
SENFVIIPDSQVVFKLQEMIHGGSPVVFDKEKVSRFGILPKYSKSSDEIQWIDVPDCFCFH
LWNAWEESDSDEIVVIGSCMTPADSIFNECDENLSSVLSEIRLNRKTGVSTRREILPNSEK
MNLEAGMVNKNKLGRKTQ

Figure 4.6. Reverse strand of coding sequence for *NCED1* product obtained from Sanger capillary sequencing (A) and associated protein sequence at 3rd reading frame (B), 2018.

†Sequencing primers used in reaction mixture: F 5'-GGTCATCATTTCTTTGACGGTGA-3' and R 5'-AATCCAGACACCTTTGGCCA-3'.

ATGGTGAAAGAAGTGTTGTTATCAAAAATGGCAGCAGGAAATGGGCATGGTGAAGA
ATCAGCCTATTTTGATGGGTGGAAAGCTTATGAAAATAACCCTTTTCACCCTGTAAA
TAATCCTCGAGGTGTTATTCAGATGGGTCTTGCTGAAAATCAGCTTTGCTTCGATCTG
GTGAAAGAGTGGATTGTGAAAAATCCAGAAGCTTCCATCTGTACAGTTGAAGGAGT
TGATTCCTTCAAAGATATTGCCATCTTTCAGGATTACCACGGTTTACCACACTTTAGA
AATGCAGTAGCAAAATTGATGGAGAAAGTGAGAGGCAATAAGGTGAGATTTGACCC
AGATAGAATAGTTATGAGCGGGGGAGCAACTGGAGCCCATGAAATGATGGTATTT
TGCTTGGCCAACCCTGGTGAAGCCTTCCTGGTTCCTACACCTTACTATCCTGCATTTG
ATAGAGATTTGAGGTGGAGAACAGGAGTACAACTTATACCAGTTGAATGTCACAGC
TCAAACAACTTCAAAGTAACGAAATCAGCCTTAGAAAAGGCATATAAAAAAGCTCA
AGACGACAACATTATAGTGAAAGGTTTGATTATAACCAACCCATCAAACCCGTTAG
GGACTGTCTTAGATAGGGAAACCTTAAAGAACATCTTAGCTTTCACTACTGATAAAA
ACATCCATTTAGTATGTGATGAGATTTATGGAGCAACTGTATTTGGTTATCCTAATTT
TGTTAGCATAGCCGAGATACTATTAGACCAAAAACACAACCCGGATCTCATACAC
ATCGTGTATAGCCTCTCGAAAGACTTAGGTTTCCCTGGCTTTCGAGTGGGGATCGTG
TACTCTTACAACGATGATGTTGTAAGCTGTGCAAGAAAAATGTCGAGTTTTGGCCTT
GTTTCGACACAAACACAGACTCTTGTTGCTTCCATGCTCTCGGATGAGGAGTTTGTG
GACAAATTCTTAGCTGAGAGTAGGAAAAGACTAGAAAGTCGACACAATTTGTTCAC
TAGGGGACTTAGCCAATTTGGAATTCAATGCTTGAAAAGCAATGCTGGATTGTTTGT
ATGGATGGATTTAAGGAAACTTATTGAGGAGAATCCAACTGAAGAAGGCGAGCTCG
AGTTGTGGCGAGTGATTATTAATGAAGTGAAGATAAATGTATCACCAGGATGTTCA
TTTCATTGCAAAGAAGCTGGATGGTTTAGAGTATGTATTGCTAACATGGATGATGAA
ACAATGCAAGTTGCTTTAAGAAGGATTAGAAAATTTGCTGCACAAAAGGTGGTAAA
GCCTATTGTTACACCTGCAAAGAGGAAATGTTGGCATCAGAACAATCTTCAGTTAAG
GTTATCAAATAGAAGATTGGATGATTTAATGGGGGTTTCCCAAATGGGATCTCCTCA
TTCTCCATTGCCTCAATCACCTCTTGTTCGAGCTCAATATTAG

Figure 4.7. Coding sequence of *ACS1* in *A. palmeri* used for primer design, established by Giacomini et al. (2019), 2018.

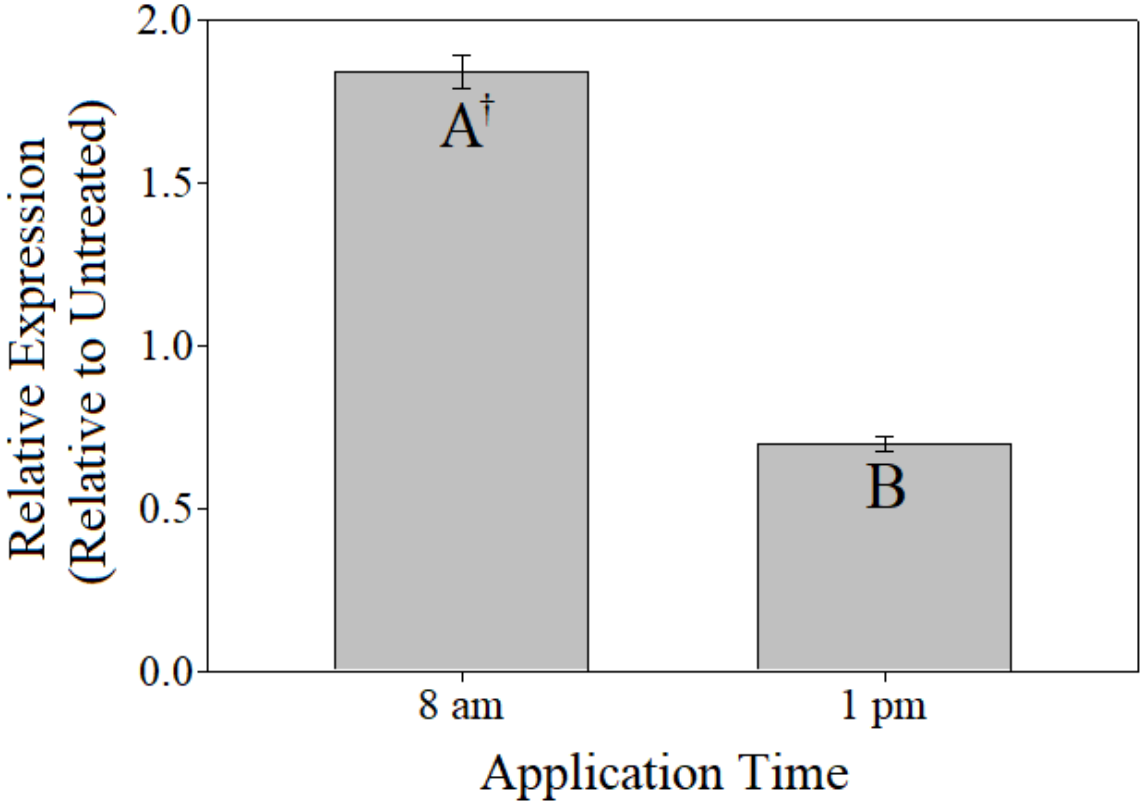

Figure 4.8. Relative expression of *NCED1* resulting from morning and mid-day herbicide applications relative to untreated control, 2018.

†Means followed by different letters differ significantly according to student's t-test at $\alpha = 0.05$.

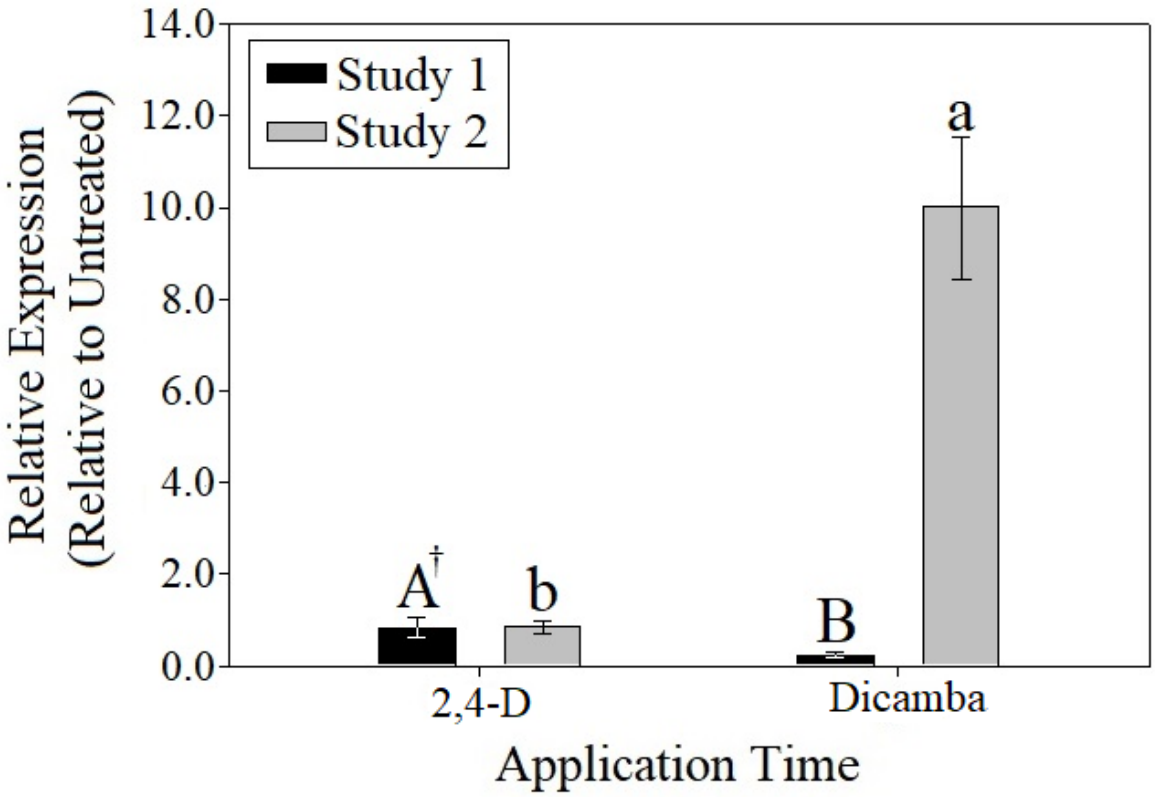

Figure 4.9. Relative expression of *ACS1* resulting from 2,4-D and dicamba applications relative to untreated control, 2018.

†Means followed by different letters differ significantly according to student's t-test at $\alpha = 0.05$. Uppercase letters correspond to comparisons within study one, whereas lowercase letters correspond to comparisons within study two

Table 4.1. Initial primers designed from multiple scaffold alignment of the *A. thaliana NCED3* gene and *A. hypochondriacus* genome, 2018.

Sequence Name	Sequence	GC	T_m
		%	°C
NCED3F1	GGTCATCATTTCTTTGACGGTGA	44	55
NCED3R1	AATCCAGACACCTTTGGCCA	50	57
NCED3F2	TGAAACCCACCGGTTTAAACAAGAA	40	57
NCED3R2	TAAGGAACTCTTGACGGAAGCTT	44	56

Table 4.2. Specific qPCR primers tested and used for quantification of transcript levels, 2018.

†Melting temperatures are based on SYBR Green master mix (intercalating dye) used for qPCR.

Sequence Name	Sequence	GC	T_m†	Amplicon Length
		%	°C	bp
NCED1F1	GGTATTGCCCGTCTACTATTG	48	60	138
NCED1R1	AGGTAAATCATCTTCCGACATAG	39	60	--
NCED1F2	GATCGTCGTAATCGGATCTTG	48	60	126
NCED1R2	TCTCTCCGGGTTGAAACT	50	60	--
NCED1F3	TTACTGTTGCCGGTTCAC	50	60	135
NCED1R3	GCACGGGAGTAGAACAATAG	50	60	--
ACS1F1	GGAGAAAGTGAGAGGCAATAAG	46	61	144
ACS1R1	GCAGGATAGTAAGGTGTAGGA	48	60	--
ACS1F2	GCTTCGATCTGGTGAAAGAG	50	60	119
ACS1R2	GTGTGGTAAACCGTGGTAAT	45	60	--
ACS1F3	AAGCTGGATGGTTTAGAGTATG	41	60	138

ACS1R3	GATGCCAACATTTCCTCTTTG	43	60	--
18SRiboF1	CCTTACGGACGAGCTATTG	53	59	132
18SRiboR1	GAGCACGCTCAAGTTCAT	50	60	--
18SRiboF2	AGTGGATGCACCCAGTATT	47	61	128
18SRiboR2	TCGATGGTTCACGGGATT	50	61	--

Table 4.3. Expression of *NCED1* resulting from morning and mid-day herbicide applications relative to untreated control, 2018.

†NRQ = normalized relative quantity of transcript. Normalized by dividing relative quantity of *NCED1* transcript by relative quantity of *18SRibo*, the reference gene.

‡SE = standard error of the mean. Standard error for relative expression means calculated as described by the equation:

$$SE(\frac{NRQ}{NRQunt}) = [\frac{NRQ\text{^}2}{NRQunt\text{^}2}(\frac{SE(NRQ)\text{^}2}{NRQ\text{^}2} + \frac{SE(NRQunt)\text{^}2}{NRQunt\text{^}2})]^{1/2}$$

where *SE* is the standard error of corresponding terms, *NRQ* is the mean normalized relative quantity for each respective treatment, and *NRQunt* is the mean normalized relative quantity for the untreated control.

§Means followed by different letters differ significantly according to student's t-test at $\alpha = 0.05$.

¶TOA = time of application.

Time of Application	NRQ† (SE‡)	Relative Expression (SE)	
8:00 AM	0.104 (0.0278)	1.842 (0.0512)	A§
1:00 PM	0.0394 (0.0179)	0.699 (0.0242)	B
Untreated	0.0563 (0.0234)		

Study*Herbicide	0.23
Study*TOA¶	0.56
Herbicide	0.37
TOA	0.049
Herbicide*TOA	0.19

Table 4.4. Expression of *ACS1* resulting from 2,4-D and dicamba applications relative to untreated control with studies presented separately, 2018.

†NRQ = normalized relative quantity of transcript. Normalized by dividing relative quantity of *ACS1* transcript by relative quantity of *18SRibo*, the reference gene.

‡SE = standard error of the mean. Standard error for relative expression means calculated as described by the equation:

$$SE(\frac{NRQ}{NRQunt}) = [\frac{NRQ\text{^}2}{NRQunt\text{^}2}(\frac{SE(NRQ)\text{^}2}{NRQ\text{^}2} + \frac{SE(NRQunt)\text{^}2}{NRQunt\text{^}2})]^{1/2}$$

where *SE* is the standard error of corresponding terms, *NRQ* is the mean normalized relative quantity for each respective treatment, and *NRQunt* is the mean normalized relative quantity for the untreated control.

§Means followed by different letters differ significantly according to student's t-test at $\alpha = 0.05$.

¶TOA = time of application.

Study	Herbicide	NRQ† (SE‡)	Relative Expression (SE)	
1	2,4-D	0.492 (0.159)	0.827 (0.249)	A§
	Dicamba	0.134 (0.0739)	0.225 (0.0903)	B
	Untreated	0.595 (0.231)		
		Herbicide	0.029	
		TOA¶	0.051	
		Herbicide*TOA	0.24	
2	2,4-D	0.176 (0.0490)	0.852 (0.123)	B
	Dicamba	2.065 (0.755)	10.027 (1.523)	A
	Untreated	0.206 (0.132)		

Herbicide	0.0034
TOA	0.37
Herbicide*TOA	0.34

CHAPTER 5

INVESTIGATION INTO INTERACTIONS OF ENVIRONMENTAL AND APPLICATION TIME EFFECTS ON 2,4-D AND DICAMBA-INDUCED PHYTOTOXICITY AND HYDROGEN PEROXIDE FORMATION[1]

[1]C. R. Johnston, W. K. Vencill, T. L. Grey, A. S. Culpepper, G. M. Henry, and M. A. Czarnota. To be submitted to *Weed Science*.

Abstract

Both environment and application time reportedly influence the efficacy of auxinic herbicides. In weed species such as Palmer amaranth (*Amaranthus palmeri* S. Watson) that display heavy seed production and high genetic variability, efficacy of auxinic herbicides recently adopted for use in resistant crops is of utmost importance to reduce selection pressure for herbicide resistance traits. Growth chamber experiments were conducted comparing the interaction of different temperature, temperature differential, and humidity treatments with application time to determine the influence of these factors on visual phytotoxicity and hydrogen peroxide (H_2O_2) formation. *Amaranthus palmeri* plants were treated with 2,4-D or dicamba at two rates in the growth chamber to reduce extraneous environmental effects on herbicide activity. Temperature displayed a high degree of influence on 2,4-D and dicamba efficacy at the 0.56 kg a.i. ha^{-1} rate, with applications at the low temperature treatment (31/20°C day/night) resulting in a 90 and 146% increase in phytotoxicity, respectively, compared to high temperature treatments (41/30°C day/night). Application time across temperature treatments significantly affected 2,4-D-induced phytotoxicity, resulting in a ≥ 30% increase in phytotoxicity across rates with treatments at 4 pm compared to those made at 8 am. Temperature differential had a significant influence on dicamba efficacy based on visual phytotoxicity data, with a ≥ 46% increase with high (37/20°C day/night) compared to low differential (41/30°C day/night). Application time within temperature differential treatments significantly affected dicamba efficacy at the rate of 0.28 kg a.i. ha^{-1}; however, increasing the rate to 0.56 kg a.i. ha^{-1} eliminated any difference. Concentration of H_2O_2 in herbicide treated plants was 34% higher under a high temperature differential compared to the low differential. Humidity treatments and application time within humidity treatments displayed undetected or inconsistent effects on visual

phytotoxicity and H_2O_2 production. Overall, temperature-related influences seem to hold the largest environmental effect on auxinic herbicides within conditions evaluated in this study. Leaf concentration of H_2O_2 appears to be generally correlated with phytotoxicity, providing a potentially useful tool in determining efficacy of auxinic herbicides in field settings.

Introduction

Maintaining optimal weed control with each herbicide application is a valuable strategy for agronomists not only to maximize cost-effectiveness, but also for resistance management. Reduced herbicide efficacy has been directly linked to increased survival of weeds possessing potential resistance-conferring alleles, leading to selection for exponential increases in the presence of weeds possessing these traits (Norsworthy et al. 2012; Neve and Powles 2005; Manalil et al. 2011). Many factors contribute to reduced herbicide efficacy, but among the most significant and relevant to current herbicide application patterns are environmental influences and diurnal variation in activity. Generally speaking, herbicides tend to be most effective under high humidity and temperature regimes; however, these conditions are by no means uniform across seasons (Friesen and Dew 1966; Anderson et al. 1993; Ritter and Coble 1981; Johnson and Young 2002). Reduced herbicidal control has been reported with applications made at dawn and/or dusk, which are times when cropping operations utilize herbicide application in order to cover large amounts of acreage in a timely manner, or to reduce drift potential and decrease evaporation of spray droplets before herbicide can penetrate leaf tissues (Johnston et al. 2018; Stewart et al. 2009; Culpepper 2014; Sellers et al. 2003; Prasad et al. 1967; Dalazen and Merotto 2016). Upon the recent advent of auxinic herbicide-resistant crops, maintaining maximum herbicide activity will promote long-term utility of these chemistries for agronomists (Bauerle et al. 2015; Johnston et al. 2018). However, more research is highly warranted on the interaction of different environmental and diurnal factors on efficacy, as little research has been done investigating the magnitude of the interplay between these two influences with auxinic herbicides.

Maintaining effective herbicide options for Palmer amaranth (*Amaranthus palmeri* S. Watson) control is one of the most troublesome weed management problems in the southern United States. Resistance of *Amaranthus* species to several herbicide mechanisms of action is widespread throughout the United States and can be attributed to not only overreliance on certain herbicide mechanisms of action, but also to the high degree of genetic variability seen in *Amaranthus* spp. due to massive seed production and obligate outcrossing (Culpepper et al. 2006; Giacomini et al. 2017; Shoup et al. 2003; Foes et al. 1998; Horak and Loughin 2000; Heap 2014; Assad et al. 2017). Increased genetic variability allows for an increased risk of selection for herbicide resistant weed biotypes (Tranel and Wright 2002). It can be theorized that continued use of 2,4-D and dicamba in resistant crops will increase selection for herbicide resistant alleles. Indeed, 2,4-D resistant waterhemp [*Amaranthus tuberculatus* (Moq.) J.D. Sauer] has already been reported, so the possibility of this phenomenon is no longer a theoretical issue (Figueiredo et al. 2017). However, taking advantage of favorable environmental conditions and times of day when applying herbicides would confer maximum efficacy would likely lesson selection pressure.

One of the main phytotoxic effects associated with auxinic herbicide application is the formation of reactive oxygen species (ROS) (Song 2014). Increased activity of enzymes involved in ureide metabolism, fatty acid oxidation, and jasmonic acid biosynthesis are generally considered a main source of ROS production (Pazmino et al. 2011; reviewed in Song 2014). One of the most prevalent herbicide-induced ROS species is hydrogen peroxide, in which production is triggered by abscisic acid-induced declines in photosynthesis and activity of NADPH oxidases (Grossmann et al. 2001; Romero-Puertas et al. 2004). A notable lack of research is present in investigating the degree of ROS production in response to auxinic

herbicides on the practical level. Investigation into the formation of hydrogen peroxide may yield important insights into the variability of 2,4-D and dicamba response across different environmental and diurnal regimens. The objectives of this research were to evaluate the degree of phytotoxicity and hydrogen peroxide formation from 2,4-D and dicamba treatments under different temperature, temperature differential, and humidity environments as well as different application times of day.

Materials and Methods

Plant Material and Treatments. Sieved seed from a glyphosate-resistant *A. palmeri* population was sown into 236 ml Styrofoam cups in potting mix (Sun Gro Professional Growing Mix, Sun Gro Horticulture, Agawam, MA) and thinned to one plant per cup following establishment. Plants were germinated and grown in a growth chamber set to a day/night temperature and humidity corresponding to environmental treatments (see below) with light from 8 am to 12 am at 600 µmol m^{-2} s^{-1} throughout the experiment. Plants were allowed to grow to the 3-5 leaf stage (~8 cm) prior to herbicide treatment. Plants were fertilized at a rate equivalent to 33.6 kg ha^{-1}.

Experimental design was a randomized complete block with four replications. Herbicide treatments included dicamba or 2,4-D at 0.28 kg a.i. ha^{-1} or 0.56 kg a.i. ha^{-1}, with each herbicide/rate combination applied at either 8 am, 8 hours after initiation of darkness (HAID), or 4 pm, 8 hours after initiation of light (HAIL). An untreated check was included. Herbicide treatments were applied with a pipette to simulate a spray coverage of 280 L ha^{-1}. Spray coverage was calculated by taking average leaf area of 4 plants (~52 cm^2), with droplets placed to the side of the midrib of each treated leaf. Herbicide was applied inside the growth chamber

in order to prevent any outside conditions from affecting herbicide penetration and absorption. The whole set of herbicide treatments were made under separate growth chamber conditions to determine the effect of differing temperature, day/night temperature differential, and humidity on phytotoxicity and hydrogen peroxide formation. For temperature treatments, herbicide applications were made under 41/30 °C (high) or 31/20°C (low) day/night temperatures, with ambient humidity at both temperature treatments (Figure 1, Figure 2). For temperature differential treatments, herbicide applications were made under either 41/30°C (low) or 37/20°C (high) temperature differentials, with ambient humidity at both temperature differential treatments. The same data for the high temperature treatment were compared with the high temperature differential treatment in analysis for determining temperature differential effects. For humidity treatments, herbicide applications were made under humidity ranging from ~66 to 89% (high) or ~35 to 44% relative humidity (low), with a day/night temperature of 36/25°C. For the high humidity treatment, a humidifier (Vicks Warm Mist, Procter & Gamble Co., Cincinnati, OH) was placed in the growth chamber, filled with tap water twice per day. For the low humidity treatment, a dehumidifier (DH-35K1SJE5, Hisense Co., Qingdao, China) was placed in the growth chamber with a drain hose connected to allow for constant moisture removal. Herbicide applications under each environmental treatment were repeated twice in time.

Phytotoxicity and Hydrogen Peroxide Determination. Visual phytotoxicity was determined at 3, 7, 10, and 14 days after treatment (DAT) using a scale of 0 to 100%, with 0% indicating no tissue damage, and 100% indicating complete desiccation and plant death. At 14 DAT, plants were moved to the laboratory and harvested for determination of hydrogen peroxide concentration.

Hydrogen peroxide concentration *in planta* was determined using a colorimetric procedure adapted from Zhou et al. (2006). A total of 0.5 g of fresh leaf material from the most acropetal leaves were harvested and frozen in liquid nitrogen. Leaf material was then ground into fresh powder in a pre-cooled mortar and pestle to prevent thawing, then added to a 15 ml centrifuge tube along with 0.15 g of activated charcoal and 5 ml of a 5% trichloroacetic acid solution. Centrifuge tubes were then vortexed for 10 s prior to centrifuging at 10,000 g for 20 min at 4 °C. Supernatant was then removed from centrifuge tubes and adjusted to pH 9 (determined to allow for maximum colorimetric resolution) using 30% ammonia solution. Adjusted supernatant was filtered using filter paper (Grade 1, Whatman plc, Maidstone, UK) to remove any remaining solids. Filtrate was separated into 2 aliquots of 0.75 ml added to 2 ml centrifuge tubes. One aliquot, treated with 6 µg of catalase dissolved in phosphate buffer to remove any hydrogen peroxide, was used as a blank. Catalase-treated aliquots were allowed to incubate at room temperature for 10 min. A colorimetric reagent was prepared containing 200 ppm 4-aminoantipyrine, 200 ppm phenol, and 100 ppm peroxidase (150 U mg^{-1}) dissolved in a 100 mM acetic acid buffer (pH 5.6). Following incubation of catalase-treated aliquots, 0.75 ml of colorimetric reagent was added to both aliquots. Aliquots were then capped and incubated in a water bath at 30°C for 10 min. Absorbance was read against the catalase blank at 505 nm and converted to µM H_2O_2 using a standard curve prepared from H_2O_2 standards contained in the same solutions used for extraction from leaf tissue (Figure 3). The standard curve was fitted and analyzed using SigmaPlot (SigmaPlot 11, Systat Software, San Jose, CA). Leaf weight was then used to finally convert to units of µmol g FW^{-1}.

Data Analysis. Visual phytotoxicity was subjected to analysis of covariance (ANCOVA) using JMP (JMP Pro 13, SAS Institute, Cary, NC), with DAT serving as the covariate. Separate overall analyses estimating the effect of the covariate and environmental treatment, herbicide, herbicide rate, time of application, and their interactions were performed under each category of environmental comparisons (temperature, temperature differential, or humidity) at a significance level of 0.05. Separate ANCOVA analyses were then performed within each significant effect to determine covariate by treatment interactions in order to compare slopes. In the case of significant covariate by treatment interactions, the null hypothesis that the slope of the covariate within each significant treatment effect was rejected, and slopes were separated using pairwise t-tests of indicator parameterization estimates. Overall means of each treatment are least squares means, and means separation was carried out using pairwise t-tests at $\alpha = 0.05$.

For hydrogen peroxide data, analysis of variance (ANOVA) was carried out via the GLM procedure in JMP to determine significant treatment effects at a significance level of 0.05, with means separation carried out using pairwise t-tests at $\alpha = 0.05$. For both visual phytotoxicity data and hydrogen peroxide concentration, significant environmental treatment by herbicide, herbicide rate, or application time interactions resulted in a comparison of environmental treatments within herbicide/rate combinations, but in the case of insignificant environmental effects, only significant effects were subjected to pairwise t-tests. All graphs of visual phytotoxicity and hydrogen peroxide data were prepared using SigmaPlot.

Results and Discussion

Temperature Effect. For visual phytotoxicity within temperature environments, no study by temperature or study by application time interactions were detected, thus data were combined

over studies. Significant temperature level by herbicide and application time by herbicide interactions were detected in the overall analysis (Table 1), thus means for temperature level and application time are presented within each herbicide/rate combination. Temperature effects pooled across application times were only statistically significant within 2,4-D and dicamba treatments at the high rate (Figure 4). Phytotoxicity from 2,4-D application at 0.56 kg ha^{-1} was 19 and 10% for the low and high temperature treatment, respectively, while phytotoxicity from dicamba applications at 0.56 kg ha^{-1} resulted in 32 and 13% phytotoxicity at the low and high temperature treatment, respectively. Differences in application time pooled across temperature treatments were statistically significant within both rates of 2,4-D, with higher phytotoxicity resulting from 4 pm applications than 8 am applications (Figure 4). Phytotoxicity with 4 pm and 8 am applications of 2,4-D at 0.28 kg ha^{-1} was 13 and 10%, respectively, while phytotoxicity with 4 pm and 8 am applications at 0.56 kg ha^{-1} was 18 and 11%, respectively. There were no significant differences across application times for dicamba at either rate.

Since significant temperature level by herbicide and application time by herbicide interactions were detected in the overall analysis, separate ANCOVAs were performed on temperature level or application time within each herbicide treatment to determine differences in slopes (Table 2). Temperature by covariate interactions were detected for all herbicide/rate combinations, with higher slopes resulting from the low temperature level in all cases. This indicates a faster progression of phytotoxicity at the low temperature level compared to the high temperature level. Application time by covariate interactions were only detected for 2,4-D at the 0.28 kg ha^{-1} rate, yielding a higher slope with the 4 pm application time, indicating a faster progression of phytotoxicity compared to applications made at 8 am.

For hydrogen peroxide concentration, significant study by treatment interactions were not detected, thus data were combined over studies. Only herbicide effects were significant within the overall ANOVA (Table 3). Dicamba application at the 0.56 kg ha^{-1} rate resulted in the highest H_2O_2 concentration at 1.62 µmol g FW^{-1}, followed by dicamba at the 0.28 kg ha^{-1} rate at 1.31 µmol g FW^{-1}. Dicamba applications at both rates resulted in significantly higher H_2O_2 concentration than untreated plants; however, 2,4-D applications at 0.28 kg ha^{-1} and 0.56 kg ha^{-1} resulted in an H_2O_2 concentration of 0.97 µmol g FW^{-1}, which was statistically similar to the untreated (0.72 µmol g FW^{-1}).

It appears that although large increases in phytotoxicity were observed going from the low rate to the high rate with both 2,4-D and dicamba under the low temperature treatment, the same trend was not nearly as dramatic with increasing rate at the high temperature treatment. This is substantiated by the statistically significant improvement of phytotoxicity with the high rate of each herbicide at the low temperature compared to the high temperature. Such trends may have to do with increased evaporation of herbicides at higher temperatures resulting in less of a rate effect. Indeed, previous research displayed a lesser degree of dicamba volatility at lower temperatures, although similar trends with 2,4-D are not as well publicized (Behrens and Lueschen 1979). Interestingly, improved translocation of 2,4-D was reported under high temperatures in hemp dogbane (*Apocynum cannabinum* L.) which may be correlated with increased phytotoxicity, although should such a phenomenon have been present in this study, it did not even out the phytotoxicity observed across temperature treatments (Schultz and Burnside 1980). Regardless, higher slopes for all herbicide treatments at the low temperature may be a result of increased spray droplet retention prior to evaporation compared to higher temperatures,

possibly resulting in faster realization of herbicidal activity. Further research is necessary to investigate these effects on absorption and activity of these herbicides.

Application time effects only being observed for 2,4-D, but not dicamba, may be related to several explanations. Dicamba, a more potent auxinic material in certain species, may have overcome any differences in auxinic herbicide efficacy across time of day due to increased efficacy associated with this herbicide (Nandula and Manthey 2002; Leon et al. 2014). Such an improvement in dicamba activity may be associated with differential binding affinities to auxin binding proteins (Webb and Hall 1995). This has important implications for growers, as applying auxinic herbicides with improved herbicidal activity may reduce the ability for efficacy to be compromised at earlier times of day. A recommendation for increased rates of 2,4-D may be desirable if more potent auxinic materials are not labeled for certain situations. For both situations, the improved penetration observed with crop oil adjuvants may remedy any reduced control related to evaporation (Jansen et al. 1961). However, the mechanism conferring the application time effect where reduced activity is observed at times of lower temperature (i.e. 8 am) demands further investigation, as this likely is not due to reduced penetration of herbicide molecules as a result of any potentially increased evaporation. Differential translocation across application times has been reported and may describe such a phenomenon (Johnston et al. 2018).

For H_2O_2 concentration pooled across temperature treatments, no rate effect was seen with 2,4-D, but a significant improvement was seen going from the low rate to the high rate of dicamba. It is somewhat expected that an herbicide-induced marker such as H_2O_2 would be increased with dicamba, a more potent auxinic material than 2,4-D, as has been previously mentioned. It is interesting that 2,4-D applications at either rate did not result in significantly higher concentration of H_2O_2 than the untreated; this may be due to either a reduced propensity

for 2,4-D to trigger H_2O_2 formation, or simply because rates of 2,4-D were not high enough to induce this phenomenon. The fact that abscisic acid production is associated with H_2O_2 formation in response to auxinic herbicides, coupled with the aforementioned improved phytotoxic action of dicamba in certain cases, may explain the trends observed in this research (Grossmann et al. 2001; Romero-Puertas et al. 2004). As abscisic acid production is upregulated in the presence of auxinic herbicides, improved phytotoxic activity with dicamba may be associated with increased abscisic acid accumulation (and subsequent photosynthesis inhibition) and hence improved H_2O_2 formation (Grossmann 2009). Regardless, it appears that across temperature regimes with temperature differentials held constant, dicamba is a more potent herbicide in *A. palmeri* as shown by H_2O_2 data.

Temperature Differential Effect. For visual phytotoxicity within temperature differential environments, no study by differential or study by application time interactions were detected, thus data are combined over studies. Significant temperature differential by herbicide and application time by herbicide effects were detected; therefore, temperature differential and application time effects are presented within each herbicide/rate combination (Table 1). Dicamba-induced phytotoxicity was significantly higher at both rates within the high temperature differential treatment, pooled across application times (Figure 6). With dicamba applications at 0.28 kg ha^{-1}, phytotoxicity was 13 and 19% with the low and high differential, respectively, while at 0.56 kg ha^{-1} phytotoxicity was 13 and 25% with the low and high differential, respectively. No significant differences in 2,4-D phytotoxicity were observed across temperature differential treatments. Significant differences in application time pooled across

differential treatments were detected only with dicamba at the 0.28 kg ha^{-1} rate, with 21% phytotoxicity with 8 am applications and 12% with 4 pm applications.

Since significant temperature level by herbicide and application time by herbicide interactions were detected in the overall analysis, separate ANCOVAs were performed on temperature level or application time within each herbicide treatment to determine slope differences (Table 4). Significant covariate by temperature differential interactions were detected for dicamba at both rates, and the slope was higher with the high differential at both rates. No significant covariate by temperature differential interactions were detected for 2,4-D at either rate. Covariate by application time interactions were only significant with dicamba at the 0.28 kg ha^{-1} rate, with a higher slope at 8 am compared to 4 pm.

Only the temperature differential effect was significant in the H_2O_2 ANOVA. Concentration of H_2O_2 was significantly higher under the high temperature differential at 1.54 µmol g FW^{-1} compared to the 1.15 µmol g FW^{-1} observed under the low temperature differential (Figure 7).

Little to no research has been published on the role of day/night temperature differential on efficacy of auxinic herbicides. Dicamba in general appears to be more sensitive to temperature differentials and application times across a temperature differential gradient, according to the data presented in this study. No temperature differential effect was observed at all with 2,4-D; however, a significant increase in phytotoxicity of 46 and 92% was observed with dicamba at 0.28 kg ha^{-1} and 0.56 kg ha^{-1}, respectively, when the temperature differential was doubled (low to high treatment). Significantly increased slopes under the high differential at both rates of dicamba are consistent, suggesting a faster progression of phytotoxicity compared to the low differential. It would be presumed that increasing the rate of dicamba would reduce

the disparity between temperature differentials, although phytotoxicity was nearly identical at the higher rate compared to the low rate at the low temperature differential. On the contrary, a 32% increase in phytotoxicity was observed when the dicamba rate was increased from 0.28 kg ha^{-1} to 0.56 kg ha^{-1} under the high differential treatment. Overall, these results suggest that dicamba is more rate-responsive at high temperature differentials, in addition to being more potent in terms of phytotoxicity. Consistently, more H_2O_2 production was observed at the high temperature differential compared to the low treatment, when pooled across application times and herbicides. This further suggests that H_2O_2 production is well-correlated with phytotoxicity. In terms of application time, dicamba provided higher control at 8 am compared to 4 pm; however, this application time effect was removed upon increasing the rate. This is interesting, as it is the opposite trend observed with 2,4-D across different temperature environments. Such an increase in phytotoxic activity may be due to applications taking place at times of lower leaf temperature, as growth chamber lights had just turned on and temperature had just been ramped up at 8 am in this study. The fact that the higher rate eliminated the time of application effect suggests that more active ingredient made it into the target site at 4 pm compared to the low rate. This trend/observation suggests that environmental factors, particularly temperature or reduced humidity, may be the reason behind application time effects. The results in this paper are consistent with previous research that displayed improved translocation, and subsequently phytotoxicity, of dicamba in kochia [*Bassia scoparia* (L.) A.J. Scott] under lower temperature regimens (Ou et al. 2018).

Humidity Effect. Study by humidity treatment and study by application time interactions were not detected for visual phytotoxicity data within humidity environments, thus results are

combined over studies. Only herbicide effects were significant according to the overall ANOVA (Table 1). Pooled across humidity treatments and application times, dicamba at the 0.56 kg ha^{-1} rate resulted in the highest phytotoxicity at 19%, with significantly reduced phytotoxicity from dicamba application at 0.28 kg ha^{-1} and 2,4-D application at 0.56 kg ha^{-1} at 11 and 12%, respectively (Figure 8). Application of 2,4-D at 0.28 kg ha^{-1} resulted in 9% phytotoxicity. Phytotoxicity from 2,4-D and dicamba applications at the low rate were statistically similar, as was phytotoxicity from 2,4-D at the high rate and dicamba at the low rate. Herbicide by covariate interactions were detected within the herbicide effect, with the highest slope resulting from dicamba application at 0.56 kg ha^{-1}, followed by a significant decrease with 2,4-D applications at 0.56 kg ha^{-1} (Table 5). Slopes of both dicamba at the low rate and 2,4-D at the high rate were statistically similar, as were slopes for dicamba and 2,4-D at the low rate.

Study by humidity treatment interactions were detected ($p < 0.0001$) for H_2O_2 concentration, thus results are presented separately across studies. No significant effects were detected in study 1; however, significant humidity by herbicide interactions were detected in study 2 (Table 3). As a result, humidity means are presented within herbicide/rate combinations for both studies for reference (Figure 9).

Lack of humidity effects suggests temperature may be the most influential environmental factor on differential control of *A. palmeri* with 2,4-D and dicamba. When herbicide effects were pooled across humidity treatments, trends followed as would be expected; increasing the rate of both 2,4-D and dicamba resulted in significant increases in phytotoxicity, with greater phytotoxicity resulting from dicamba at the high rate compared to 2,4-D at the high rate. The lack of statistical significance in H_2O_2 production across treatments in study 1 voids the ability to draw any conclusions on humidity effects in this regard. However, if H_2O_2 production is as well

correlated with phytotoxicity as was observed under temperature-based environmental treatments, there is likely a lack of true, reproducible significant differences across humidity levels using conditions employed in this research. The lack of humidity effects observed in this research is inconsistent with previous research on 2,4-D and dicamba, linking high humidity to decreased dicamba volatility and/or increased absorption, which would intuitively result in increased activity (Behrens and Lueschen 1979; Pallas 1960; Al-Khatib et al. 1992).

Overall, it appears that temperature-related effects provide the greatest environmental influence of factors tested in this research. In addition, application time effects are significant with 2,4-D and dicamba under different temperature and day/night temperature differential regimens, respectively. Increased rates of dicamba resulted in greater phytotoxicity to *A. palmeri* in general when application time effects resulted in decreased efficacy; however, increasing rates appears to only improve control significantly at lower temperatures. As such, applying dicamba under lower temperatures and conditions where the day/night temperature differential is greatest likely provides the best strategy for maximizing efficacy according to this research. Similarly, increasing 2,4-D rates appears to improve phytotoxicity more at low temperatures; however, equal control may be observed at high temperatures at higher rates than those used in this research. 2,4-D-induced phytotoxicity in general was insensitive to temperature differentials, indicating potentially greater flexibility for growers to apply this herbicide with fluctuating day/night temperatures compared to dicamba. In addition, applications of 2,4-D appear to have greater efficacy at mid-day across a temperature gradient, but applying 2,4-D with higher temperature differentials appears to eliminate the application time effect. Development of a rapid H_2O_2 assay in herbicide-treated plant tissues may provide a useful tool for agronomists to determine the efficacy of 2,4-D and dicamba applications, as correlation with phytotoxicity

appeared to be promising in this research. In the face of rapidly-evolving herbicide resistance and the need for maintaining stewardship of auxinic herbicide chemistries, it is critical that agronomists maintain application strategies for 2,4-D and dicamba that take time of application and temperature influences into consideration.

References

Al-Khatib K, Parker R, Fuerst EP (1992) Foliar absorption and translocation of herbicides from aqueous solution and treated soil. Weed Sci. 40:281-287

Anderson DM, Swanton CJ, Hall JC, Mersey BG (1993) The influence of temperature and relative humidity on the efficacy of glufosinate-ammonium. Weed Res. 33:139-147

Assad R, Reshi ZA, Snober J, Rashid I. (2017) Biology of Amaranths. Bot. Rev. 83:382-436

Bauerle MJ, Griffin JL, Alford JL, Curry AB, Kenty MM (2015) Field evaluation of auxin herbicide volatility using cotton and tomato as bioassay crops. Weed Technol. 29:185-197

Behrens R, Lueschen WE (1979) Dicamba volatility. Weed Sci. 27:486-493

Culpepper AS, Grey TL, Vencill WK, Kichler JM, Webster TM, Brown SM, York AC, Davis JW, Hanna WW (2006) Glyphosate-resistant Palmer amaranth (*Amaranthus palmeri*) confirmed in Georgia. Weed Sci. 54:620-626

Culpepper S (2014) Application time of day influence on Roundup, Reflex, and Clarity. Unpublished raw data

Dalazen G, Merotto A (2016) Physiological and genetic bases of the circadian clock in plants and their relationship with herbicides efficacy. Planta Daninha 34:191-198

Figueiredo MRA, Leibhart LJ, Reicher ZJ, Tranel PJ, Nissen SJ, Westra P, Bernards ML, Kruger GR, Gaines TA, Jugulam M (2017) Metabolism of 2,4-dichlorophenoxyacetic acid contributes to resistance in a common waterhemp (*Amaranthus tuberculatus*) population. Pest Manag. Sci. doi:10.1002/ps.4811

Foes MJ, Tranel PJ, Wax LM, Stoller EW (1998) A biotype of common waterhemp (*Amaranthus rudis*) resistant to triazine and ALS herbicides. Weed Sci. 46:514-520

Friesen HA, Dew DA (1966) The influence of temperature and soil moisture on the phytotoxicity of dicamba, picloram, bromoxynil, and 2,4-D ester. Can. J. Plant Sci. 46:653-660

Giacomini DA, Umphres AM, Nie H, Mueller TC, Steckel LE, Young BG, Scott RC, Tranel PJ (2017) Two new *PPX2* mutations associated with resistance to PPO-inhibiting herbicides in *Amaranthus palmeri*. Pest Manag. Sci. 2017:10.1002/ps.4581

Grossmann K, Kwiatkowski J, Tresch S (2001) Auxin herbicides induce H_2O_2 overproduction and tissue damage in cleavers (*Galium aparine* L.). J. Exp. Bot. 52:1811-1816

Grossmann K (2009) Auxin herbicides: current status of mechanism and mode of action. Pest Manag. Sci. 66:113-120

Heap I (2014) Herbicide resistant weeds. *In* Pimentel D, Peshin R eds. Integrated Pest Management. Dordrecht, Netherlands: Springer Dordrecht. Pp. 281-301

Horak MJ, Loughin TM (2000) Growth analysis of four *Amaranthus* species. Weed Sci. 48:347-355

Jansen LL, Center WA, Shaw WC (1961) Effects of surfactants on the herbicidal activity of several herbicides in aqueous spray systems. Weeds 9:381-405

Johnson BC, Young BG (2002) Influence of temperature and relative humidity on the foliar activity of mesotrione. Weed Sci. 50:157-161

Johnston CR, Eure PM, Grey TL, Culpepper AS, Vencill WK (2018) Time of application influences translocation of auxinic herbicides in Palmer amaranth (*Amaranthus palmeri*). Weed Sci. 66:4-14

Leon RG, Ferrell JA, Brecke BJ (2014) Impact of exposure to 2,4-D and dicamba on peanut injury and yield. Weed Technol. 28:465-470

Manalil S, Busi R, Renton M, Powles SB (2011) Rapid evolution of herbicide resistance by low herbicide dosages. Weed Sci. 59:210-217

Nandula VK, Manthey FA (2002) Response of kochia (*Kochia scoparia*) inbreds to 2,4-D and dicamba. Weed Technol. 16:50-54

Neve P, Powles S (2005) Recurrent selection with reduced herbicide rates results in the rapid evolution of herbicide resistance in *Lolium rigidum*. Theor. Appl. Genet. 110:1154-1166

Norsworthy JK, Ward SM, Shaw DR, Llewellyn RS, Nichols RL, Webster TM, Bradley KW, Frisvold G, Powles SB, Burgos NR, Witt WW, Barrett M (2012) Reducing the risks of herbicide resistance: best management practices and recommendations. Weed Sci. 60:31-62

Ou J, Stahlman PW, Jugulam M (2018) Reduced absorption of glyphosate and decreased translocation of dicamba contribute to poor control of kochia (*Kochia scoparia*) at high temperature. Pest Manag. Sci. 74:1134-1142

Pallas JE (1960) Effects of temperature and humidity on foliar absorption and translocation of 2,4-dichlorophenoxyacetic acid and benzoic acid. Plant Physiol. 35:575-580

Pazmino DM, Rodriguez-Serrano M, Romero-Puertas MC, Archilla-Ruiz A, Del Rio LA, Sandalio LM (2011) Differential response of young and adult leaves to herbicide 2,4-dichlorophenoxyacetic acid in pea plants: Role of reactive oxygen species. Plant Cell Environ. 34:1874-1889

Prasad R, Foy CL, Crafts AS (1967) Effects of relative humidity on absorption and translocation of foliarly applied dalapon. Weeds 15:149-156

Ritter RL, Coble HD (1981) Influence of temperature and relative humidity on the activity of acifluorfen. Weed Sci. 29:480-485

Romero-Puertas MC, Mccarthy I, Gómez M, Sandalio LM, Corpas FJ, Del Rio LA, Palma JM (2004) Reactive oxygen species-mediated enzymatic systems involved in the oxidative action of 2,4-dichlorophenoxyacetic acid. 2004. Plant Cell Environ. 27:1135-1148

Schultz ME, Burnside OC (1980) Absorption, translocation, and metabolism of 2,4-D and glyphosate in hemp dogbane (*Apocynum cannabinum*). Weed Sci. 28:13-20

Sellers BA, Smeda RJ, Johnson WG (2003) Diurnal fluctuations and leaf angle reduce glufosinate efficacy. Weed Technol. 17:302-306

Shoup DE, Al-Khatib K, Peterson DE (2003) Common waterhemp (*Amaranthus rudis*) resistance to protoporphyrinogen oxidase-inhibiting herbicides. Weed Sci. 51:145-150

Song Y (2014) Insight into the mode of action of 2,4-dichlorophenoxyacetic acid (2,4-D) as an herbicide. J. Integr. Plant Biol. 56:106-113

Stewart CL, Nurse RE, Sikkema PH (2009) Time of day impacts postemergence weed control in corn. Weed Technol. 23:346-355

Tranel PJ, Wright TR (2002) Resistance of weeds to ALS-inhibiting herbicides: what have we learned? Weed Sci. 50:700-712

Webb SR, Hall JC (1995) Auxinic herbicide-resistant and -susceptible wild mustard (*Sinapis arvensis* L.) biotypes: effect of auxin herbicides on seedling growth and auxin-binding activity. Pestic. Biochem. Physiol. 52:137-148

Zhou B, Wang J, Guo Z, Tan H, Zhu X (2006) A simple colorimetric method for determination of hydrogen peroxide in plant tissues. Plant Growth Regul. 49:113-118

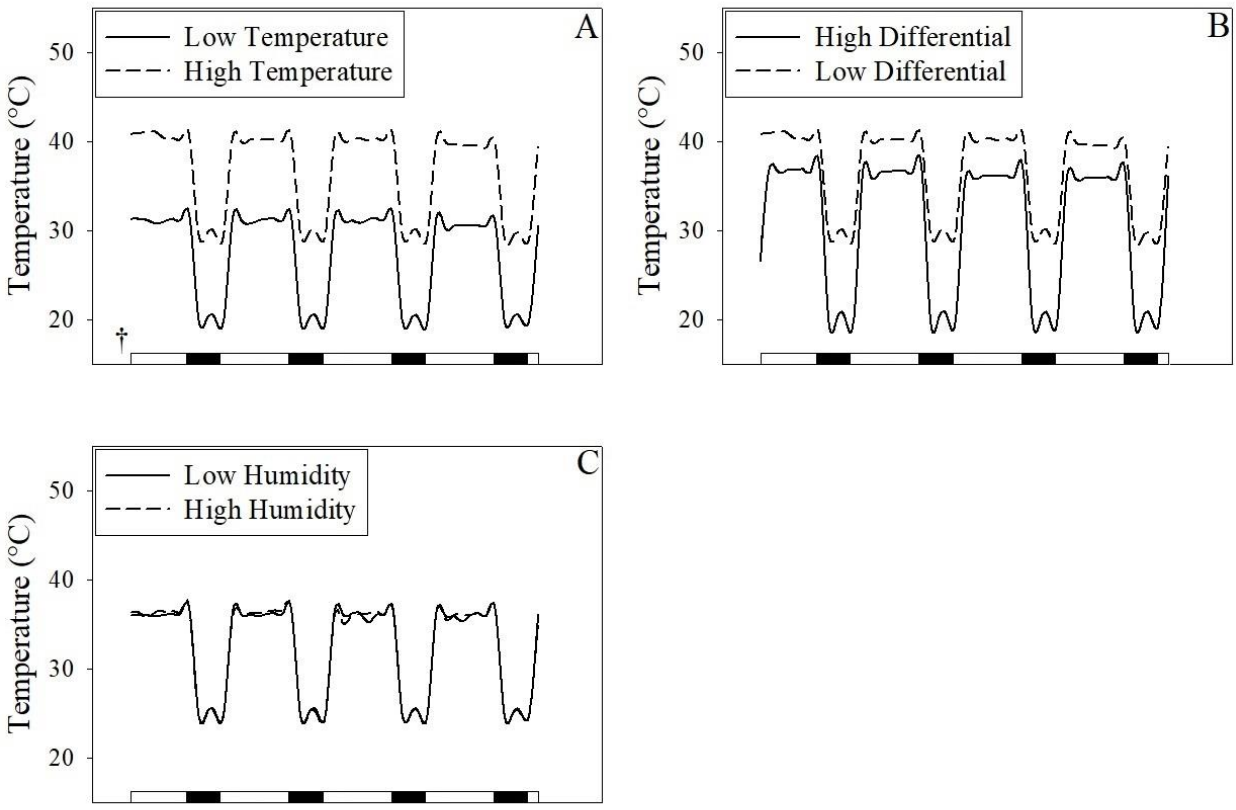

Figure 5.1. Temperature under different temperature treatments (A), temperature differential treatments (B), and humidity treatments (C) in growth chamber experiments, 2018.

†White bars across x-axis represent simulated daytime (8 am to 12 am), and black bars represent simulated evening (12 am to 8 am).

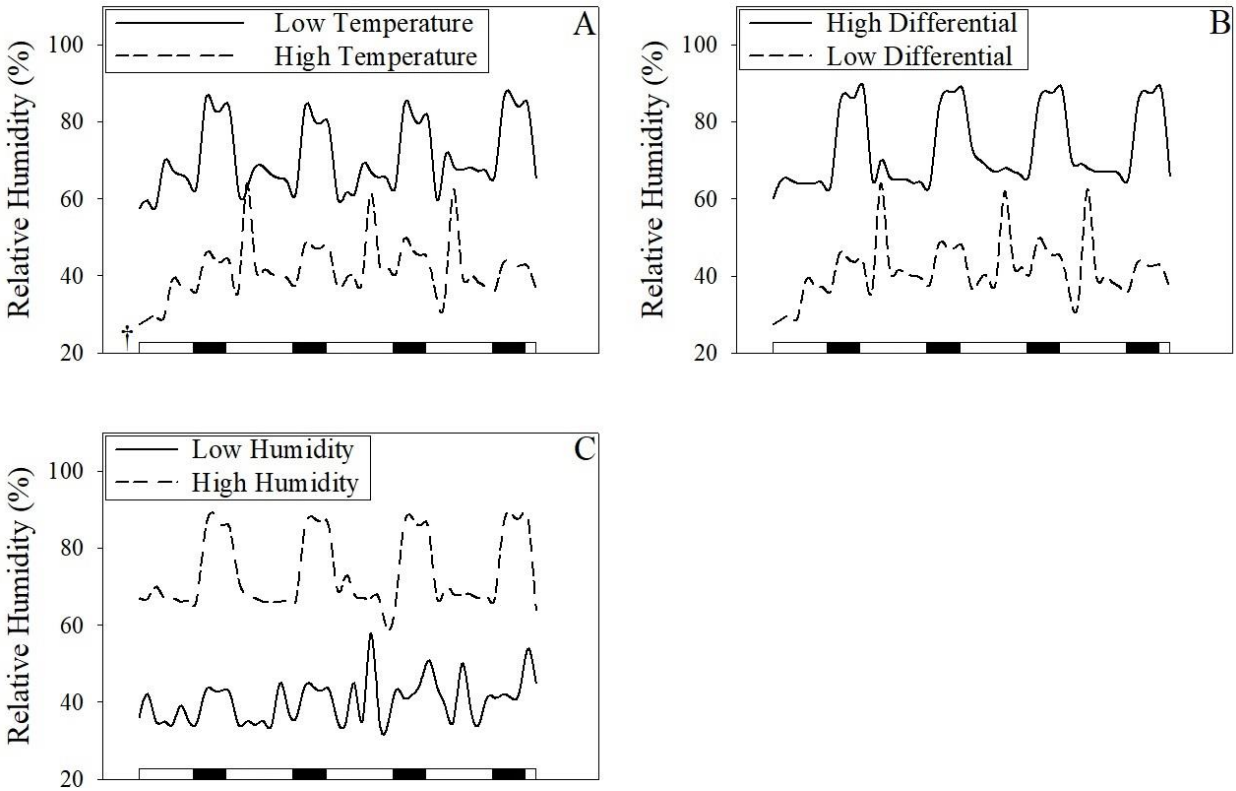

Figure 5.2. Relative humidity under different temperature treatments (A), temperature differential treatments (B), and humidity treatments (C) in growth chamber experiments, 2018. †White bars across x-axis represent simulated daytime (8 am to 12 am), and black bars represent simulated evening (12 am to 8 am).

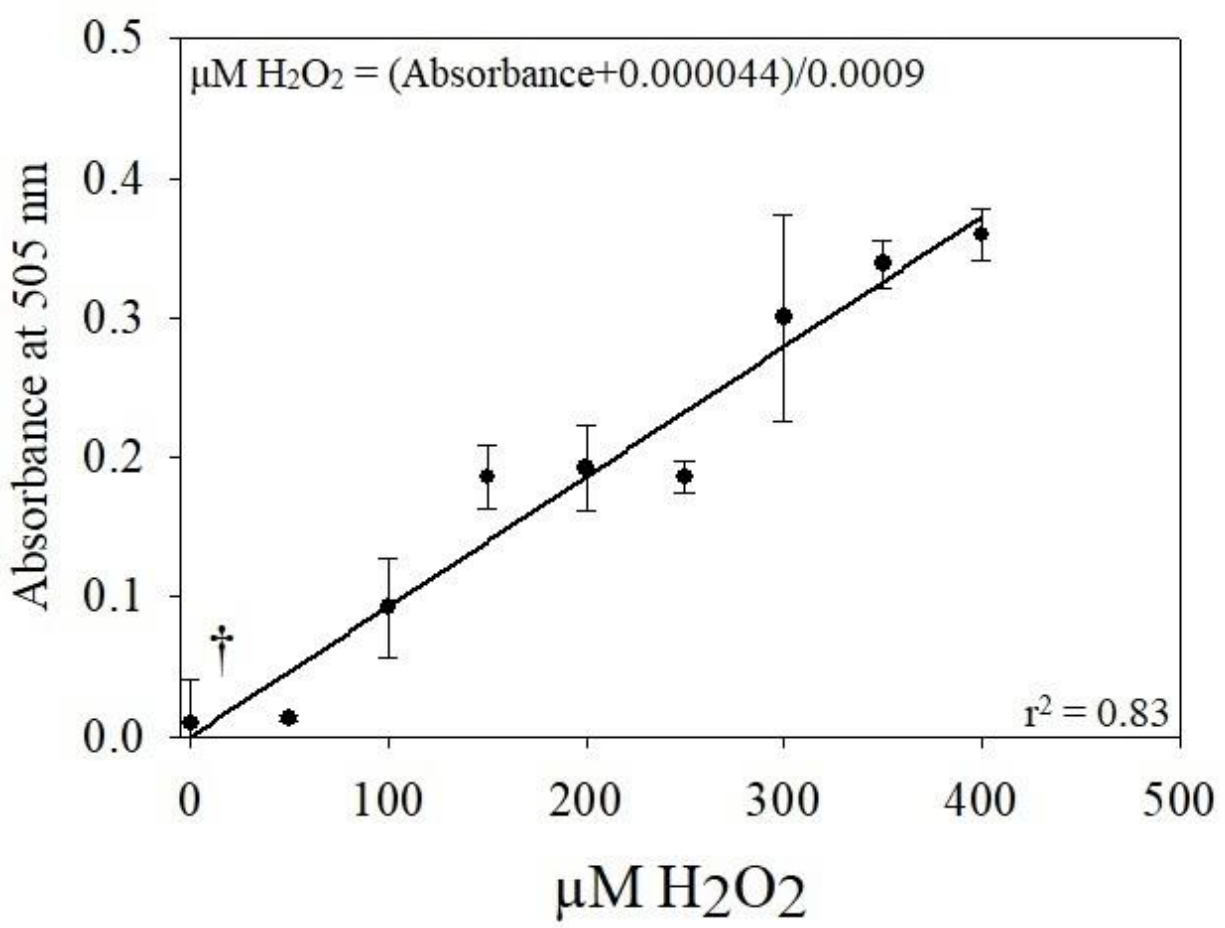

Figure 5.3. Standard curve used for converting absorbance of H_2O_2 extraction solution at 505 nm to µM H_2O_2, 2018.

†Vertical bars represent standard error of the mean.

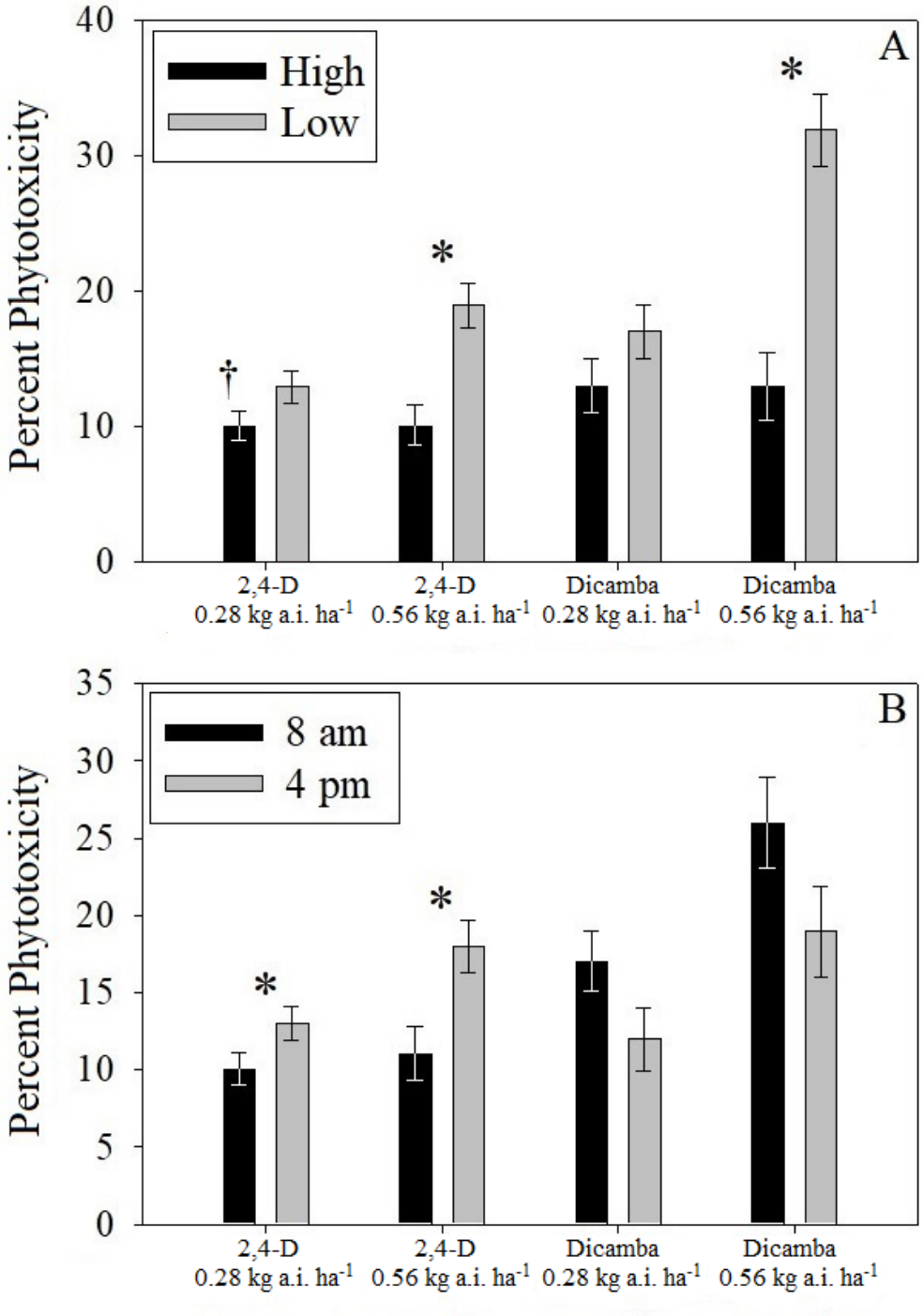

Figure 5.4. Means for effects of different temperature treatments pooled across application times (A) and application times pooled across temperature treatments (B) with different herbicide/rate combinations in growth chamber experiments, 2018.

[†]Vertical bars represent standard error of the mean.

[‡]Means are based on results from ANCOVA analysis using days after treatment as a covariate.

[§]Asterisks represent significant differences within herbicide/rate combinations based on t-test results at $\alpha = 0.05$.

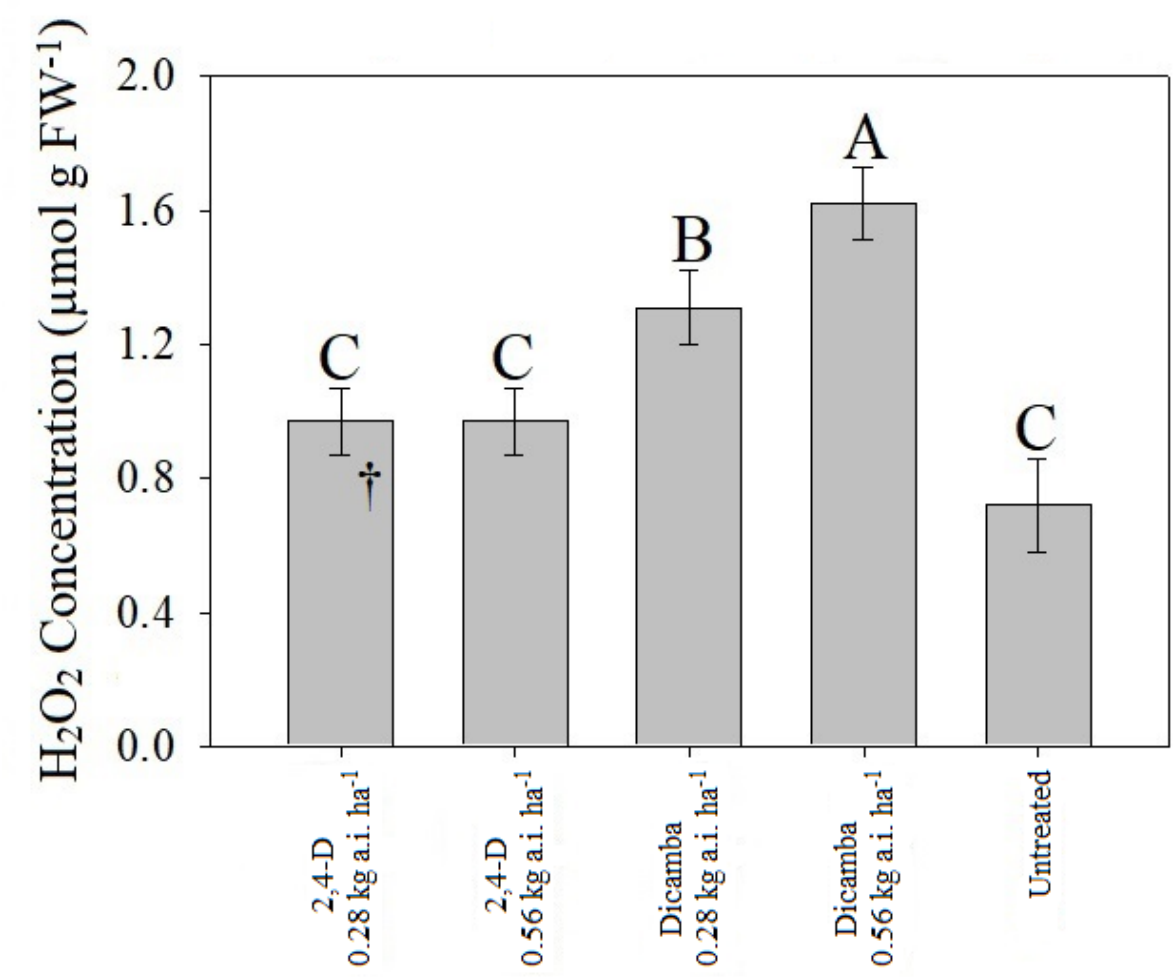

Figure 5.5. Means for hydrogen peroxide concentration in *A. palmeri* leaf tissue treated with 2,4-D and dicamba at two rates pooled across two temperature treatments and two application times in growth chamber experiments, 2018.

†Vertical bars represent standard error of the mean.

‡Means followed by the same letter do not differ statistically based on pairwise t-tests at α = 0.05.

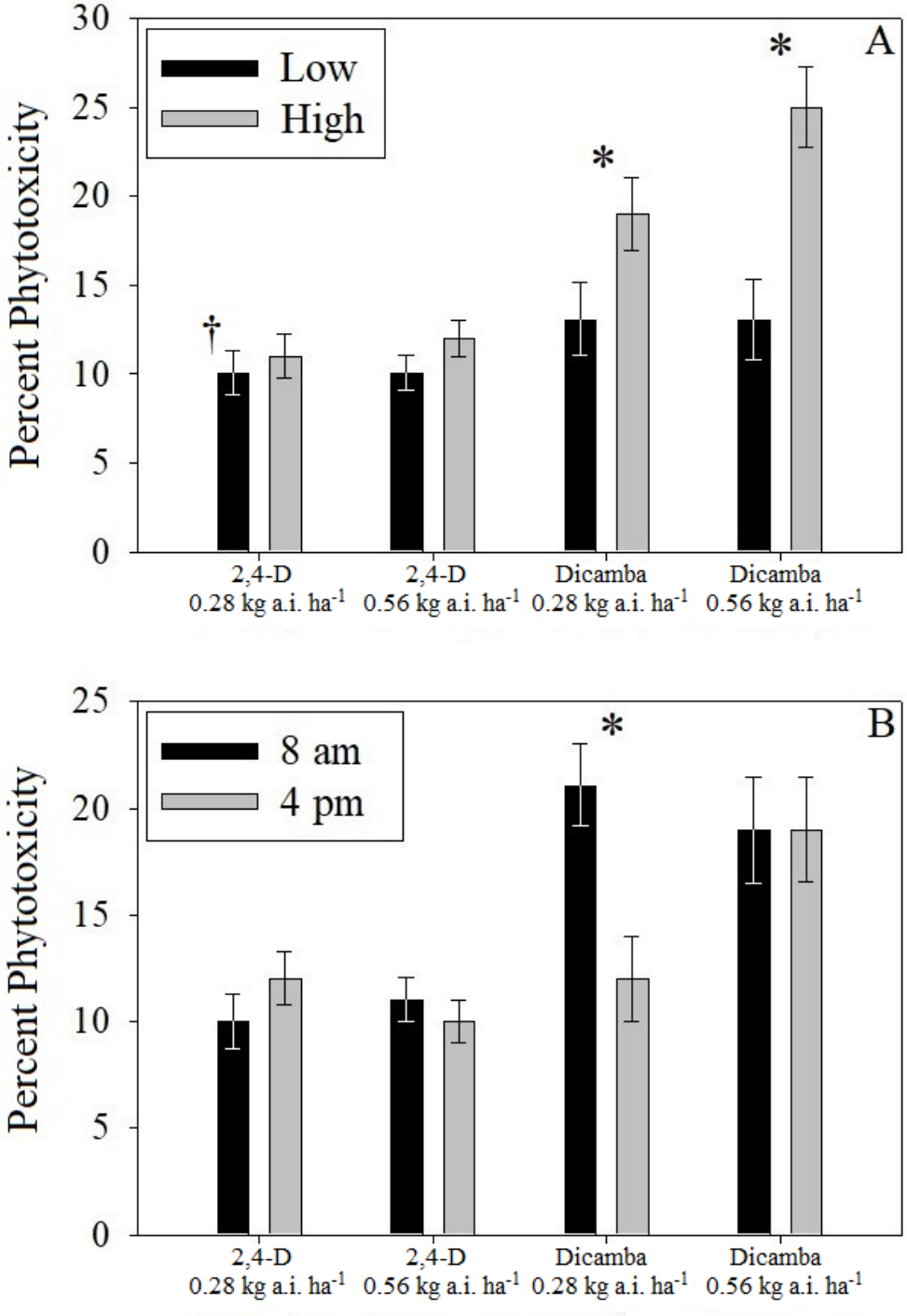

Figure 5.6. Means for effects of different temperature differential treatments pooled across application times (A) and application times pooled across temperature differential treatments (B) with different herbicide/rate combinations in growth chamber experiments, 2018.

[†]Vertical bars represent standard error of the mean.

[‡]Means are based on results from ANCOVA analysis using days after treatment as a covariate.

[§]Asterisks represent significant differences within herbicide/rate combinations based on t-test results at $\alpha = 0.05$.

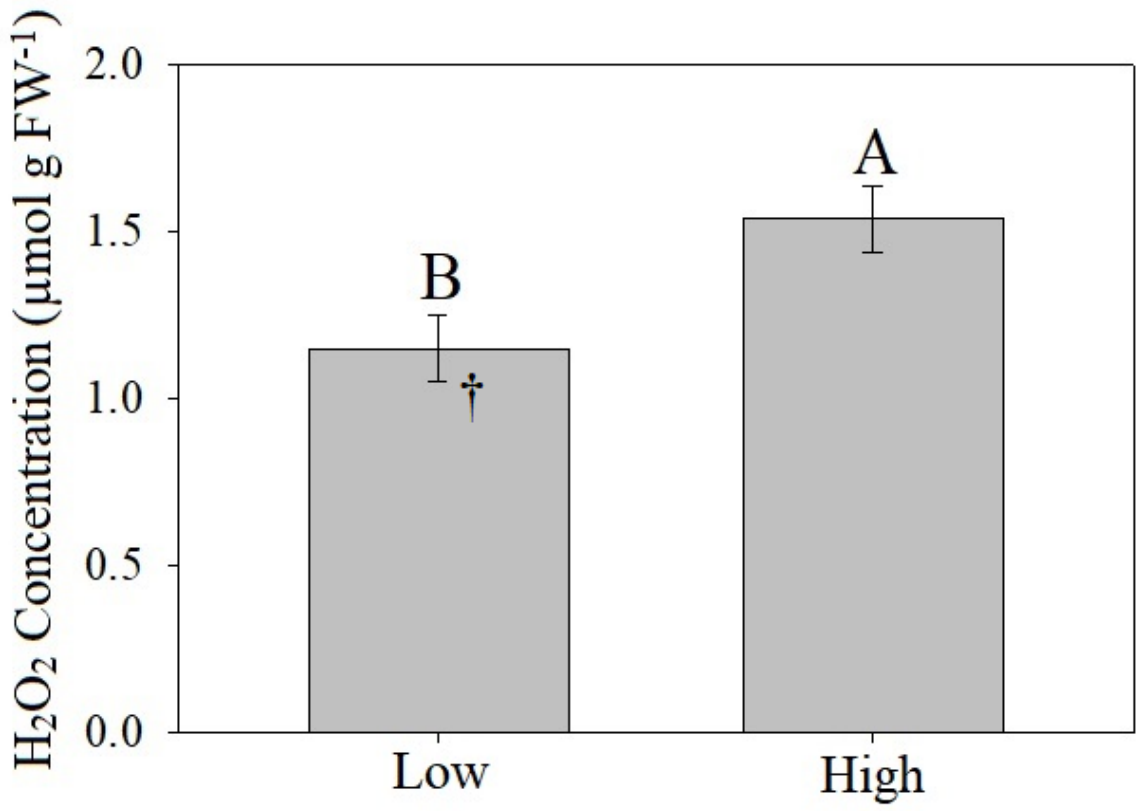

Figure 5.7. Means for hydrogen peroxide concentration in *A. palmeri* leaf tissue treated with 2,4-D and dicamba at two temperature differential treatments, pooled across rates and application times in growth chamber experiments, 2018.

†Vertical bars represent standard error of the mean.

‡Means followed by the same letter do not differ statistically based on pairwise t-tests at α = 0.05.

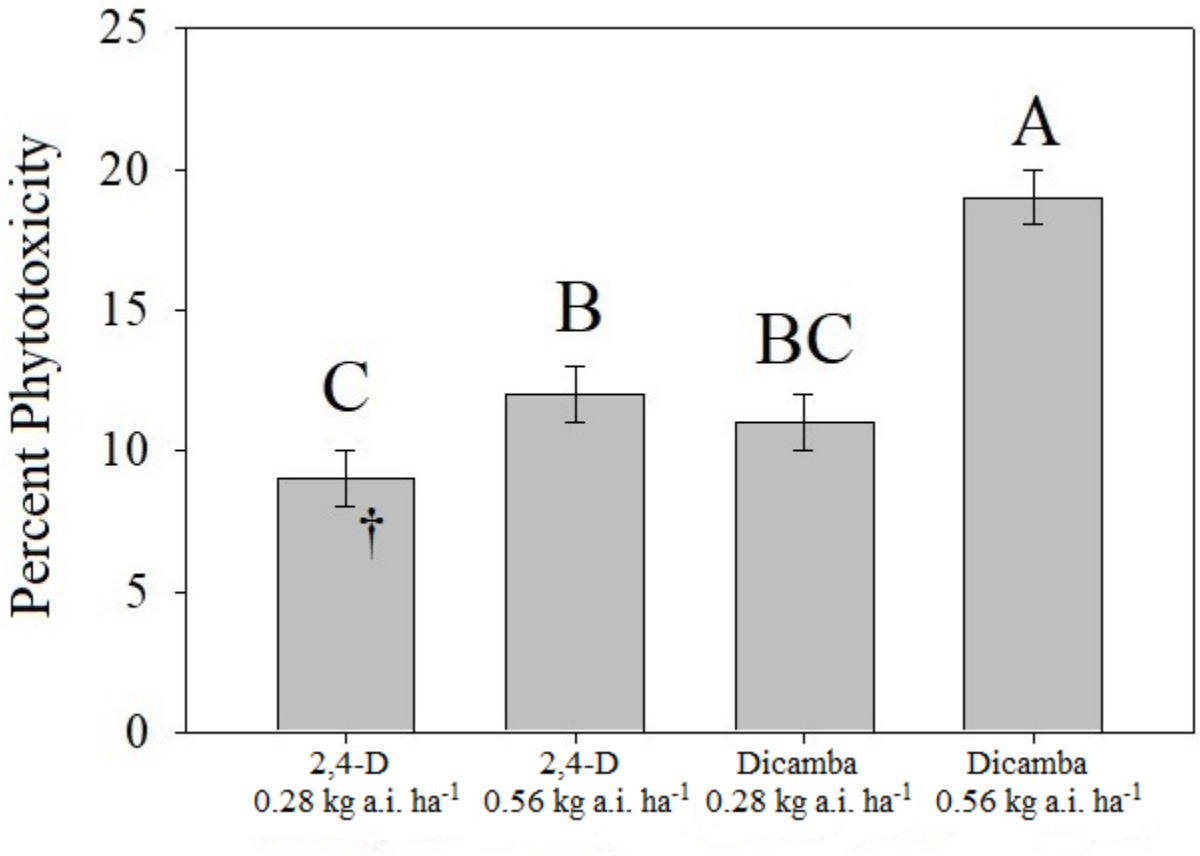

Figure 5.8. Means for effect of herbicide/rate combinations pooled across application times and two humidity treatments in growth chamber experiments, 2018.

†Vertical bars represent standard error of the mean.

‡Means are based on results from ANCOVA analysis using days after treatment as a covariate.

§Means followed by the same letter do not differ statistically based on pairwise t-tests at $\alpha = 0.05$.

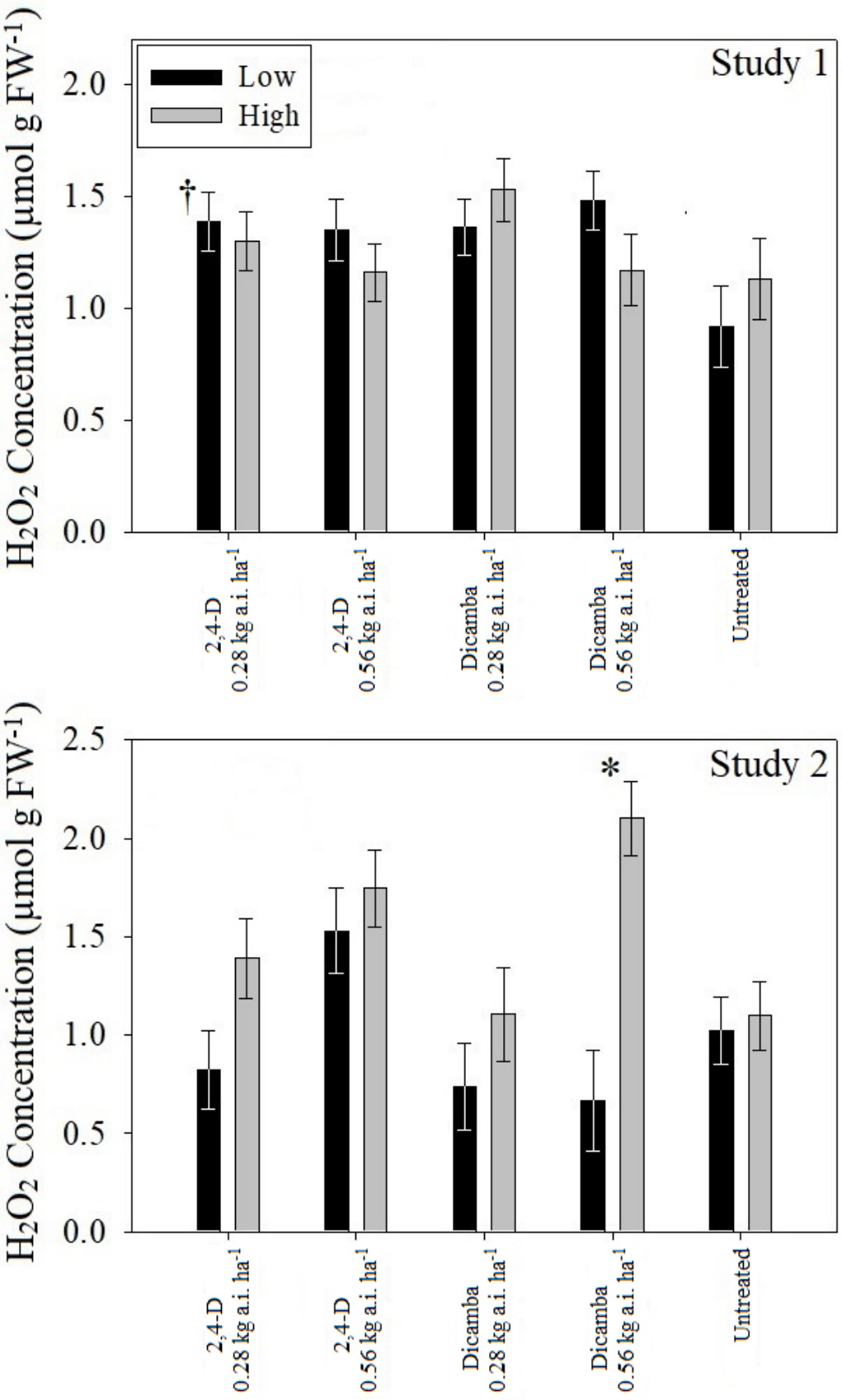
Study 1
Low
High
H_2O_2 Concentration (µmol g FW^{-1})
2.0
1.5
1.0
0.5
0.0
†
2,4-D 0.28 kg a.i. ha^{-1}
2,4-D 0.56 kg a.i. ha^{-1}
Dicamba 0.28 kg a.i. ha^{-1}
Dicamba 0.56 kg a.i. ha^{-1}
Untreated
Study 2
H_2O_2 Concentration (µmol g FW^{-1})
2.5
2.0
1.5
1.0
0.5
0.0
*
2,4-D 0.28 kg a.i. ha^{-1}
2,4-D 0.56 kg a.i. ha^{-1}
Dicamba 0.28 kg a.i. ha^{-1}
Dicamba 0.56 kg a.i. ha^{-1}
Untreated

Figure 5.9. Means for hydrogen peroxide concentration in *A. palmeri* leaf tissue treated with 2,4-D and dicamba under two humidity treatments with different herbicide/rate combinations, pooled across application times in growth chamber experiments, 2018.

[†]Vertical bars represent standard error of the mean.

[‡]Means are based on results from ANCOVA analysis using days after treatment as a covariate.

[§]Asterisks represent significant differences within herbicide/rate combinations based on t-test results at $\alpha = 0.05$.

Table 5.1. ANCOVA tables for covariate and interaction of application time, herbicide, and environmental treatment under different temperature, temperature differential, and humidity treatments in growth chamber experiments, 2018.

[†]DAT = days after treatment, serving as the covariate in analyses.

[‡]Study by application time and environmental treatment not detected for temperature, temperature differential, or humidity comparisons at a significance level of 0.05, thus effect of study and study by treatment interactions omitted from analyses and all tables represent effects combined over both studies.

Environmental Treatment	Source	Degrees of Freedom	Sum of Squares	Mean Square	F-ratio	Prob > F
Temperature	[†]DAT (Covariate)	1	62775.96	62775.96	283.4066	<0.0001
	Temperature	1	9468.125	9468.125	42.7445	<0.0001
	Application Time	1	14.805	14.805	0.0668	0.7961
	Herbicide	3	9406.921	3135.640333	14.1561	<0.0001
	Temperature*Application Time	1	45.127	45.127	0.2037	0.6519
	Temperature*Herbicide	3	4976.21	1658.736667	7.4885	<0.0001
	Application Time*Herbicide	3	4307.931	1435.977	6.4828	0.0003
	Block	3	6313.522	2104.507333	9.501	<0.0001
	Error	471	104328.82	221.5049257		
	Total	487	199188.52			
Temperature Differential	DAT (Covariate)	1	48587.22	48587.22	234.2688	<0.0001
	Differential	1	3417.732	3417.732	16.479	<0.0001
	Application Time	1	575.277	575.277	2.7738	0.0965
	Herbicide	3	7133.615	2377.871667	11.4652	<0.0001

	Differential*Application Time	1	685.434	685.434	3.3049	0.0697
	Differential*Herbicide	3	2098.766	699.5886667	3.3731	0.0184
	Application Time*Herbicide	3	2399.276	799.7586667	3.8561	0.0096
	Block	3	667.546	222.5153333	1.0729	0.3602
	Error	483	100173.95	207.3994824		
	Total	499	165672.95			
Humidity	DAT (Covariate)	1	39688.223	39688.223	306.3802	<.0001
	Humidity	1	116.958	116.958	0.9029	0.3425
	Application Time	1	62.529	62.529	0.4827	0.4875
	Herbicide	3	6754.287	2251.429	17.3803	<.0001
	Humidity*Application Time	1	11.437	11.437	0.0883	0.7665
	Humidity*Herbicide	3	240.403	80.13433333	0.6186	0.6032
	Application Time*Herbicide	3	349.685	116.5616667	0.8998	0.4412
	Block	3	758.388	252.796	1.9515	0.1205
	Error	466	60365.23	129.5391202		
	Total	482	108347.14			

Table 5.2. Slope comparisons for ANCOVA results comparing effect of temperature treatment and application time within herbicide/rate combinations in growth chamber experiments, 2018.

[†]Parentheses represent standard error of the slope estimate.

[‡]Slope estimates followed by different letters do not differ statistically based on pairwise t-tests of indicator parameterization estimates at $\alpha = 0.05$.

[§]DAT = days after treatment, serving as the covariate in analyses. Insignificant temperature or application time by covariate effects at a significance level of 0.05 resulted in one slope being reported for each temperature or application time effect within herbicide/rate combinations.

[¶]Time = application time.

Effect					
Temperature	Herbicide	Temperature	Slope		Equation
	2,4-D 0.28 kg ha^{-1}	High	1.33 [†](0.25)	[‡]B	y = 1.33x - 1.19
		Low	2.40 (0.30)	A	y = 2.40x - 7.37
		Temperature	0.0627		
		DAT	<0.0001		
		[§]Temperature*DAT	0.0069		
	2,4-D 0.56 kg ha^{-1}	High	1.39 (0.19)	B	y = 1.39x - 1.94
		Low	3.40 (0.52)	A	y = 3.40x - 9.46
		Temperature	<0.0001		

		DAT	<0.0001		
		Temperature*DAT	0.0006		
	Dicamba 0.28 kg ha^{-1}	High	1.97 (0.35)	B	y = 1.97x - 3.60
		Low	3.50 (0.61)	A	y = 3.50x -12.79
		Temperature	0.1887		
		DAT	<0.0001		
		Temperature*DAT	0.0299		
	Dicamba 0.56 kg ha^{-1}	High	2.46 (0.45)	B	y = 2.46x - 7.32
		Low	6.21 (0.77)	A	y = 6.21x - 20.16
		Temperature	<0.0001		
		DAT	<0.0001		
		Temperature*DAT	<0.0001		
Application Time	Herbicide	Application Time	Slope		Equation
	2,4-D 0.28 kg ha^{-1}	8:00 AM	1.45 (0.22)	B	y = 1.45x - 2.44
		4:00 PM	2.28 (0.32)	A	y = 2.28x - 6.19
		Time	0.0412		
		DAT	<0.0001		
		¶Time*DAT	0.0383		
	2,4-D 0.56 kg ha^{-1}	8:00 AM	2.43 (0.31)		y = 2.43x - 5.93
		4:00 PM			
		Time	0.0079		
		DAT	<0.0001		
		Time*DAT	0.0788		
	Dicamba 0.28 kg ha^{-1}	8:00 AM	2.73 (0.35)		y = 2.73x - 8.25

	4:00 PM		
	Time	0.0679	
	DAT	<0.0001	
	Time*DAT	0.0522	
Dicamba 0.56 kg ha^{-1}	8:00 AM 4:00 PM	4.28 (0.51)	y = 4.28x -13.65
	Time	0.0616	
	DAT	<0.0001	
	Time*DAT	0.2423	

Table 5.3. ANCOVA tables for covariate and interaction of application time, herbicide, and environmental treatment under different temperature, temperature differential, and humidity treatments in growth chamber experiments, 2018.

[†]Study by application time and environmental treatment not detected for temperature or temperature differential comparisons at a significance level of 0.05, thus effect of study and study by treatment interactions omitted from analyses and both tables represent effects combined over both studies. Study by humidity interactions were detected for humidity comparisons ($p < 0.0001$), thus separate analyses were performed for each study.

Environmental Treatment	Source	Degrees of Freedom	Sum of Squares	Mean Square	F Ratio	Prob > F
Temperature	Temperature	1	0.7495175	0.7495175	2.4018	0.1247
	Application Time	1	0.2879474	0.2879474	0.9227	0.3393
	Herbicide	3	8.6963347	2.898778233	9.2892	<.0001
	Temperature*Application Time	1	0.5311225	0.5311225	1.702	0.1953
	Temperature*Herbicide	3	1.6413884	0.547129467	1.7533	0.1617
	Application Time*Herbicide	3	0.9965817	0.3321939	1.0645	0.3682
	Block	3	2.6188032	0.8729344	2.7973	0.0446
	Error	91	28.397462	0.312060022		
	Total	106	43.9191574			
Temperature Differential	Differential	1	3.9921646	3.9921646	8.0121	0.0057
	Application Time	1	1.3649275	1.3649275	2.7393	0.1014
	Herbicide	3	2.2728409	0.757613633	1.5205	0.2147

	Differential*Application Time	1	0.0495746	0.0495746	0.0995	0.7532
	Differential*Herbicide	3	0.5033551	0.167785033	0.3367	0.7988
	Application Time*Herbicide	3	1.6833617	0.561120567	1.1261	0.3429
	Block	3	2.3359656	0.7786552	1.5627	0.204
	Error	89	44.345872	0.498268225		
	Total	104	56.548062			
Humidity (Study 1)	Humidity	1	0.15622576	0.15622576	1.055	0.3101
	Application Time	1	0.00225615	0.00225615	0.0152	0.9023
	Herbicide	3	0.27580983	0.09193661	0.6208	0.6054
	Humidity*Application Time	1	0.00018727	0.00018727	0.0013	0.9718
	Humidity*Herbicide	3	0.38938405	0.129794683	0.8765	0.4607
	Application Time*Herbicide	3	0.24038595	0.08012865	0.5411	0.6567
	Block	3	0.19551155	0.065170517	0.4401	0.7255
	Error	43	6.3676301	0.148084421		
	Total	58	7.62739066			
Humidity (Study 2)	Humidity	1	5.2010046	5.2010046	18.4889	0.0001
	Application Time	1	0.0950854	0.0950854	0.338	0.5645
	Herbicide	3	3.7193683	1.239789433	4.4073	0.0095
	Humidity*Application Time	1	0.6510978	0.6510978	2.3146	0.1367
	Humidity*Herbicide	3	2.6176662	0.8725554	3.1018	0.0383
	Application Time*Herbicide	3	1.3401494	0.446716467	1.588	0.2087
	Block	3	0.8007471	0.2669157	0.9489	0.427
	Error	37	10.408234	0.281303622		
	Total	52	24.8333528			

Table 5.4. Slope comparisons for ANCOVA results comparing effect of temperature differential treatment and application time within herbicide/rate combinations in growth chamber experiments, 2018.

[†]Differential = temperature differential.

[‡]Parentheses represent standard error of the slope estimate.

[§]DAT = days after treatment, serving as the covariate in analyses. Insignificant temperature differential or application time by covariate effects at a significance level of 0.05 resulted in one slope being reported for each temperature differential or application time effect within herbicide/rate combinations.

[¶]Slope estimates followed by different letters do not differ statistically based on pairwise t-tests of indicator parameterization estimates at $\alpha = 0.05$.

Effect				
Temperature	Herbicide	[†]Differential	Slope	Equation
	2,4-D 0.28 kg ha^{-1}	Low High	1.63 [‡](0.22)	y = 1.63x - 3.17
		Differential	0.4887	
		DAT	<0.0001	
		[§]Differential*DAT	0.1833	
	2,4-D 0.56 kg ha^{-1}	Low High	1.57 (0.18)	y = 1.57x - 2.63
		Differential	0.2297	
		DAT	<0.0001	

		Differential*DAT	0.3187		
	Dicamba 0.28 kg ha^{-1}	Low	1.97 (0.35)	¶B	y = 1.97x - 3.60
		High	3.71 (0.64)	A	y = 3.71x - 11.98
		Differential	0.0356		
		DAT	<0.0001		
		Differential*DAT	0.0198		
	Dicamba 0.56 kg ha^{-1}	Low	2.46 (0.45)	B	y = 2.46x - 7.32
		High	4.87 (0.66)	A	y = 4.87x - 16.24
		Differential	0.0006		
		DAT	<0.0001		
		Differential*DAT	0.0031		
Application Time	Herbicide	Application Time	Slope		Equation
	2,4-D 0.28 kg ha^{-1}	8:00 AM 4:00 PM	1.63 (0.22)		y = 1.63x - 3.18
		Time	0.2934		
		DAT	<0.0001		
		Time*DAT	0.267		
	2,4-D 0.56 kg ha^{-1}	8:00 AM 4:00 PM	1.57 (0.18)		y = 1.57x - 2.58
		Time	0.3518		
		DAT	<0.0001		
		Time*DAT	0.2037		
	Dicamba 0.28 kg ha^{-1}	8:00 AM	3.91 (0.65)	A	y = 3.91x - 11.79
		4:00 PM	1.88 (0.31)	B	y = 1.88x - 4.30
		Time	0.0011		

	DAT	<0.0001	
	Time*DAT	0.0054	
Dicamba 0.56 kg ha^{-1}	8:00 AM 4:00 PM	3.70 (0.43)	y = 3.70x - 11.96
	Time	0.9275	
	DAT	<0.0001	
	Time*DAT	0.5544	

Table 5.5. Slope comparisons for ANCOVA results comparing effect of herbicide/rate combinations pooled across humidity treatments and application times in growth chamber experiments, 2018.

[†]Parentheses represent standard error of the slope estimate.

[‡]Slope estimates followed by different letters do not differ statistically based on pairwise t-tests of indicator parameterization estimates at $\alpha = 0.05$.

[§]DAT = days after treatment, serving as the covariate in analyses. Insignificant herbicide by covariate effects at a significance level of 0.05 resulted in one slope being reported for each herbicide/rate combination.

Herbicide	Slope		Equation
2,4-D 0.28 kg ha^{-1}	1.46 [†](0.17)	[‡]C	y = 1.46x - 3.60
2,4-D 0.56 kg ha^{-1}	1.97 (0.24)	B	y = 1.97x - 4.46
Dicamba 0.28 kg ha^{-1}	1.92 (0.25)	BC	y = 1.92x - 5.75
Dicamba 0.56 kg ha^{-1}	3.62 (0.31)	A	y = 3.62x - 12.02
Herbicide	<0.0001		
DAT	<0.0001		
[§]Herbicide*DAT	<0.0001		

CHAPTER 6

OVERALL CONCLUSIONS

The reduction in auxinic herbicide efficacy near dawn and dusk, particularly with 2,4-D and dicamba, is a concern for growers that must treat large acreages. In cases where sequential applications must be made, increased production costs arise. Additionally, the threat of proliferation of problematic herbicide-resistant weed biotypes due to sublethal herbicide activity warrants a proactive approach to stewardship of these chemistries. This is particularly critical to maintaining effective alternative chemical control options for Palmer amaranth (*Amaranthus palmeri* S. Watson), a weed with widespread resistance to glyphosate and acetolactate synthase-inhibiting herbicides.

Differential auxinic herbicide translocation has been reported in *A. palmeri*. A reduced sensitivity of 2,4-D translocation in this species to N-1-napthylphthalamic acid (NPA) was observed with 8 am herbicide applications compared to those at 1 pm. This in combination with a lack of differential activity of 2,3,5-triiodobenzoic acid (TIBA), a selective PIN transport inhibitor, on 2,4-D translocation across both times of day suggest that ABCB-mediated 2,4-D transport may be upregulated at dawn. Similarly, dicamba translocation displayed a reduced sensitivity to the selective ABCB transport inhibitor 5-[*N*-(3,4-dimethoxyphenylethyl)methylamino]-2-(3,4-dimethoxyphenyl)-2-isopropylvaleronitrile hydrochloride (verapamil) with 8 am herbicide applications compared to those made at 1 pm. It is therefore suggested that differential ABCB activity at dawn is the reasoning behind improved translocation at this time.

Ethylene is one of the major markers of auxinic herbicide activity, with increases in production presumably indicating greater phytotoxicity in susceptible weeds. No significant difference in ethylene evolution in *A. palmeri* was detected across application times of 2,4-D, providing potential evidence that diurnal variation in the activity of this herbicide is negligible. However, significant differences in ethylene production were observed with dicamba, with a higher degree of evolution at 1 pm compared to 8 am. This provides real evidence for diurnal variation in the activity of a widely used auxinic herbicide. The role of translocation in ethylene production was illustrated by a marked increase in ethylene evolution when 2,4-D and dicamba translocation was inhibited by TIBA and NPA after 8 am herbicide applications, respectively. Furthermore, inhibition of dicamba translocation with NPA resulted in a complete reversal of the reduced ethylene production observed at 8 am.

Research utilizing qPCR indicated a significantly higher degree of *NCED1* expression with 2,4-D and dicamba applications at dawn compared to mid-day. This increase in the transcript levels of an abscisic acid (ABA) biosynthesis gene may reduce the ability of *A. palmeri* plants to perceive and carry out ABA-mediated signal transduction from auxinic herbicide presence in cells due to a reduction in plant biochemical activity. However, should an ABA-induced reduction in plant biochemical activity reduce the efficacy of auxinic herbicides due to stomatal closure and thus decreased carbon fixation, this does not appear to coincide with reduced auxinic herbicide translocation reported from previous research.

Temperature, day/night temperature differential, and humidity are all environmental effects that have reported influence on herbicide efficacy. Furthermore, the time of application may have more significant affects on phytotoxicity under certain environmental conditions. Temperature and day/night temperature differential were observed to have a marked affect on

both 2,4-D and dicamba activity in *A. palmeri*, with a notable lack of difference across differing humidity conditions. At the experimental high rate, 2,4-D and dicamba showed more activity at low temperatures. The time of application effect appears to be preserved with 2,4-D across a temperature gradient; however, no time of application effect was observed with dicamba across this same gradient. Interestingly, pooled across temperature differentials, dicamba showed a time of application effect at the low rate, but this was eliminated with increase to the high rate. These results suggest that application at lower temperatures is preferred with these two herbicides when possible. Furthermore, in the case of differing day/night temperature differentials, using a high rate of dicamba will potentially eliminate any time of application effects. The production of H_2O_2 in *A. palmeri* leaf tissue was found to have a relatively close association with observed phytotoxicity, suggesting that development of a rapid field test for H_2O_2 content may prove to be a valuable tool for growers who are suspecting reduced herbicide performance.